



# Max-Planck-Institut für Astronomie Heidelberg-Königstuhl

## Annual Report **2001**



**Cover Picture:**

This infrared image of Saturn was taken with the adaptive optics system NAOS and the infrared camera CONICA at the 8.2 meter telescope YEPUN of the VLT on Cerro Paranal in Chile (ESO). The image was taken shortly after first light of NAOS- CONICA in November 2001. With this device the diffraction-limited angular resolution of the large telescope is reached. The consortium responsible for development and construction of CONICA was led by the MPIA. A detailed description is given on p. 13 – 17.

# Max-Planck-Institut für Astronomie

Heidelberg-Königstuhl

## Annual Report

## 2001



## **Max Planck Institute for Astronomy**

### *Academic Members, Governing Body, Directors:*

Prof. Thomas Henning (since 1. 11. 2001)  
Prof. Hans-Walter Rix (Managing Director)

### *Emeritus Scientific Members:*

Prof. Hans Elsässer, Prof. Guido Münch

### *External Scientific Members:*

Prof. Immo Appenzeller, Heidelberg  
Prof. Steven Beckwith, Baltimore  
Prof. Karl-Heinz Böhm, Seattle  
Prof. George H. Herbig, Honolulu  
Prof. Rafael Rebolo, Teneriffa

### *Scientific Oversight Committee:*

Prof. Lodewijk Woltjer, Saint-Michel-l'Observatoire (Chair)  
Prof. Ralf-Jürgen Dettmar, Bochum  
Prof. Ewine van Dishoek, Leiden,  
Prof. Pierre Léna, Meudon  
Prof. Dieter Reimers, Hamburg,  
Prof. Anneila Sargent, Pasadena  
Prof. Rens Waters, Amsterdam,  
Prof. Simon D. M. White, Garching  
Prof. Robert Williams, Baltimore,  
Prof. Harold Yorke, Pasadena

### *Staff:*

The MPIA currently employs a staff of 185 (including externally funded positions). There are 35 scientists and 43 junior and visiting scientists. Students of the Faculty of Physics and Astronomy of the University of Heidelberg work on dissertations at the degree and doctorate level in the Institute. Apprentices are constantly undergoing training in the Institute's workshops.

*Address:* MPI für Astronomie, Königstuhl 17, D-69117 Heidelberg

*Telephone:* 0049-6221-5280, *Fax:* 0049-6221-528 246

*E-mail:* Sekretariat@mpia.de, Anonymous ftp: ftp.mpia.de

*Isophot Datacenter:* phthelp@mpia.de

*Internet:* <http://www.mpia.de>

## **Calar Alto Observatory**

*Address:* Centro Astronómico Hispano Alemán,  
Calle Jesús Durbán 2/2, E-04004 Almería, Spanien

*Telephone:* 0034-50-230 988, - 632 500, *Fax:* 0034-50-632 504

*E-mail:* name@caha.de

## **Masthead**

© 2002 Max-Planck-Institut für Astronomie, Heidelberg

All rights reserved. Printed in Germany

*Editors:* Dr. Jakob Staude, Prof. Hans-Walter Rix

*Text:* Dr. Thomas Bürhke

*Translation:* Margit Röser

*Illustrations:* MPIA and others

*Graphics and picture editing:* Dipl.-Phys. Axel M. Quetz, Martina Weckauf, Karin Meißner-Dorn

*Layout:* Marita Beyer, Modautal

*Printing:* Laub GmbH+Co., Elztal-Dallau

ISSN 1437-2924; Internet: ISSN 1617 – 0490

# Contents

<b>I General</b> .....	<b>5</b>	Barnard 68 – a Globule on the Verge of Collapsing? .....	37
I.1 Research Goals at the MPIA.....	5	Active Star Formation within CB 34 .....	40
Objectives of the Institute .....	5	Origin of CB 34.....	42
A Retrospect .....	5	Interstellar Icy Dust Grains .....	43
International Cooperation in Ground-based Astronomy .....	7	Core-mantle Model of Dust Grains.....	43
Adaptive Optics and Interferometry.....	8	Detection of Icy Dust Using ISOPHOT.....	44
Extraterrestrial Research .....	10	Formation of Binary Stars: New Answers and New Questions .....	46
Teaching and Public Relations .....	11	Evolution of Orbital Periods .....	48
I.2 Scientific Questions .....	12	Early Chemical Evolution of the Milky Way System ..	50
Galactic Research .....	12	A Model of the Chemical and Dynamical Evolution of the Halo .....	50
Extragalactic Research .....	12	Evolution of Metal Abundances.....	51
<b>II. Highlights</b> .....	<b>13</b>	IV.2 Extragalactic Astronomy.....	54
II.1. NAOS-CONICA: the High Performance Camera for the VLT.....	13	The Deepest Infrared Image – an Inventory of Stellar Masses in High Redshift Galaxies.....	54
Adaptive Optics .....	15	The Faint Infrared Extragalactic Survey (FIRES) .....	54
NAOS-CONICA Compared to HUBBLE .....	15	Bright and Massive Galaxies in the Early Universe.....	55
First Results and Future Tasks .....	16	An Extraordinary Large Disk Galaxy at $z = 3$ .....	56
II.2. Most Distant Quasar Shining through Primordial Matter .....	18	Old Galaxies at $z = 2?$ .....	57
The Re-ionization Phase.....	18	Limits and Future Tasks .....	58
Observing the Most Distant Quasars.....	18	Dust in Galaxy Clusters.....	58
The Sloan Digital Sky Survey (SDSS) .....	20	The Jet of the Quasar 3C 273 .....	61
II.3. COMBO-17 Reveals Dark Matter in Galaxy Clusters	21	Particle Acceleration and Synchrotron Emission .....	61
The Strategy of COMBO-17.....	21	Observations with the HST and the VLA .....	62
Weak Gravitational Lensing due to the Supercluster Abell 901/902 .....	21	Two Populations of Electrons .....	63
Dark Matter within the Abell Clusters .....	24	Spiral Systems in Elliptical Galaxies .....	64
<b>III Instrumental Development</b> .....	<b>27</b>	Simulations of the Kinematics .....	64
Adaptive Optics .....	27	Dark Matter and Galaxy Formation .....	70
Multiconjugate Adaptive Optics (MCAO) .....	28	The Angular Momentum Content of the Halos and Disks.....	70
LUCIFER and LINC – Two Instruments for the LBT .....	29	The Far-Infrared Sky Background.....	72
OMEGA 2000 – a Wide Field Infrared Camera for Calar Alto .....	31	Confusion Noise .....	73
LAICA – the Wide Field Camera for Calar Alto .....	31	Extragalactic Background Radiation.....	74
MIDI – an Infrared Interferometer for the VLT .....	32	IV.3 The Solar System .....	75
PACS - the Infrared Camera for HERSCHEL (formerly FIRST).....	34	ISO Observes Dust and Ice in Comet Hale-Bopp.....	75
<b>IV. Scientific Work</b> .....	<b>37</b>	Dust and Ice in the Coma of Hale-Bopp.....	76
IV.1 Galactic Astronomy .....	37	<b>Staff</b> .....	<b>79</b>
Evolutionary Stages of Bok Globules .....	37	<b>Working Groups</b> .....	<b>80</b>
		<b>Cooperation with Industrial Firms</b> .....	<b>82</b>
		<b>Teaching Activities</b> .....	<b>84</b>
		<b>Meetings, Talks and Public Lectures</b> .....	<b>84</b>
		<b>Service in Committees</b> .....	<b>86</b>
		<b>Publications</b> .....	<b>87</b>



# I General

## I.1 Research Goals at the MPIA

---

### Objectives of the Institute

From the formation and evolution of the Universe as a whole to the formation of stars and planets, it is the goal of the MPIA to advance astrophysical research on world standards by building telescopes and their auxiliary instruments, by direct observations, and by interpretation of the data obtained. Technological developments concentrate on the instrumentation for the optical and infrared wavelength range as well as for ground-based and satellite-borne observations.

The scientific work of one scientific department aims on understanding the formation and evolution of galaxies, their nuclei, and stellar populations from the big bang up to now. The research goal of the second department is to study star formation as well as to detect pla-

nets around other stars and study their formation and properties.

---

### A Retrospect

In 1967, the Senate of the Max Planck Society decided to establish the Max Planck Institute for Astronomy in Heidelberg with the intention to enable astronomical research in Germany to catch up with international stan-

**Fig. I.1:** The Max Planck Institute for Astronomy in Heidelberg with the Landessternwarte and the Neckar river valley in the background.

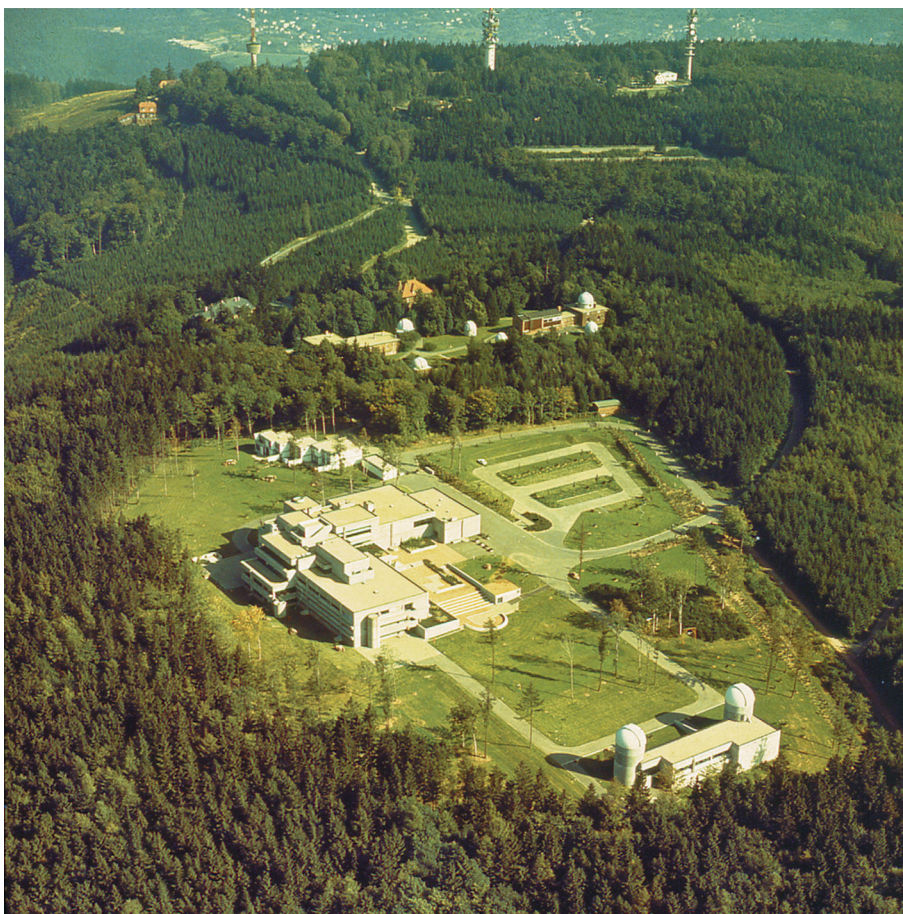




**Fig. I.2:** The Calar Alto Observatory. A view from the west shows the domes of the Schmidt telescope, the 1.23m telescope, the 2.2m telescope and the 3.5m telescope (from left to right).

dards. Two years later, the Institute commenced its work in temporary accommodation on the Königstuhl, and in 1975 it moved into its new buildings (Fig. I.1). As a long-term goal, MPIA was assigned with the construction and operation of two efficient observatories, one in the northern and one in the southern hemisphere. For the northern site, the Calar Alto Mountain (height: 2168 meters), in the province of Almería in southern Spain, was chosen, offering good climatic and meteorological conditions for astronomical observations. In 1972, the German-Spanish Astronomical Center (DSAZ) was established, generally known as the Calar Alto Observatory.

Between 1975 and 1984, the 1.23m reflector financed by the German Research Society (DFG) as well as the 2.2m and the 3.5m telescopes started operation on Calar Alto. With the Calar Alto Observatory, the MPIA commands one of the two most efficient observatories in Europe.

Today, MPIA operates the Calar Alto Observatory, which is available to all German astronomers, and takes

care to maintain the observatory's international competitive capacity. This includes the development of new instruments for the telescopes and the preparation of observing programs.

The original plans to build a southern observatory on the Gamsberg in Namibia could not be realized for political reasons. The 2.2m telescope intended for this location has instead been loaned to the European Southern Observatory (ESO) for a period of 25 years. Since 1984, it has been in operation on La Silla in Chile, where 25 % of its observing time is granted to astronomers within the Max Planck Society.

Since it was established, MPIA has been involved in extraterrestrial research, too. In particular, an early start in infrared astronomy associated with these activities has been of great significance for the later development of the Institute as a whole. In the 1970's, two photometers were developed and built at MPIA which flew successfully on board the two solar probes **HELIOS 1** and **2**. At about the same time, the **THISBE** infrared telescope (Telescope of Heidelberg for Infrared Studies by Balloon-borne Experiments) was developed. It was carried by a high-altitude research balloon up to a height of 40 km where mid/far infrared observations are possible.



**Fig. I.3:** Presentation of the mounting of the Large Binocular Telescope in November 2001. (image: Carlucci)

MPIA was participating significantly in the world's first Infrared Space Observatory (ISO) of the European Space Agency ESA: **ISOPHOT**, one of four scientific instruments on board of ISO, was built under the coordinating leadership of a principal investigator at the Institute. For over two years, ISO provided excellent data. It was switched off on 8 April 1998, after its coolant supply had been exhausted.

### International Cooperation in Ground-based Astronomy

Together with the University of Arizona and Italian institutes, MPIA is one of the major partners in an international consortium, which is building the **Large Binocular Telescope (LBT, Fig. I.3)**. The LBT is a double telescope, with two mirrors of 8.4 m diameter each, fixed on a common mount. Together, the two mirrors have a light-gathering power equivalent to a single 11.8 m mirror. This will make the LBT the world's most powerful single telescope. Furthermore, the double telescope is planned to be

used for interferometric observations. In this case, its spatial resolution will correspond to that of a single mirror 22.8 m across. First light with only one primary mirror is currently planned for mid-2004. One year later, the entire telescope will be put into operation.

Under the leadership of the Landessternwarte Heidelberg, the German partners are building a near-infrared spectrograph for the LBT, called **LUCIFER** (see Chapter III). MPIA will supply the entire detector package and develop the overall design of the cooling system. Integration and tests of the instrument will also be carried out in the laboratories of MPIA.

Simultaneously, planning of the LBT interferometer, which will be equipped with an adaptive optics system, is in full swing. For this instrument, MPIA is developing the optics of the LINC beam combiner, which finally will allow interferometry over a wavelength range between 0.6  $\mu\text{m}$  and 2.2  $\mu\text{m}$ . This requires an extremely demanding optical design. Moreover, an informal consortium with colleagues from the Universität Köln and the Astrophysical Institute Arcetri in Italy was formed.



**Fig. I.4:** The Very Large Telescope, situated in the Chilean Andes. (Image: ESO)

Building new instruments for Calar Alto and the LBT as well as for the ESO Very Large Telescope (VLT) is a major part of the MPIA's activities (see Chapter III). For this purpose, the Institute is equipped with ultra-modern precision mechanics and electronics workshops.

Participation in multinational observatories and projects are of major importance, too. In the year under report, the high-resolution infrared camera CONICA was put into operation at the ESO Very Large Telescope (VLT) on Cerro Paranal in Chile (Fig. I.4). This camera, equipped with an adaptive optics system, has fully met the expectations, being one of the highlights of the Institute's activities in 2001 (see Chapter II.1).

Construction of MIDI, an interferometric instrument for the VLT, was progressing well. From 2002 on, this trend-setting instrument will allow for the first time the interferometric coupling of two big telescopes in the infrared.

The MPIA is also participating in the **Sloan Digital Sky Survey (SDSS)**. This is the hitherto most extensive sky survey, imaging about a quarter of the entire sky in five wavelength ranges. The final catalogue will provide positions and colors of an estimated one hundred million celestial bodies as well as redshifts of about one million galaxies and quasars. The observations are performed using a 2.5m telescope, which was specially built for this purpose, located at Apache Point Observatory in New Mexico (Fig. I.5). The project is conducted by an international consortium of American, Japanese and German institutes. In Germany, the MPIA at Heidelberg and the MPI for Astrophysics in Garching are involved. In exchange for material and financial contributions from the MPIA, a team of scientists at the Institute gets full access to the data. After a testing phase of a little more than a year, the survey officially started in April 2000.

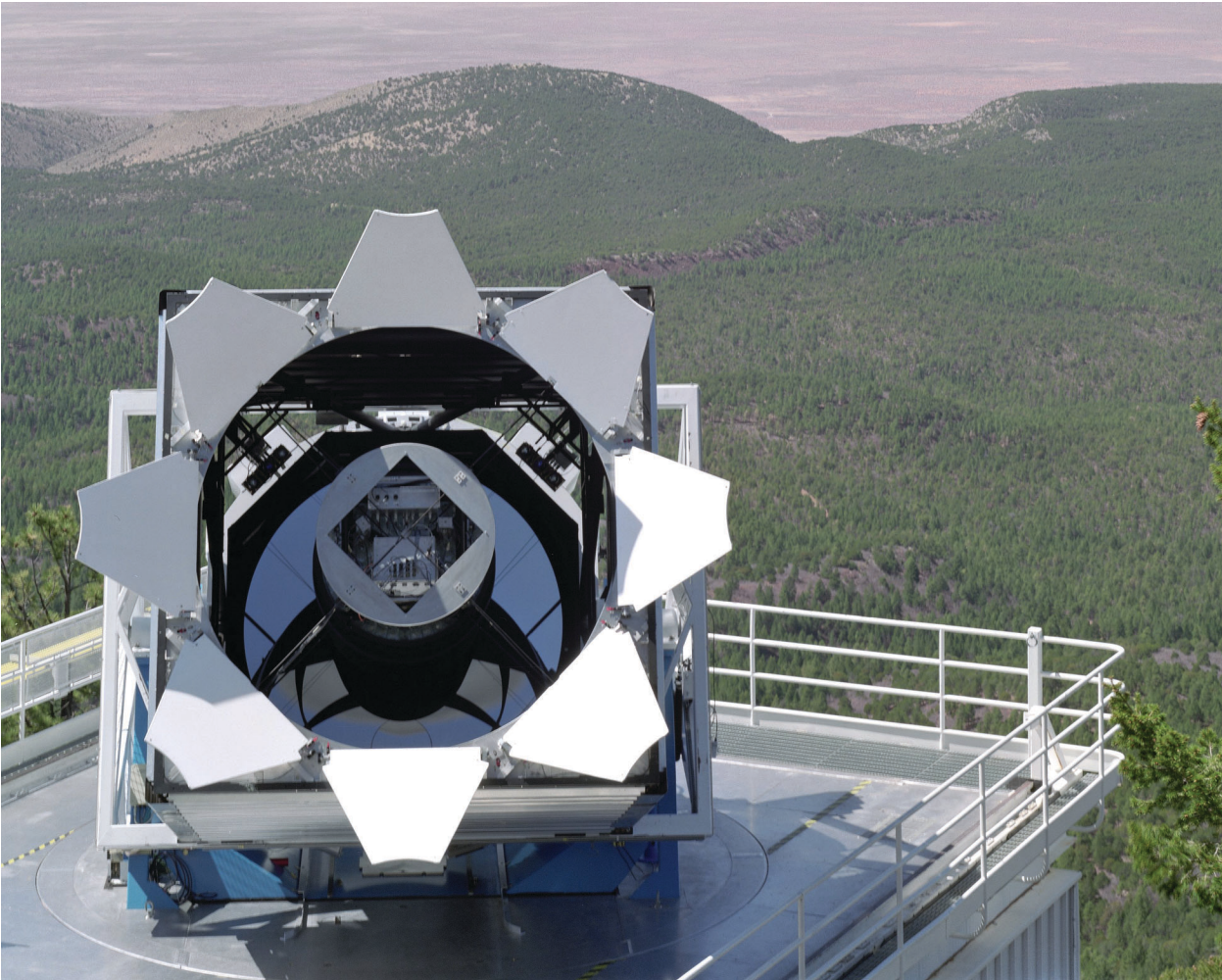


**Fig. 1.5:** The 2.5m telescope of the Sloan Digital Sky Survey (image: SDSS)

### Adaptive Optics and Interferometry

Research concentrates on the “traditional” visible spectral range as well as on the infrared, attributing much importance to the advancement of new techniques. So, e.g., the Institute is contributing considerably to the new technique of adaptive optics systems by the development of the **ALFA** system using an artificial laser guide star. Currently, this field of research is being carried on by developing a multiconjugate adaptive optics system (Chapter III). Experience gained in this work will be incorporated into the development of new instruments for the Very Large Telescope and the Large Binocular Telescope.

The establishment of the **German Center for Infrared and Optical Interferometry** (Frontiers of Interferometry in Germany, or **FrInGe** for short), located at MPIA, also emphasizes the Institute’s consequent ori-

entation towards future astronomical techniques. Recently, infrared and optical interferometry has globally experienced a great impetus. Most of it is due to the latest success of the Very Large Telescope Interferometer (VLTI). Here, the MIDI and AMBER instruments will soon yield first scientific data.

Interferometric instruments enable ground-based telescopes to reach unprecedented spatial resolution. Moreover, precise astrometry will allow the detection of moving celestial objects, particularly the motion of stars caused by orbiting planets.

In interferometry, the process of planning and scheduling observations, data reduction and interpretation are much more tightly connected than in traditional astronomy. In fact, the technique of data interpretation is strongly influenced by the very design of the instrument - and vice versa.

For these reasons, FrInGe was created in September 2001. Its goal is to co-ordinate efforts by German institutions in this field. FrInGe will gather tools and software developed by participating institutes. A team at the MPIA, e.g., is currently developing software for planning interferometric observations, called SimVLTI.

Apart from MPIA, the following institutes are participating in FrInGe: the Astrophysikalische Institut Potsdam

(AIP), the Astrophysikalische Institut and Universitätssternwarte der Universität Jena (AIU), the Kiepenheuer-Institut für Sonnenphysik in Feiburg (KIS), the MPI für extraterrestrische Physik in Garching (MPE), the MPI für Radioastronomie in Bonn (MPIfR) and the I. Physikalisches Institut der Universität zu Köln (UK).

Another goal of FrInGe is defining the next generation of interferometric instruments. This includes the extension of VLTI and contributions to the planned space interferometer DARWIN.

FrInGe will seek to establish cooperation with other interferometric centers in Europe. The long-term perspective is to establish a European interferometric center for infrared and optical interferometry.

---

### Extraterrestrial Research

For one thing, current activities at MPIA include exploiting the scientific results of the ISO mission.

During the last year of the ISO post-operative phase (starting 1998), activities in program development and calibration analysis for version 10 of the automatic data analysis have been completed within the framework of the ISOPHOT data center at MPIA. This was the last upgrade of the software used at the ISO data center VILSPA in Spain to create the ISO Legacy Archive.

In the year under report, eight visitors used the ISOPHOT data center in Heidelberg for several days. By the end of 2001, about 190 publications based on ISOPHOT data have appeared in refereed journals, corresponding to an analysis of about 25% of the scientific data base. In summer, preparations for the five-year long active archive phase started which follows the post-operative phase. During this active archive phase, the remaining 75% of the data will be analyzed and the accuracy and user friendliness of the ISO data archive will be increased. In addition, the ISO data base will be expanded to be part of a globally accessible “virtual observatory” for all wavelength ranges.

Concerning the scientific aspect, there were quite a number of important studies, including observations of interstellar icy dust grains (Chapter IV.1), the completion of studies on intergalactic dust (Chapter IV.2) and observations of comet Hale-Bopp (Chapter IV.3).

The experience gained with ISOPHOT was decisive for the MPIA's significant participation in the construction of the PACS **infrared camera and spectrometer** (Chapter III). This instrument will operate on board the European HERSCHEL infrared observatory (formerly the Far Infrared and Submillimeter Telescope, FIRST). The launch of this 3.5m space telescope is planned for 2007.

Furthermore, the Institute is expected to participate in the development of the successor to the HUBBLE space telescope, the so-called **New Generation Space Telescope** (NGST) (Fig. I.6). The NGST is planned to be equipped with a third focal-plane instrument, an instrument for the

mid-infrared range from 5 - 28  $\mu\text{m}$ . This consists of a high-resolution camera and a spectrometer of medium resolution. The instrument will be built fifty percent each by American and European institutes, which will be granted guaranteed observation time in exchange for their contributions. As part of the European consortium, the MPIA offers the development of all cryo-mechanics for the positioning of optical components such as gratings, filter wheels and mirrors in the cryo-vacuum (with a temperature of about 7K). Due to the successful development of ISOPHOT and PACS, the Institute is well prepared for this task. In the last quarter of the year under report, a phase A study financed by ESA started under the leadership of ATC Edinburgh; to this study, MPIA will contribute the cryo-mechanics and electric design packages.

The Institute is participating in a satellite experiment proposed to NASA by Johns Hopkins University, Baltimore. This telescope, known as **PRIME** (Primordial Explorer), is intended to map a large part of the sky down to a magnitude of 24.5 in the wavelength range between 0.9 and 3.4  $\mu\text{m}$ . PRIME would be a predecessor of NGST (New Generation Space Telescope), the planned successor to the HUBBLE Space Telescope. It would comprise a 75 cm telescope moving around Earth in a polar orbit at 650 km altitude. The telescope's focal plane is split by three mirrors into four wavelength channels, which are equipped with newly developed infrared arrays.

Prime could scan a quarter of the entire sky within three years with an unprecedented accuracy, providing new findings in virtually every field of modern astronomy. For example, the telescope could detect at least 1000 supernovae of type Ia in the redshift range  $1 < z < 5$  and measure their light curves, as well as finding hundreds of brown dwarfs at distances up to 1000 parsecs, extrasolar planets the size of Jupiter at distances up to 50 parsecs, quasars with redshifts up to  $z = 25$  and protogalaxies up to  $z = 20$ .

An industry feasibility study of the PRIME telescope was completed in the middle of the year and the project was submitted by the German side to the consultative panel of the DLR. In an international cooperation of the participating institutes, the phase A report was completed and sent to NASA in December. NASA will decide on the project in July 2002. MPIA is to provide the telescope.

With this widely spread instrumentarium, MPIA will continue to contribute significantly to astronomical research.

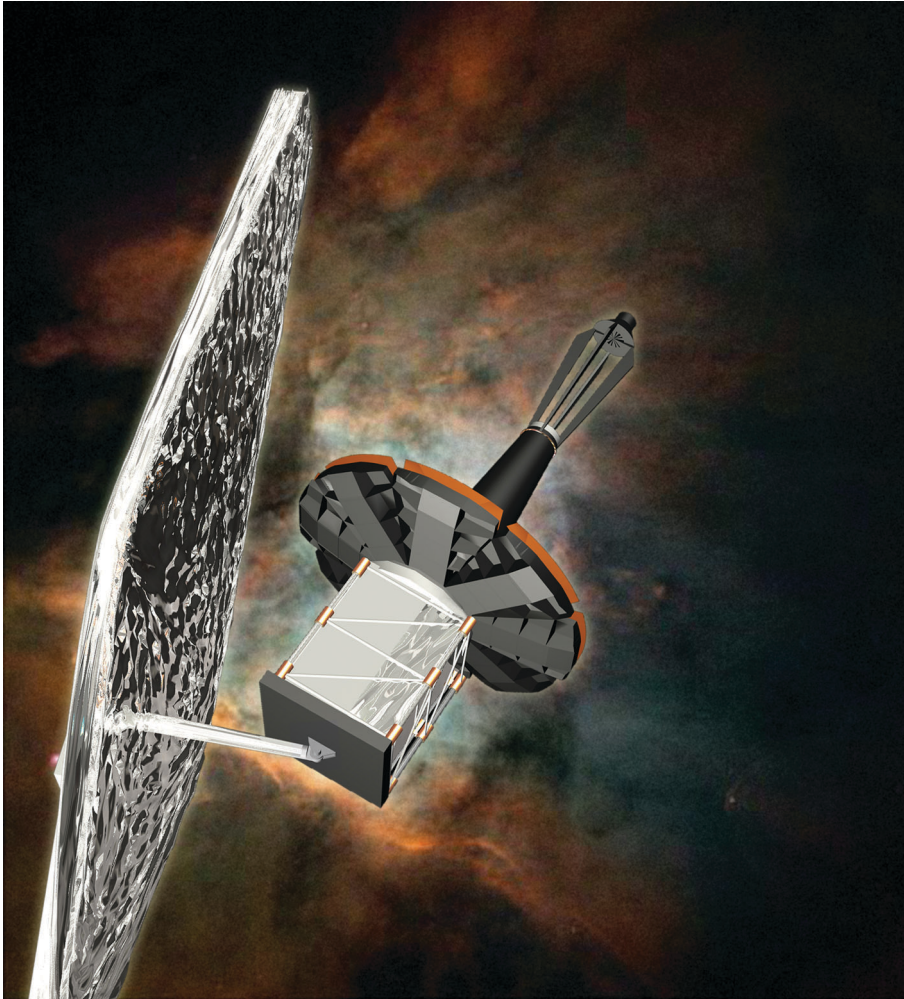


**Fig. I.6:** Possible design of the NGST. (image: Lockheed-Martin)

---

### Teaching and Public Relations

The Institute's tasks also include informing the general public about results of astronomical research. Members of the Institute give talks at schools, adult education centers and planetaria. They also appear at press conferences or on radio and television programs, in particular on the occasion of astronomical events, which attract major public attention. Numerous groups of visitors come to the MPIA on the Königstuhl and to the Calar Alto Observatory.

Since 1976, a regular one-week teacher training course is held in autumn at the MPIA which is very popular among teachers of physics and mathematics in Baden-Württemberg.

Finally, the monthly astronomical journal *Sterne und Weltraum* (Stars and Space), co-founded by Hans Elsässer in 1962, is published at the MPIA. This journal is intended for the general public but also offers a lively forum both for professional astronomers and for the large community of amateurs in this field.

## I.2 Scientific Questions

The central issue of all cosmological and astronomical research deals with the formation and evolution of the universe as a whole as well as of stars and galaxies, the Sun and its planets. The MPIA's research program is oriented to these questions.

In the field of galactic research, the Institute concentrates on star formation in huge interstellar clouds of gas and dust. In the field of extragalactic astronomy, the focus is on large-scale structure of the universe, the search for primordial galaxies and the investigation of active galaxies and quasars. These are remote stellar systems with enormous luminosities. The observational research is supported by a group of theoreticians who use computer simulations to reconstruct processes in the universe extending over tens of thousands or millions of years. Thus, a fertile synthesis of observation and theory is achieved at the MPIA.

---

### Galactic Research

A central field of galactic research at the MPIA is star formation. The first stages of this process take place in the interiors of dust clouds, and hence remain hidden from our view in visible light. Infrared radiation, however, can penetrate the dust, which is why the early stages of star formation are being studied preferentially in this wavelength range.

Using ISOPHOT, it was possible to detect very cold and dense regions within large dust clouds. These are protostellar cores, which are on the verge of collapse or already contracting to form stars. In the year under report, observations of Bok globules – small, compact dark clouds in which only few stars can form - were of special interest (Chapter IV.1). There were also new findings on the formation and evolution of binary stars – another important research field at the Institute (Chapter IV.1).

---

### Extragalactic Research

Extragalactic research is dealing with galaxies and clusters of galaxies. In this field, one of the major tasks is to reconstruct galactic evolution. What was the star formation rate in the early universe? Did galaxies merge, thereby reducing their total number in the course of billions of years? And how did dark matter affect these processes? These are only three of the crucial questions.

In this context, great progress was made thanks to the Faint Infrared Extragalactic Survey (FIRES). It combines images of the HUBBLE Space Telescope in visible light with new near-infrared images obtained with the Very Large Telescope (VLT) of the European Southern Observatory (ESO). Up to now, these are the deepest and best images in this wavelength region. The goal is, among other things, to determine the magnitude distribution, sizes and shapes of galaxies over a wide redshift range and the evolution of their stellar masses. First results confirm the strategy of the method and have already revealed a number of interesting facts (Chapter IV.2).

Dark matter is still a great mystery to cosmologists. So far, neither its nature nor its spatial distribution is known. In collaboration with colleagues from Great Britain, astronomers at MPIA have mapped the spatial distribution of dark matter in superclusters of galaxies (Chapter II.3). At the same time, theoreticians investigated how dark matter could have advanced or even initiated the formation of galaxies in the early universe. This work illustrates again fundamental deficits in the understanding of dark matter and its role in the evolution of the universe.

## II Highlights

### II.1 NAOS-CONICA: the High Performance Camera for the VLT

At the end of 2001, the infrared camera CONICA, built under the leadership of the MPIA, was put into operation at the ESO Very Large Telescope. Together with the adaptive optics system NAOS, built in France, the instrument reaches the theoretical resolution limit of the telescope. Thus, European astronomers are setting new standards for ground-based near infrared observations.

The four telescopes of the VLT (Fig. II.1) provide space for a total of twelve scientific instruments at both of their Nasmyth foci and at the Cassegrain focus. NAOS-CONICA is used at the Nasmyth focus of the telescope named YEPUN (Venus or Evening Star in English) and is designed for the near infrared region.

CONICA (Coudé Near Infrared camera) was built under the leadership of the MPIA in collaboration with scientists of the MPI für extraterrestrische Physik (Garching) and of

the ESO. The adaptive optics system NAOS (Nasmyth Adaptive Optics System) was built in France.

Before “first light” at the telescope (Fig II.2), ten years of planning and construction had passed during which new developments kept requiring conceptual modifications. The most fundamental of these was necessary when ESO decided to install CONICA at the Nasmyth focus (focal ratio of  $f/15$ ) instead of the Coudé focus ( $f/51$ ). At the same time, ESO decided to attach CONICA rigidly to an adaptive optics system.

**Fig. II.1:** Schematic illustration of the VLT and its instruments (in parentheses the dates of the prospective “first light”). The VST (Survey Telescope) is a 2.5m-telescope with a very large field of view, which will be used for wide area surveys. In the lower part, three smaller so-called auxiliary telescopes are to be seen which will be employed for interferometry in addition to the large telescopes. (ESO)

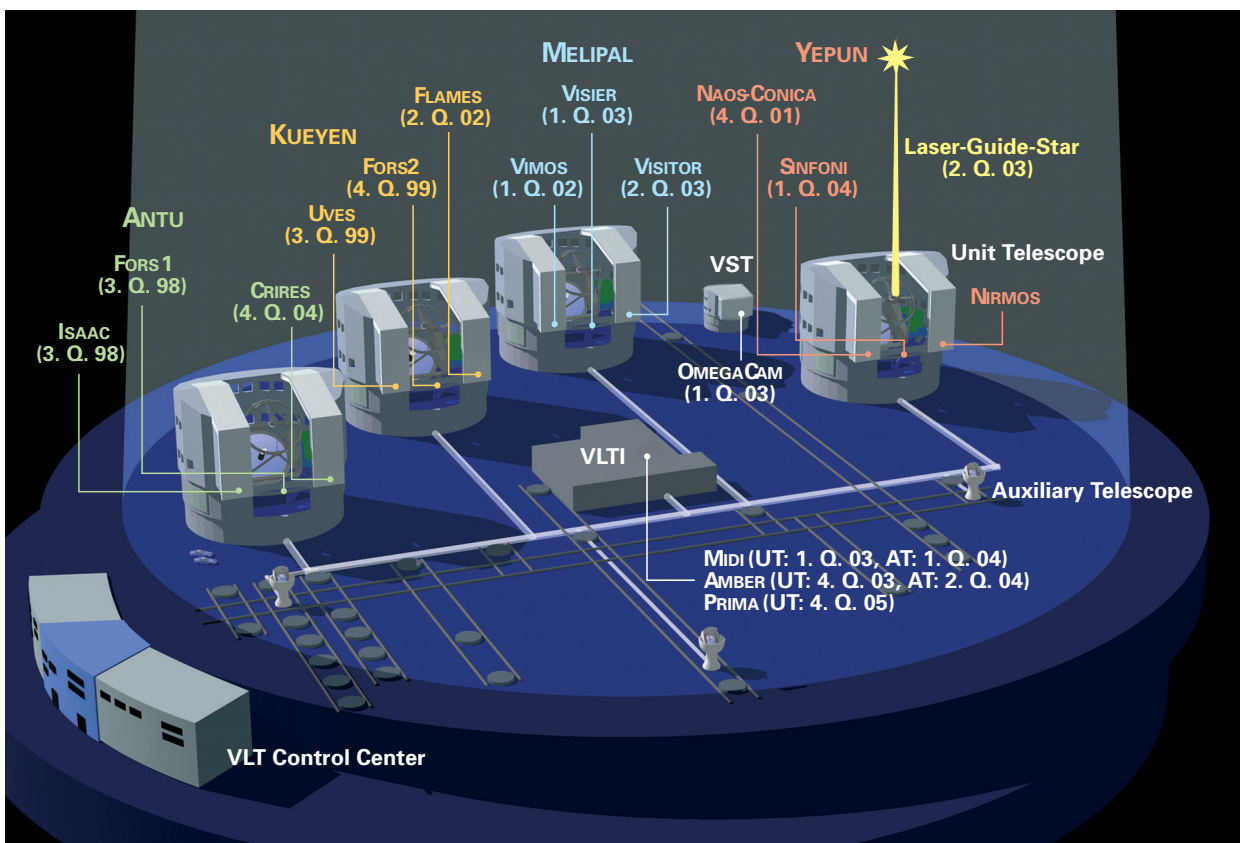




**Fig. II.2:** The Heidelberg team during the set-up of CONICA at the Nasmyth focus of the YEPUN telescope. (MPIA)

Constructing CONICA involved an estimated 40 man-years of work. ESO took over the material costs of about 2.3 million D-Mark while the MPIAs contributed their workshop equipment and the expertise of their staff.

CONICA provides several different operation modes (Fig. II.3):

*Direct imaging:* A total of seven cameras with different focal ratios provide almost perfect imaging capability. They are mounted on a big wheel with which they can be inserted into the optical beam. Four cameras are operating in the  $1 - 2.5 \mu\text{m}$  wavelength region and three in the  $2 - 5 \mu\text{m}$  region. The image scale varies between 0.11 arc seconds per detector pixel at  $f/6.4$  and 0.014 arc seconds per pixel at  $f/51$ . The field of view also depends on the focal ratio and decreases

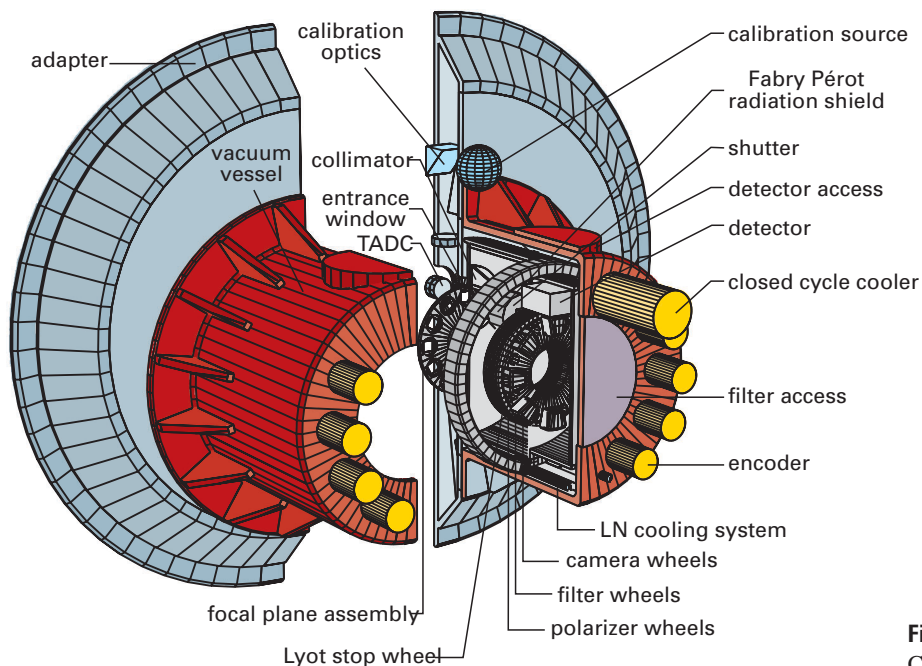


**Fig. II.3:** Conceptual overview of CONICA. (MPIA)

from  $73 \times 73$  arc seconds ( $f/6.4$ ) to  $14 \times 14$  arc seconds ( $f/51$ ).

*Polarimetry:* Measuring the degree and angle of polarization gives important clues about, *e.g.*, the spatial distribution of circumstellar dust. For this kind of observations CONICA is provided with four wire grid analyzers and two Wollaston prisms. The entire instrument can be rotated to arbitrary position angles on the sky.

*Spectroscopy:* The spectral energy distribution of the infrared radiation allows one to determine temperatures, velocities, redshifts and also the chemical compositions of cosmic bodies and clouds of gas and dust. For this purpose, CONICA contains four so-called grisms – optical elements consisting of a prism and a diffraction grating. They allow spectroscopy with low resolution ( $200 < \lambda/\Delta\lambda < 1000$ ) over the whole range from  $1 - 5 \mu\text{m}$ .

In addition, there are a number of other *optical elements*. CONICA has about 40 color filters which are mounted in two additional wheels and which can be inserted individually into the optical beam. They also include several narrow band filters as well as a tunable Fabry-Perot etalon which allow to search for the spectral signatures of certain substances. Moreover, slits and coronagraphic masks can be inserted into the focal plane. The latter is used to occult bright objects which outshine neighboring faint objects.

Another interesting element is a tunable dispersion corrector consisting of two double prisms which can be rotated against one another. They are used to correct atmospheric dispersion effects (the wavelength dependent refraction of light by air). The corrector is working in a wavelength range between  $1$  and  $2.5 \mu\text{m}$  down to zenith distances of  $60$  degrees.

Observing in the infrared region puts special demands on the instruments as all bodies at room temperature emit thermal radiation in this wavelength region. To avoid blinding the instrument by its own thermal emission, it has to be cooled down significantly. A closed cycle cooler cools the optical system as well since the cameras down to  $-210$  degrees Celsius and the detector down to  $-240$  degrees Celsius. This cryostat turned out to be a major problem concerning the stability of the entire instrument as during long exposures the entire camera is rotating on the telescope in order to compensate for the apparent sky rotation. Therefore care had to be taken that the instrument weighing  $1$  ton was not flexing mechanically by more than a few thousandths of a millimeter during this motion. Meeting this requirement was especially difficult for the thermally insulated cold part of CONICA.

---

## Adaptive Optics

The turbulence of the atmosphere prevents large telescopes from reaching their theoretical resolution, the so-called diffraction limit, because the light of a celestial body passing the different atmospheric layers experiences spatially and temporally rapidly changing disturbances (“seeing”). Thus, the originally flat wavefront undulates during its passage through the atmosphere, similar to a flag fluttering in the wind. As a result, longer-exposure images get blurred.

An adaptive optics system corrects seeing effects during the observations (cf. Annual Report 1998, p. 38). This is achieved by a tip-tilt mirror, which compensates for the motion of the image point on the detector. Moreover, the “distorted” wave front is straightened by a flexible mirror, whose surface is distorted in such a way, that it shows exactly the opposite pattern of the wave front. After being reflected by this adaptive mirror the distortion of the wave front is eliminated and an undistorted diffraction limited image appears on the detector.

However, this method only works under certain conditions. For one thing, NAOS requires a reference star with a certain minimum brightness within the field of view. The limiting magnitude in the visible range is  $18$  mag, and  $14$  mag at  $2.2 \mu\text{m}$ . The seeing has to be below about  $2$  arc seconds for NAOS to work optimally. NAOS corrects the field of view within  $60$  arc seconds of the reference star, but the quality of the correction decreases with increasing distance to the reference star (anisoplanatism). The quality of the correction also declines with decreasing brightness of the reference star and increasing seeing.

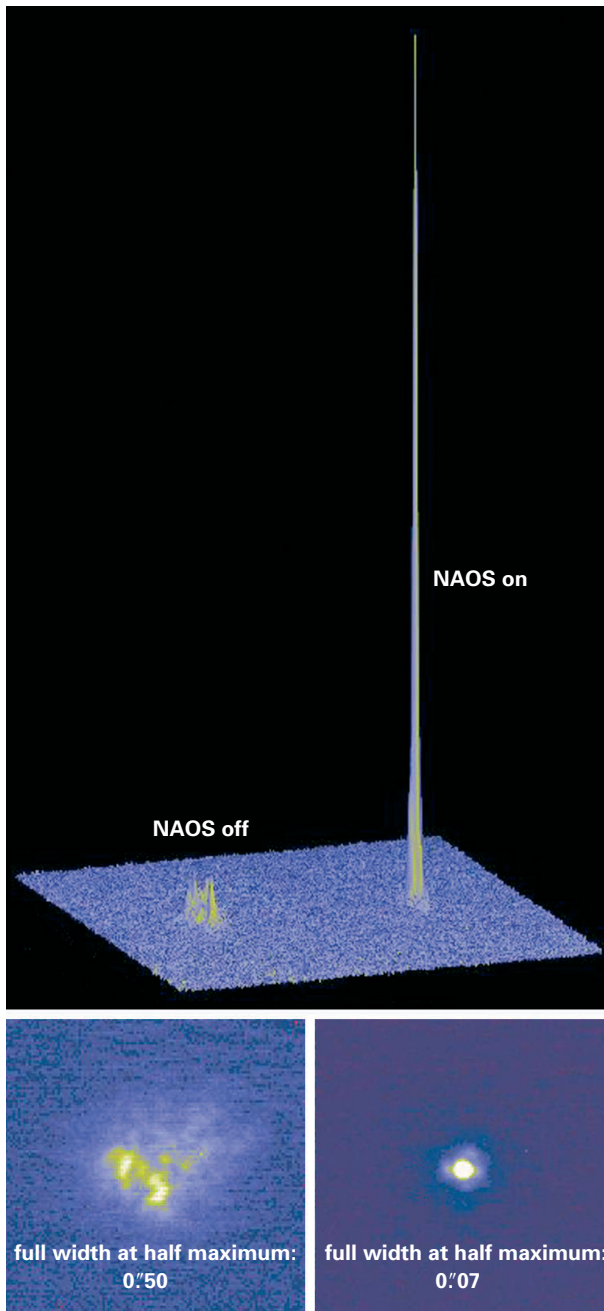
---

## NAOS-CONICA Compared to HUBBLE

This list of restrictions and requirements for employing adaptive optics should not give the impression that this technique could only be used in a very limited way. Even the first results demonstrate impressively that NAOS-CONICA will be in serious competition with the HUBBLE Space Telescope in many cases. Obviously, CONICA has fundamental advantages: The diameter of the VLT’s primary mirror is  $3.4$  times as large as that of the HST. Thus, the diffraction limit at a given wavelength is smaller by the same factor for the VLT, while the light gathering area is ten times as large for the VLT. At a wavelength of  $2.2 \mu\text{m}$ , NAOS-CONICA reaches a limiting magnitude of about  $25$  mag in an one hour exposure. Moreover, newly developed detectors, can be employed on a ground-based telescope much faster and more cheaply than on HUBBLE.

On the other hand, the space telescope also has evident advantages. It does not depend on fields with a suitable reference star, and the resolution hardly varies over the entire field of view. Besides that, there are wavelength regions where the atmosphere is not transparent, like aro-

und  $1.4\ \mu\text{m}$  and  $1.9\ \mu\text{m}$  or in wide ranges between  $2.5\ \mu\text{m}$  and  $3.4\ \mu\text{m}$  as well as between  $4.2\ \mu\text{m}$  and  $4.7\ \mu\text{m}$ . In these regions, observations from the ground are impossible. Finally, HUBBLE is not affected by the brightness of the night sky.



### First Results and Future Tasks

As a first test object for NAOS-CONICA, the telescope was aimed at an unnamed star of 8 mag in the Milky Way. The uncorrected image showed a seeing of 0.5 arc seconds. Immediately after turning on NAOS, the stellar image shrunk (Fig. II.4). At  $1.2\ \mu\text{m}$  and  $2.2\ \mu\text{m}$  wavelength, the system almost reached the theoretical diffraction limit with resolutions of 0.04 and 0.07 arc seconds, respectively, in the first attempt.

An image of the star cluster NGC 3603 compared to a HUBBLE image is showing the potential of the new camera (Fig. II.5). A magnificent image of Saturn was taken as well (Fig. II.6). It is a superposition of two images, taken at  $1.6\ \mu\text{m}$  and  $1.2\ \mu\text{m}$  with 20 and 24 seconds exposure times, respectively. Saturn's moon Tethys (seen below) was used as a reference object for the adaptive optics. The resolution is 0.07 arc seconds, corresponding to 410 kilometers at the location of the planet. A high-resolution image of the Jovian moon Io was also obtained (Fig. II.7). It was taken with an exposure time of 230 seconds through a small-band filter at  $2.166\ \mu\text{m}$  wavelength (Bracket-gamma line). Although the disk of the moon has an apparent diameter of only 1.2 arc seconds, many surface features of the volcanically active moon can be recognized at 0.068 arc seconds resolution, corresponding to 210 kilometers on Io.

NAOS-CONICA will stay as an instrument at the YEPUN telescope and will be available to guest observers. Astronomers of both MPIs are granted 45 observing nights in return for their efforts. The French colleagues, too, will get a number of guaranteed observing nights. The new instrument can be used for a multitude of research areas, such as:

- Study of the formation and evolution of galaxies and galaxy clusters, whose spectra are highly redshifted due to the large distances involved.
- Observation of the centers of active galaxies harboring black holes, which presumably are surrounded by large masses of dust.

**Fig. II.4: Below:** The first image taken with NAOS-CONICA. Left: the uncorrected image; right: after turning on the adaptive optics. **Above:** A three-dimensional illustration of the intensity distribution of both images. (ESO)

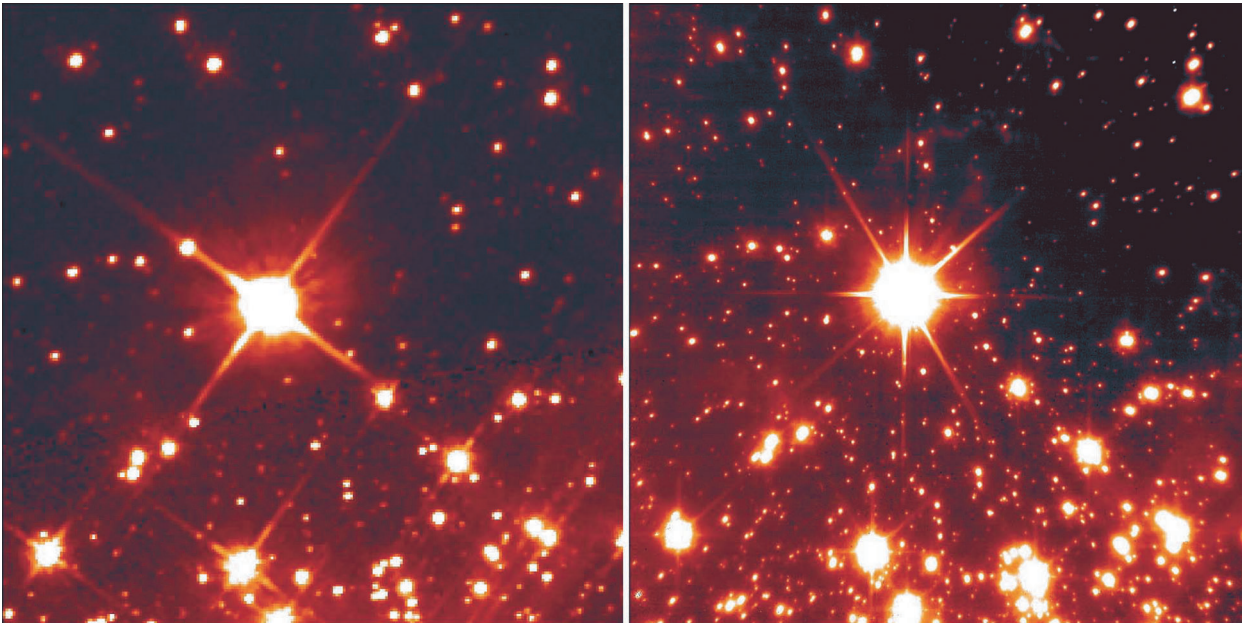


**Fig. II.5:** The star cluster NGC 3603, imaged by the HUBBLE Space Telescope (left) and NAOS-CONICA (right). (NASA/ESO)

- Discovery of very low-mass stars and brown dwarfs, radiating mainly in the infrared region.
- Study of star formation regions where the young stars frequently are obscured by clouds of dust, which are transparent in the infrared region.
- Study of circumstellar dusty disks, in which planets may be forming.

Discovery and direct observation of extrasolar planets. In the infrared, the brightness contrast between star and planet is significantly smaller than in visible light.

*(Rainer Lenzen, P. Bizenberger, M. Hartung, W. Laun, N. Münch, R.-R. Rohloff, C. Storz, K. Wagner)*



**Fig. II.6:** Saturn, photographed in the near infrared with 0.07 arc seconds resolution. (ESO)

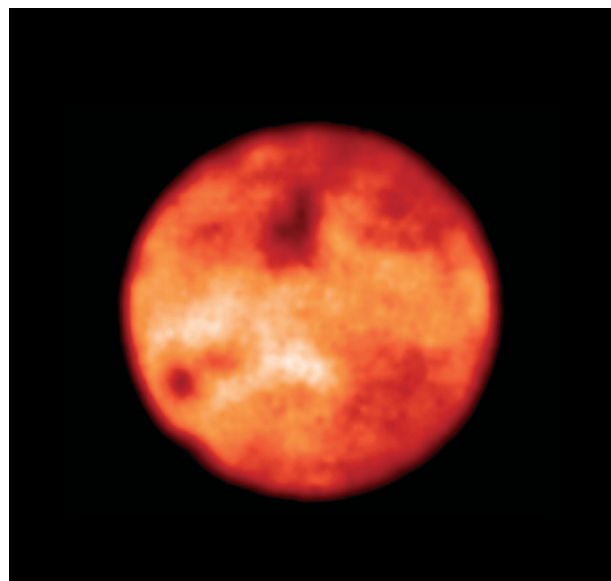


**Fig. II.7:** Jupiter's moon Io, photographed at 2.166  $\mu\text{m}$  wavelength. The resolution is 0.068 arc seconds. (ESO)

## II.2 Most Distant Quasar Shining through Primordial Matter

**In the course of the large Sloan Digital Sky Survey (SDSS), carried out by American, German and Japanese astronomers, the most distant quasar to date has been discovered. It has radiated the light, which we detect today at a time when the Universe was only about 700 million years old. Astronomers at the MPIA obtained a spectrum of this celestial object using the Very Large Telescope (VLT) of the European Southern Observatory (ESO). The spectrum shows that the quasar is still located within the mainly neutral intergalactic matter, which filled the very early Universe. Thus, astronomers succeeded for the first time in reaching with their observations the boundary of the "genuine" primordial matter.**

After the Big Bang, the Universe was filled with a hot ionized gas, in which protons and electrons were moving around freely. Only after about 300 000 years, had the medium cooled down enough for atoms to form. This happened at a redshift of  $z = 1100$  to  $1500$ , the exact value depending on the cosmological model. After this recombination phase, the gas in the entire Universe was neutral. In this medium, consisting almost exclusively of hydrogen and helium, the first stars, galaxies and quasars formed. The UV-radiation, which they emitted, ionized their surroundings anew. This so-called re-ionization marks the phase of the very first structure formation within the early Universe, which made it bright again.

---

### The Re-ionization Phase

When and how the re-ionization phase occurred, is a fundamental issue of present-day cosmology, which until now could only be addressed theoretically. According to present models, re-ionization occurred at redshifts between  $z = 6$  and  $z = 20$ , that is, several hundred million years after the Big Bang. However, this value is very uncertain, as re-ionization was a very complex process. Computer simulations have to take into account, *e.g.*, gas dynamics, star formations processes, atomic and molecular processes as well as radiative transport phenomena. Moreover, it is not clear whether the dominating contribution to re-ionization came from the UV radiation of hot stars or of accreting black holes.

One of the uncertainty factors is, the stellar mass function. Very probably, it had a different shape at that time than it has today because the gas did not contain heavy elements. There is some evidence that the fraction of massive stars was larger in the first stellar generation than to-

day. As a result, there were more supernova explosions which significantly affected the enrichment of the surrounding medium with heavy elements as well as the number of energetic ionizing UV photons. The evolution of the re-ionization phase is additionally complicated by inhomogeneities of the gas, clumping locally into denser clouds, or of the dark matter whose nature is still unknown to us but which acted in a way as "condensation seeds" for the forming galaxies.

According to current ideas, the re-ionization phase can probably be roughly divided into three stages: First, single regions of ionized gas (HII regions) formed around the stars or quasars. In a second stage, these regions overlapped, strongly increasing the intensity of the UV radiation. During the third stage, the still existing neutral hydrogen within dense regions finally became ionized, too. In such models, the second stage sets in at a redshift around  $z = 7$  and the third stage at  $z = 6$ .

---

### Observing the Most Distant Quasars

In the end, a clear picture of this earliest phase of structure formation in the Universe can only be obtained by observations. But detection and spectroscopic studies of objects with redshifts larger than  $z = 6$  became possible only recently. The Sloan Digital Sky Survey (SDSS, see below) offers the possibility to find the proverbial needles within a haystack while the new generation of large telescopes provides the necessary capability to study them in detail.

With the SDSS, it is possible, among other things, to detect quasars by their characteristic spectral energy distribution. Quasars are very compact central regions of galaxies harboring a massive black hole. This is surrounded by a disk of hot gas which is radiating very intensely in the UV region. As quasars are the most luminous celestial objects known they should still be observable at redshifts  $z > 6$ .

In the year under report, two new distance record holders among the quasars were discovered within the data of the SDSS. In subsequent observations with the Keck telescope their redshifts were determined to be  $z = 6.28$  and  $z = 5.99$ . The most distant quasar, which was designated SDSS 1030+0524, is thus seen at a time when the age of the Universe was only 5 % of its present value, that is, about 700 million years ( $q_0 = 0.5$ ,  $H_0 = 65$  km/s/Mpc)

Simultaneously to the Keck observations, astronomers of MPIA observed the record holder SDSS 1030+0524 in the near infrared, using the ISAAC camera at the VLT (Fig.

II.8). Moreover, they obtained spectra of both quasars, using ISAAC and FORS 2 also at the VLT (Fig. II.9).

The spectrum of SDSS 1030+0524 exhibits a dramatic effect: the Lyman- $\alpha$  emission line emitted by the quasar itself is redshifted on its way to us from the UV region into the infrared region and lies at a wavelength of  $\lambda = 885$  nanometers. Normally, it is joined towards the shorter wavelengths by continuum emission. In the spectrum on hand, however, the continuum between  $\lambda = 845$  and  $871$  nm is no longer detectable. It is reduced to at most 0.5 % of its original value. In the second quasar with  $z = 5.99$  the flux is only reduced to 7 % and in a third quasar with  $z =$

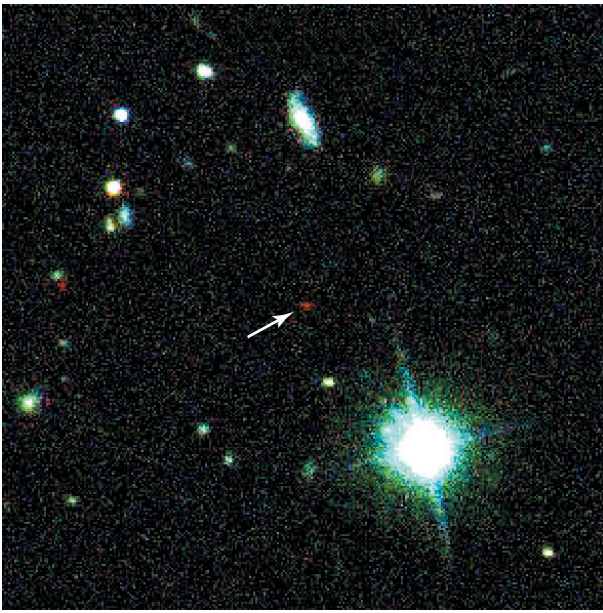


**Fig. II.8:** The most distant quasar (arrow) appears as a faint, unusually red object on the discovery image. (SDSS)

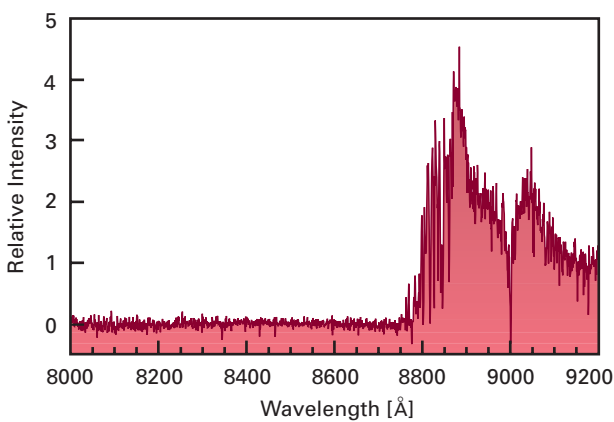


**Fig. II.9:** Spectrum of the new distance record holder SDSS 1030+0524. In the region between  $\lambda = 845$  nm and  $871$  nm, the continuum is no longer detectable.

5.8, also discovered with the SDSS, it is only diminished to 9 %.

The disappearance of the continuum is caused by absorption of radiation by the neutral intergalactic gas, which is located in a redshift range between about  $z = 6.0$  and  $z = 6.3$ . Thus, the new observations show that the re-ionization was not yet completed at the time at which we see the quasar at  $z = 6.28$ . In quasars with smaller redshifts, the continuum emission slowly increases, as the Universe is gradually re-ionized by stars and quasars.

From the observational data of the most distant quasar and some other quasars, first cautious conclusions about the conditions during the re-ionization era can be drawn. First, the spectrum of SDSS 1030+0524 shows that the emission towards the “blue” side of the Lyman- $\alpha$  emission is not completely absorbed. This is caused by the fact that the quasar is ionizing the surrounding gas to a high degree and so prevents absorption by neutral gas. This is called the “proximity effect”. Matter lying immediately in front of the quasar is less redshifted and therefore absorbs at shorter wavelengths. From the spectrum, the radius of the ionized surrounding is estimated to be about 15 million light years. Assuming that the entire gas had been neutral before the quasar started to shine, the luminous period of the quasar is given by the time, in which the light took to cross this volume of space, namely 15 million years.

From the existing spectroscopic data of the most distant quasars known up to now, the degree of suppression of the Lyman continuum can be obtained as a function of redshift. The result shown in Fig. II.10 matches qualitatively the expected one. Absorption of the Lyman- $\alpha$  emission of the quasars increases with increasing redshift (Fig. II.10, above). Above  $z = 6$ , the medium gets virtually opaque, that is, it is neutral. The lower part of Fig. II.10 shows the corresponding optical depth as a function of increasing redshift.

These new observations demonstrate that very distant quasars can be used to “probe” the genuine primordial medium and indicate how soon after the Big Bang the first quasars formed. The centers of these objects contain black holes of typically several hundred million solar masses. How these formed is still largely a mystery.

“Classically”, a black hole forms when a massive star explodes at the end of its life, blowing off its outer layers while the central core collapses into a black hole. Such a stellar black hole, however, only has about ten solar masses. In order to grow to the size of a quasar core, it has to accrete a great deal of material from its surroundings. Therefore it would be very interesting if the evolution of quasars themselves as a function of redshift could be determined.

Up to now, the analysis is based on data of only a few quasars. But astronomers estimate they may detect about 20 more quasars of redshifts between  $z = 6.0$  and  $6.6$  in the course of SDSS. These new quasars will offer the opportunity to study in detail the intergalactic medium during the recombination phase of the early Universe.

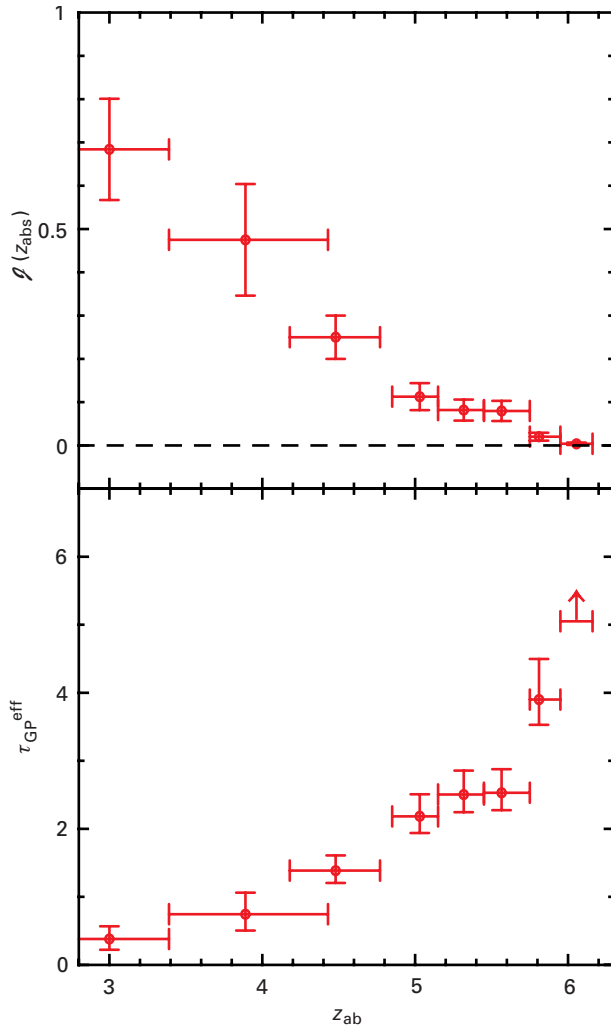


**Fig. II.10:** Evolution of the Lyman- $\alpha$  emission as a function of  $z$ . **Above:** Ratio of the observed and the theoretically possible unabsorbed Lyman- $\alpha$  emission. **Below:** Optical depth of the Lyman- $\alpha$  photons. (Fan et al.)

Thereby, temporal evolutions as well as the expected spatial inhomogeneities will be investigated.

With even more distant quasars, however, SDSS reaches its limit. At redshifts beyond  $z > 6.6$ , the Lyman- $\alpha$  emission is shifted into the near infrared, which is outside the sensitivity range of this survey. In this region, infrared surveys like the planned PRIME mission could accomplish the task. MPIA is also participating in the preparation of this mission (see Chapter III).

### The Sloan Digital Sky Survey (SDSS)

The Sloan Digital Sky Survey (SDSS), started in April 2000, is the most extensive digital sky survey so far. For this purpose, a 2.5 m telescope equipped with a mosaic CCD camera was built on Apache Point, New Mexico. The project is conducted by a consortium of US-American, Japanese and German institutes. In Germany, MPIA and MPI für Astrophysik in Garching are involved. The survey will image half the Northern sky in numerous color bands while particularly interesting and peculiar objects are studied spectroscopically.

The final catalogue of all recorded objects will provide positions and colors of more than one hundred million celestial bodies. Many unusual objects have already been identified by their colors. In all, redshifts of about one million galaxies and 100 000 quasars will be measured. More than 13 000 quasars have been found already, among them 26 of the 30 known most distant quasars and the record holders described above.

SDSS data will allow one to determine the spatial distribution of galaxies and quasars in a volume one hundred times as large as before. From that, far-reaching conclusions about the early evolution of galaxies and quasars as well as about the structure of our Milky Way system will be drawn.

*(Laura Penterecci, Hans-Walter Rix)*

## II.3 COMBO-17 Reveals Dark Matter in Galaxy Clusters

**The major fraction of the total matter in the Universe is invisible. So far, neither the nature nor the spatial distribution of this dark matter is known. Astronomers at MPIA, in collaboration with colleagues in Great Britain, have mapped the spatial distribution of dark matter in galaxy superclusters. This was done using the Wide Field Imager at the 2.2 m telescope on La Silla which had been built by astronomers at the Institute and colleagues from ESO.**

Instruments with high light-gathering power and large fields of view are of increasing importance for many astronomical studies. Presently, several sky surveys are conducted all over the world in order to reveal the evolution of galaxies across a redshift range as broad as possible, *i.e.*, to distances as far as possible. Scientists at MPIA have initiated such a project and conducted it together with colleagues at the University of Bonn and at the Institute for Astronomy in Edinburgh. The name of the survey, COMBO-17 (Classifying Objects by Medium-Band Observations with 17 Filters) indicates that galaxy magnitudes are measured in 17 color ranges using images taken through as many filters.

These observations are not only useful for problems of galaxy evolution but also for other questions, like the distribution of dark matter in galaxy clusters.

---

### The Strategy of COMBO-17

The key requirement for the project is the large field of view of the wide field camera (Wide Field Imager, WFI, cf. Annual Report 1998, p. 33) at the MPG/ESO 2.2 m telescope on La Silla. It has a field of view of  $32 \times 32$  square arc minutes - a little more than the size of the full moon. The CCD array consisting of eight individual chips with  $2046 \times 4096$  pixels each is sensitive over a wide spectral range, from UV ( $\lambda = 350$  nm) to the near infrared ( $\lambda = 950$  nm).

In the course of COMBO-17, a total of five widely separated fields on the sky are imaged through 17 filters, including five broad-band filters (standard ranges U, B, V, R, I) and 12 medium-band filters (relative width about 3%). Sophisticated software allows one first to distinguish the pointlike stars and quasars from the extended galaxies in the images. Due to the different colors, the remaining objects can be classified very precisely. For stars, spectral types A to M8, for galaxies, classes E (elliptical) to Sc (spiral galaxy with high star formation rate) as well as star burst galaxies with unusually high star formation rates can be identified. Moreover, for each galaxy down to an R-magnitude of 24 mag, a redshift can be determined,

with an uncertainty varying according to magnitude and type between  $\Delta z = 0.005$  and  $\Delta z = 0.1$ . Quasars, too, are identified and their redshifts measured with an accuracy better than  $\Delta z = 0.1$ .

At the end of the COMBO-17 survey, a field of sky of at least one square degree will be searched completely for stars, galaxies and quasars. For comparison: Both HUBBLE Deep Fields, the deep images in the northern and southern sky taken by the HUBBLE Space Telescope, cover only one hundredth of the field of view of the WFI. Thus, COMBO-17 will be able to provide comparatively secure information on the evolution of galaxies because a significantly larger and therefore more representative volume of space is included. COMBO-17 will determine redshifts and spectral energy distributions of a total of 50 000 galaxies brighter than 24 mag.

---

### Weak Gravitational Lensing due to the Supercluster Abell 901/902

While the galaxy evolution data analysis is still in progress, astronomers could already use some images to study the field around the supercluster Abell 901/902 (Fig. II.11). This region was chosen deliberately for COMBO-17 because it contains at least three rich clusters of galaxies with almost identical redshifts. In this area, astronomers plan to investigate to what extent the galaxy distribution in the Universe matches the mass distribution, as it is suspected for some time that the distribution of dark matter does not correspond exactly to the distribution of visible matter in the form of stars and galaxies. Early studies, however, had yielded only vague and rather contradictory results.

The supercluster Abell 901/902 is suited excellently for COMBO-17. With a diameter of about 30 arc minutes, it fits perfectly into the WFI's field of view. At a redshift of  $z = 0.16$ , this field corresponds to a diameter of about 17 million light years at the location of the cluster. The field was exposed for 80 to 300 minutes through the medium-band filters, the total exposures being the sums of 10 to 20 shorter exposures. In addition to the multi-color images, an extremely deep image in the red spectral range was taken of the field when the seeing was better than 0.7 arc seconds with a total exposure time of 6.5 hours. Thus, a limiting magnitude of 26 mag was reached for point sources. This image (Fig. II.12b) is perfectly suited to identify and classify galaxies with redshifts around  $z = 0.3$  as extended objects.

This extremely sharp image is essential for the mapping of the dark matter, a method working on the following principle. Space is bent by the gravitational field of



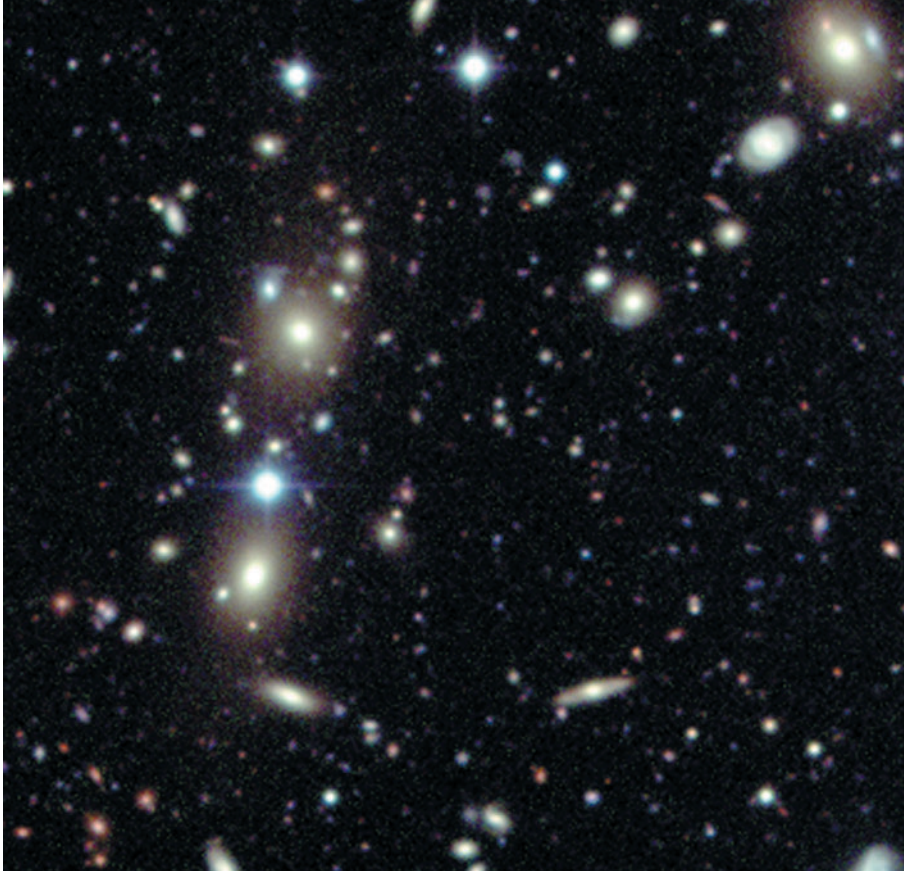
**Fig. II.11:** This field (of about the size of the full moon) contains the galaxy clusters Abell 901 and 902 and has been imaged by the WFI. It is a composite image, taken through a blue, a visual and a red filter.

any kind of matter. So if, for instance, light of a distant galaxy is falling through the gravitational field of a cluster of galaxies, it is bent in a similar way as in an optical lens. Observed from Earth, this lensing effect has different consequences: The observed position of the galaxy is shifted against its real position, the galaxy image appears magnified in brightness and its shape is distorted. This latter distortion is used in the so-called weak lensing effect: Usually, spiral galaxies appear – seen edge-on – as elongated images with random orientation of their axis of symmetry or – seen from above – as circular disks. But if a cluster in the foreground acts as a gravitational lens, the images of the galaxies in the background of the cluster are slightly stretched tangentially to the gravitational centers.

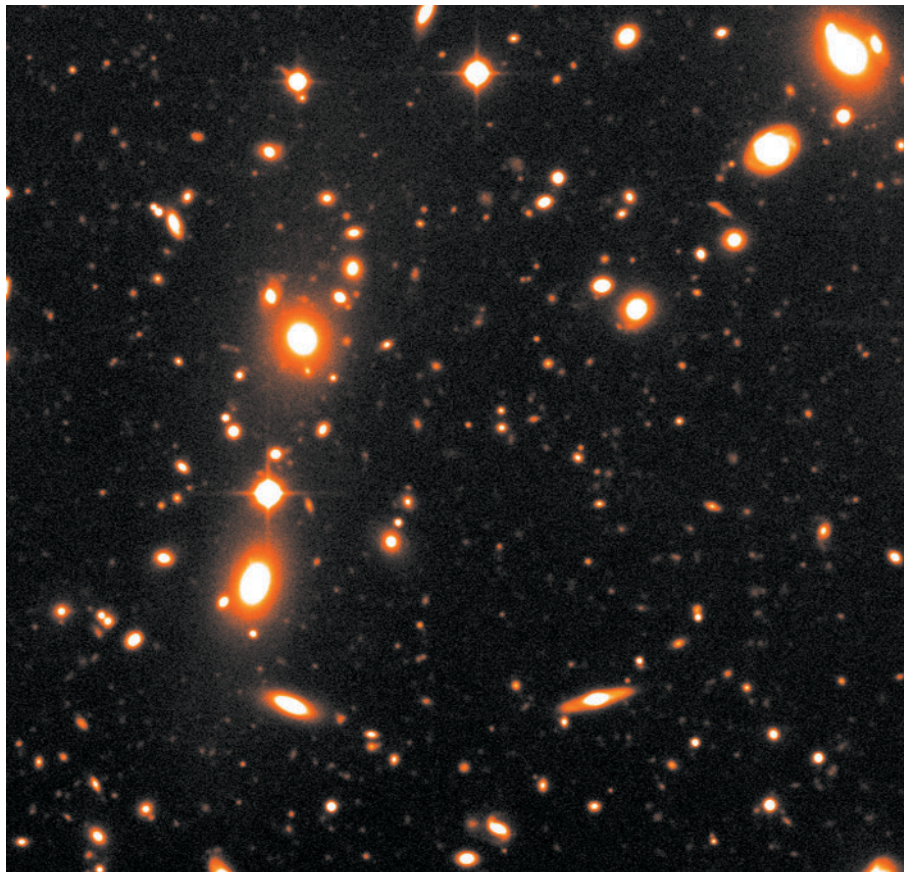
From an observed non-random orientation of the galaxy images, the spatial distribution and the amount of matter within the lensing cluster can be inferred directly using sophisticated mathematical procedures (Fig. II.13 and II.14.) A problem with this method, however, is the extremely small effect: the average elongation is only a few tenths of an arc second. These tiny distortions are not detectable in individual galaxies but only as a general statistical trend.

Two images were sufficient for the simplest studies of galaxy distortion: the high-resolution red image for analyzing the distortion of the structure and the blue image to distinguish galaxy populations lying before or behind the Abell clusters.

The final purpose of COMBO-17 is not only to apply this simple method, which has been proofed successfully on other clusters, but to use in addition the exact knowledge of the distances (redshifts) of the background galaxies. This way, the mass of the clusters can be determined directly without additional assumptions.



**Fig. II.12:** Central region of the galaxy cluster Abell 902; **a)** detail from Fig. II.11; **b)** high-resolution red image of the same field at a seeing of 0.7 arc seconds.



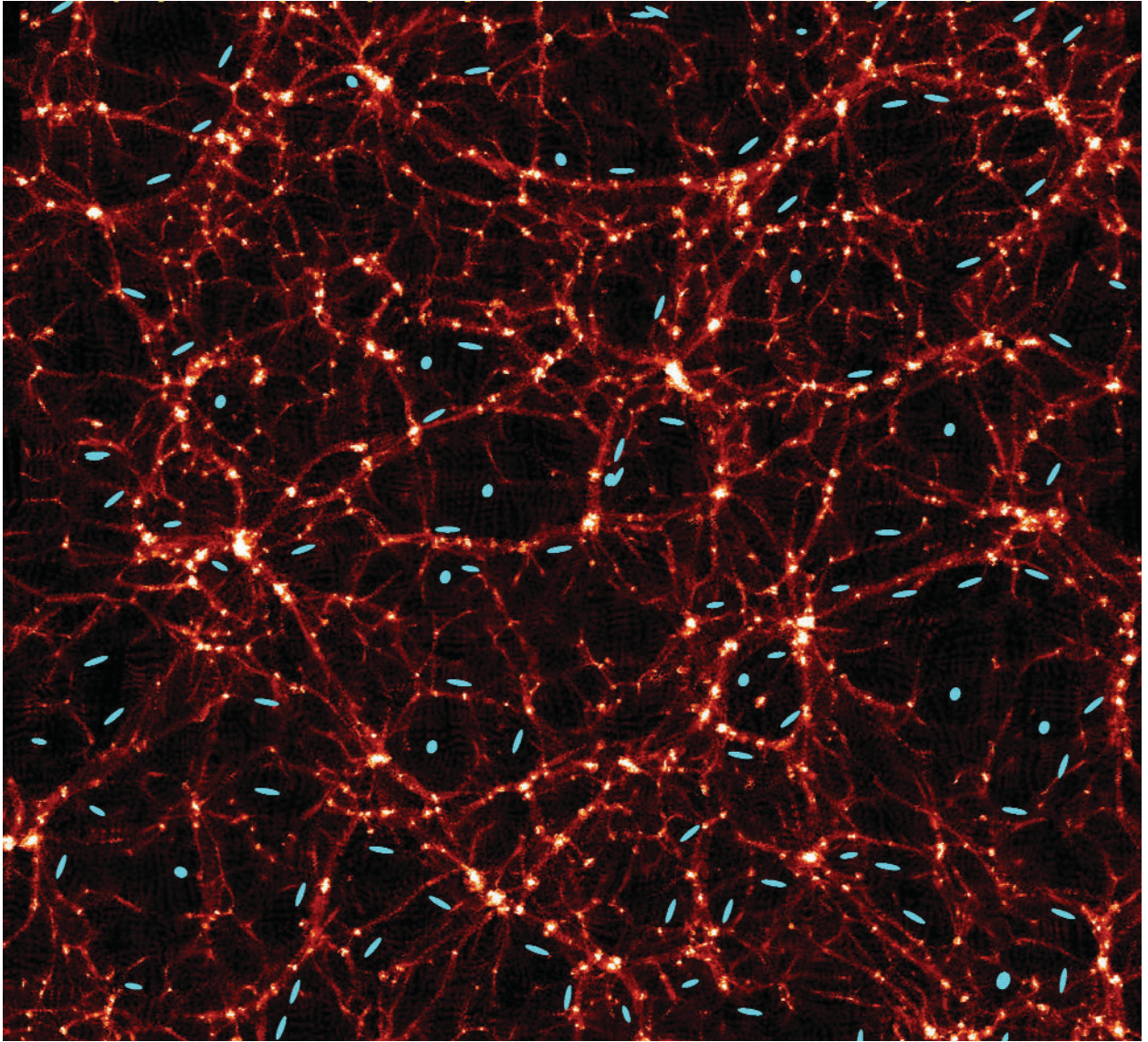


**Fig. II.13:** Schematic illustration of the weak gravitational lensing effect. The computer simulation shows a branching net of galaxy clusters. Their gravity causes the galaxy images (blue) to be orientated tangentially to the centers of the clusters. (MPA)

#### Dark Matter within the Abell Clusters

Earlier studies had already shown that the supercluster Abell 901/902 comprises three sub-clusters, Abell 901a, 901b and 902, which have very different properties. Abell 901a appears to be an undisturbed, relaxed cluster dominated by a central massive elliptical galaxy. Abell 901b also contains an elliptical galaxy at its center, but appears more irregular in shape. Abell 902 is the most irregular of the three, although here two elliptical galaxies define the optical center, too.

A total of about 40 000 galaxy images were used for the morphological analysis. Assuming simply that all background galaxies are at a fixed distance of about  $z = 1$

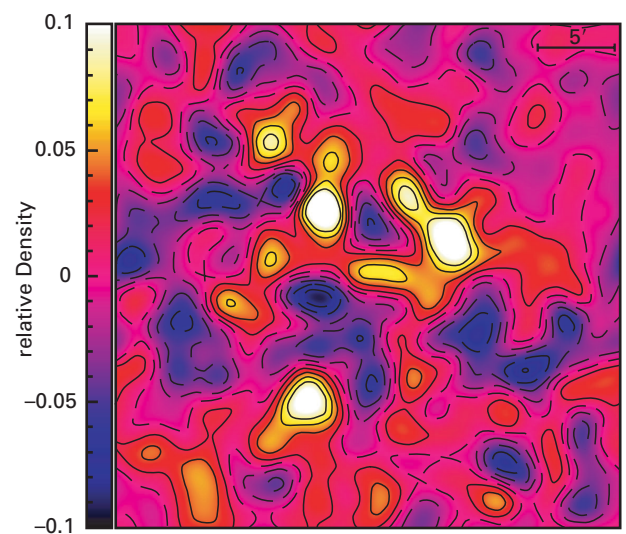


**Fig. II.14:** Reconstruction of the total mass within the observed field. In addition to the three galaxy clusters, a faint bridge of matter connecting Abell 901a and 901b is indicated.

and that the clusters can be described as spherical mass distributions of constant temperature, the total mass can be calculated. It turns out to be about 1014 solar masses for each of the three clusters.

The power of the new method of weak gravitational lensing is mainly given by the fact that it can be used to trace the *distribution* of the dark matter. The map derived from existing data shows several interesting details in comparison with the brightness distribution of the galaxies (corresponding to the visible matter) (Fig. II.15).

On first sight, the galaxies especially in Abell 901a and Abell 902 seem to trace relatively well the distribution of the total matter within the achieved spatial resolution. As mentioned above, Abell 901a is the most symmetric of the three clusters of galaxies.

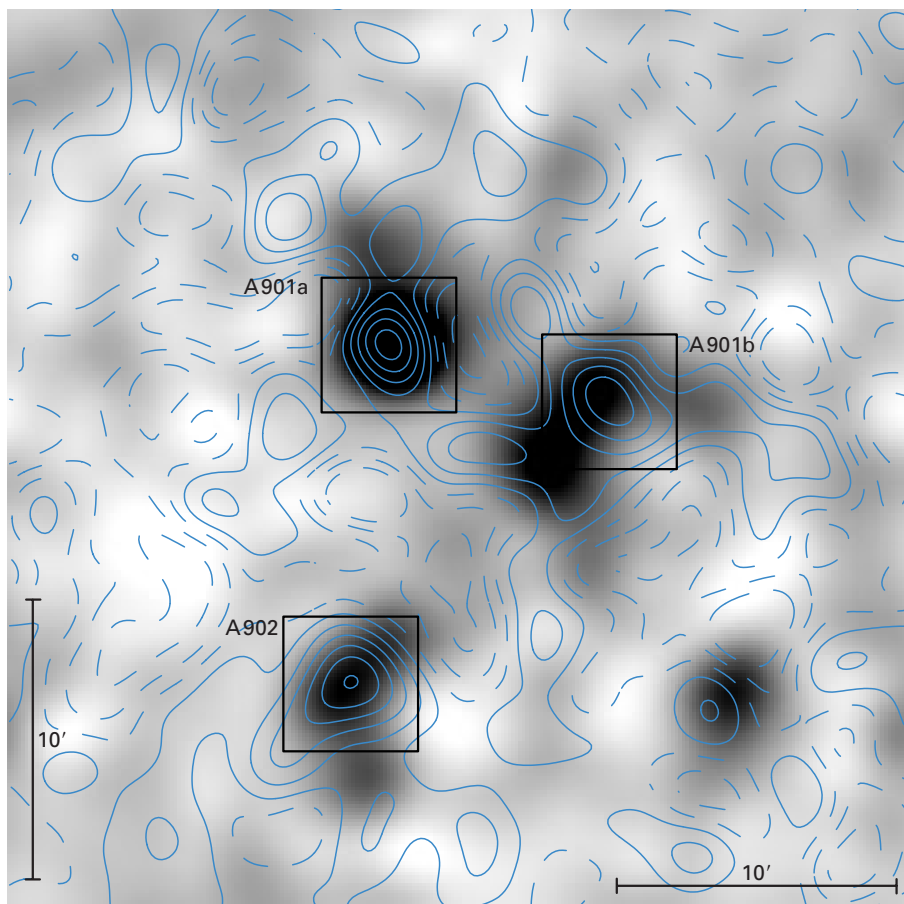
Abell 901b, however, presents a different picture. Here, the dark matter appears to be dislocated to the west with respect to the optical center. Moreover, there is evidence of dark matter connecting Abell 901a and its neighboring cluster Abell 901b. In the optical images a faint bridge of matter is indicated in this location, too. Furthermore, it appears that the gravitating dark matter in Abell 901b is distributed more regularly and symmetrically while the galaxies occupy an elongated region.

These results suggest that dark matter is not always aligned with the galaxy distribution – a fact which is also reflected in the so-called mass/luminosity ratio. This cos-

mologically very important parameter is defined as follows: From the apparent magnitude and distance of a given galaxy, the total luminosity  $L$  of its luminous matter (stars and gas) can be determined, measured in units of solar luminosity. This value can be related to the total mass  $M$  (measured in solar mass units), which makes itself conspicuous only by gravitational effects.

A typical value of  $M/L = 10$  is found for elliptical galaxies. The  $M/L$  values derived in this study, however, show a considerable variance between the three clusters as well as within each cluster, lying in a range from  $M/L = 100$  to  $M/L = 800$  (Fig. II.16). When integrated over the entire cluster (at a radius of 6 arc minutes), the value converges to  $M/L = 200$ . Thus, the cluster contains, on average, several tens as much dark matter as luminous matter. The scatter of the measured  $M/L$  ratios is another indication that the dark matter density is not proportional to the density of the luminous matter. In addition, the constancy of the values at  $M/L = 200$  at large radii suggests that the dark matter does not extend significantly beyond the distribution of the galaxies.

**Fig. II.15:** Comparison of the luminosity distribution of the galaxies and the dark matter distribution (contour lines). (Gray et al.)



The  $M/L$  ratio is of great importance for different cosmological aspects. For one thing, it is suspected that its value in galaxy superclusters is representative for the Universe as a whole, making it possible to determine the mean matter density of the Universe, a crucial parameter for the evolution of the Universe.

But  $M/L$  is also of special interest for theories of galaxy formation. The currently most favored theory of galaxy formation assumes that hydrogen gas accumulated mainly near the largest concentrations of dark matter, greatly enhancing the efficiency of galaxy formation in these regions. Accordingly, one would expect the  $M/L$  ratio to increase in the outer reaches of a great mass concentration like Abell 901/902. The observations described above clearly question this idea.

However, this analysis is based - like its predecessors - on the greatly simplifying assumption that the gravitational lens (the supercluster) can be described as a relatively thin distribution of matter at  $z = 0.167$ , while all background galaxies are assumed to be at  $z = 1$ , which is certainly unrealistic. Actually, COMBO-17 was able to detect another rich galaxy cluster behind Abell 901/902 at  $z = 0.43$ . Moreover, there also seems to be an enhanced galaxy concentration at even larger redshifts around  $z = 1$ . To be exact, the gravitational lensing effect therefore has to be considered as a superposition of at least three lenses lying one behind the other.

As the multi-color method of COMBO-17 yields reliable redshifts for all galaxies down to  $R = 24$  mag, unimagined possibilities open up to take into account the exact spatial distributions of mass concentrations responsible for gravitational lensing. The real distance-dependent mass distribution of Abell 901/902 will only be deciphered by this completely novel analysis. And from this distribution one can then derive reliable values of the  $M/L$  ratio.

At present, COMBO-17 is the globally unique attempt to perform a three-dimensional gravitational lens analysis. It is expected to provide new insights into the question of the universal  $M/L$  ratio or how mass concentrations of dark matter have aided galaxy formation.

(Christian Wolf, Klaus Meisenheimer, A. Borch,  
S. Phleps, H.-W. Rix, H.-J. Röser)

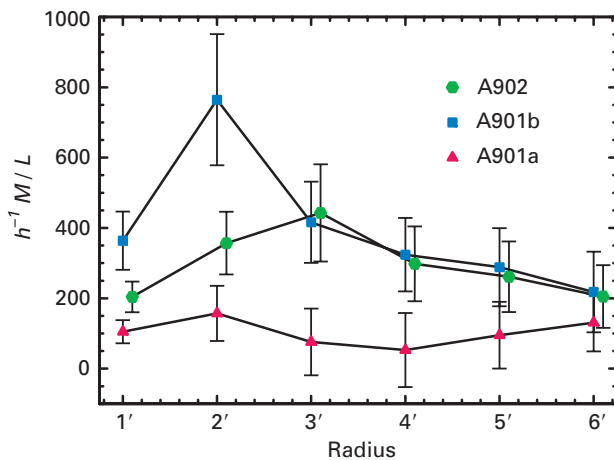


**Fig. II.16:**  $M/L$  ratios within the three clusters as a function of distance to the central galaxy. (Gray et al.)

### III Instrumental Development

**The performance of a telescope depends critically on the quality and efficiency of the instruments mounted in the focal plane. During recent years, a series of scientific instruments has been developed and built at the MPIA to significantly increase the telescopes' efficiency and broaden their range of application. Currently, several instruments are under construction at the Institute, which will be used at ground-based observatories as well as in space telescopes. These high-tech devices will contribute significantly to progress in astronomy.**

The instruments are built in the workshops at MPIA, often in cooperation with small and large companies. The requirements set by the scientists keep presenting these firms with new challenges, the know-how gained in this way strengthening their competitive capacity on the global market.

Here is a summary of the MPIA's recent instruments and of their actual status in the year under report.

#### Adaptive Optics

In theory, the angular resolving power of a telescope, *i.e.*, its capability to produce separate images of two objects lying close together on the sky, increases with the diameter of the primary mirror. Practically, however, the turbulence of the atmosphere blurs longer-exposure images to such a degree that the resolution is only one half to one arc second at its best, independent of the mirror size.

In recent years, astronomers and engineers at the MPIA, together with colleagues at the MPI für extraterrestrische Physik (MPE) in Garching, have built an adaptive optics system for the near-infrared wavelength range for the Calar Alto Observatory. This system, called ALFA, corrects image fluctuations during the exposure (cf. Annual Report 2000, p. 31). In this way, the theoretically possible resolution, that is the diffraction limit, can be achieved.

On Calar Alto, it was shown that ALFA can be operated using an artificial laser guide star. This is created by a laser beam shot parallel to the telescope's optical axis toward the sky. At an altitude of about 90 kilometers, the beam excites atmospheric sodium atoms, which start to glow. The spot of light created in this way serves as a reference star for the adaptive optics system. The experiences gained with this instrument are very useful in building similar systems for the ESO Very Large Telescope and the Large Binocular Telescope.

The VLT 8 m telescope YEPUN will be the first to be equipped with a laser-guide-star device. Here, a sodium laser, named PARSEC, will produce a continuous beam with a power of 10 to 15 watts (Fig. III.1). This instrument is being developed in collaboration with researchers at MPIA and MPE. The MPIA is contributing a so-called LIDAR (Light Detecting and Ranging) – a pulsed laser,

**Fig. III.1:** The prototype of PARSEC mounted in the MPE laboratory: The main laser is to be seen in the rear left, the amplifier in front. (Picture: MPE)



which can be used to measure the altitude of the atmospheric sodium layer and the concentration of sodium atoms there.

Experience acquired with ESO has been incorporated into the development of LIDAR. It turns out that a laser guide star can only be used efficiently if the atmospheric conditions are known in detail. In 2000, experiments with LIDAR at the 3.5 m telescope on Calar Alto were successful, so it was decided to build a similar device for PARSEC.

The construction of LIDAR recently started. Acceptance by ESO is planned for May 2003, so that in October of the same year, PARSEC can be put into operation. In the beginning, PARSEC will be used together with NAOS/CONICA (Chapter II.1). In 2004, SINFONI, the second focal instrument on YEPUN, will presumably be put into operation and will also use the laser guide star.

For the LBT, another instrument is being tested currently – a SCIDAR (Scintillation Detection and Ranging), which helps optimize the adaptive optics system of the LBT. Adaptive optics systems on large telescopes can only partially compensate image distortions due to atmos-

pheric turbulences. This mostly affects objects outside the central correction axis of the adaptive optics. The strength of this so-called anisoplanasy effect depends mainly on the vertical structure of the atmospheric turbulence. If there are several bright stars in the field of view during an exposure with adaptive optics, the strength of the effect can be estimated to yield good photometric and astrometric measurements. Unfortunately, this is not always the case, and these estimates are highly uncertain. This is where SCIDAR will be put into action.

SCIDAR observes a binary star, producing a defocused image of it (actually it is an image in the pupil plane). Then the vertical structure of the atmospheric turbulence can be determined up to an altitude of about 20 km by measuring the intensities of the pupil images of both stars. While measurements of the phase distortions within the pupil cannot yield information on the vertical structure of the turbulence, the strength of the scintillation depends on the distance between a turbulence layer and the observational plane. Thus, the brightness distribution within the pupil contains information on the vertical distribution of the turbulence (Fig. III.2).

The SCIDAR hardware has been built at Steward Observatory while MPIA contributed the software for the data analysis. In the year under report, the instrument has been tested on the Vatican Advanced Technology Telescope. Afterwards, it will be operated on the LBT. If it is working satisfactorily, a similar device could be used at the VLT as a kind of “extended weather station”.

(S. Hippler, M. Feldt, M. Kasper,  
R.-R. Roloff, K. Wagner)

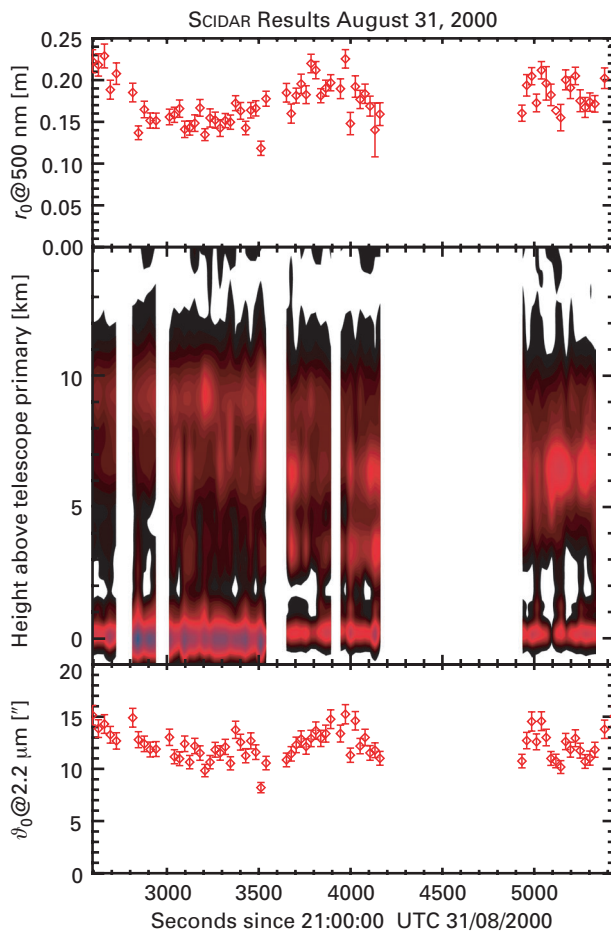


**Fig. III.2:** Characteristic results of SCIDAR measurements obtained at the Calar Alto Observatory. The values above and below indicate two important quantities of adaptive optics, the Fried parameter and the isoplanatic angle. In the middle, the turbulent structure of the atmosphere can be recognized.

### Multiconjugate Adaptive Optics (MCAO)

Adaptive optics systems always need a reference star of a certain minimum brightness. Furthermore, optimal correction is only possible within a certain angle around this star. Beyond this, the image becomes increasingly blurred. This limitation can be avoided by using so-called multiconjugate adaptive optics (MCAO).

To make this technique practicable for the first time, a special team was established at MPIA. On a long-term basis, a MCAO is to provide the LBT with diffraction-limited images in the combined focus – not only in the near infrared but also at wavelengths down to 800 nm. At an observing wavelength of 1  $\mu\text{m}$ , the diffraction limit of the LBT is 9 milli-arc seconds. The goal is to get such a diffraction-limited image over the entire field of view, which has a size of 1 arc minute.

With the classical adaptive optics, only one direction within the field of view is corrected. With MCAO, this technique is applied to several directions and reference stars, assuming the atmosphere to consist of only a few thin turbulent layers (Fig. III.3).

During the next three years, MCAO will be added to the LINC/NIRVANA instrument of the LBT (see below).

Light coming from one LBT mirror is divided by a beam splitter. One fraction travels to a wavefront sensor, which controls the adaptive secondary mirror of one of the LBT's primary mirrors. The fraction of the light, which passes the beam splitter is directed by two flexible mirrors with 349 actuators each and by several other mirrors to the focus. The light beam coming from the second LBT primary mirror is subjected to the same procedure. Wave trains in phase then interfere in the joint focus.

In this instrument, a total of six wavefront sensors as well as six adaptive mirrors with a total of 2740 actuators will be used – a unique concept so far, which will render the spatial resolution of ground-based telescopes almost independent of atmospheric influences over a large field of view. Moreover, the fact that the wavefront sensors have fields of view of one to two arc minutes facilitates the choice of reference stars of sufficient brightness for the adaptive optics. This is crucial for conducting as many scientific projects as possible with this instrument.

### LUCIFER and LINC – Two Instruments for the LBT

As mentioned in chapter I, MPIA, together with the MPI für extraterrestrische Physik in Garching, the MPI für Radioastronomie in Bonn, the Astrophysikalisches Institut Potsdam, and the Landessternwarte Heidelberg, will have a 25% share in costs and use of the Large Binocular Telescope (LBT), under the auspices of the "LBT Beteiligungsgesellschaft". Unlike all previously-built telescopes, the LBT will be equipped with two light-gathering mirrors, each having a diameter of 8.4 m. Commissioning of the telescope with the first mirror will take place in 2004. After the commissioning of the second mirror one year later, interferometry will also be possible.

Under the direction of the Landessternwarte Heidelberg, the German partners are building a pair of near-infrared spectrographs, called LUCIFER, for the LBT. MPIA will supply the entire detector package and develop the overall design of the cooling system. Integration and tests of the instrument will also be carried out in the laboratories of MPIA. Apart from MPIA and LSW, the MPI für extraterrestrische Physik, the Universität Bochum and the Fachhochschule für Technik und Gestaltung in Mannheim are involved in the LUCIFER project.

In 2004, the first LUCIFER unit will begin operations in the focal plane of the first mirror. The second instrument arrives 18 months later at the focus of the second mirror. With LUCIFER, both direct imaging and long-slit spectroscopy in the wavelength range between 0.85 and 2.45  $\mu\text{m}$  wavelength will be possible. In order to reduce thermal background radiation of the instrument, LUCIFER will be cooled to 77 K. A total of six observing modes are planned:

- Seeing-limited direct imaging with a field of view of 4',
- Long-slit spectroscopy with a slit length of 4',

- Multi-object spectroscopy,
- Diffraction-limited direct imaging with a field of view of 0.5',
- Long-slit spectroscopy,
- Integral field spectroscopy.

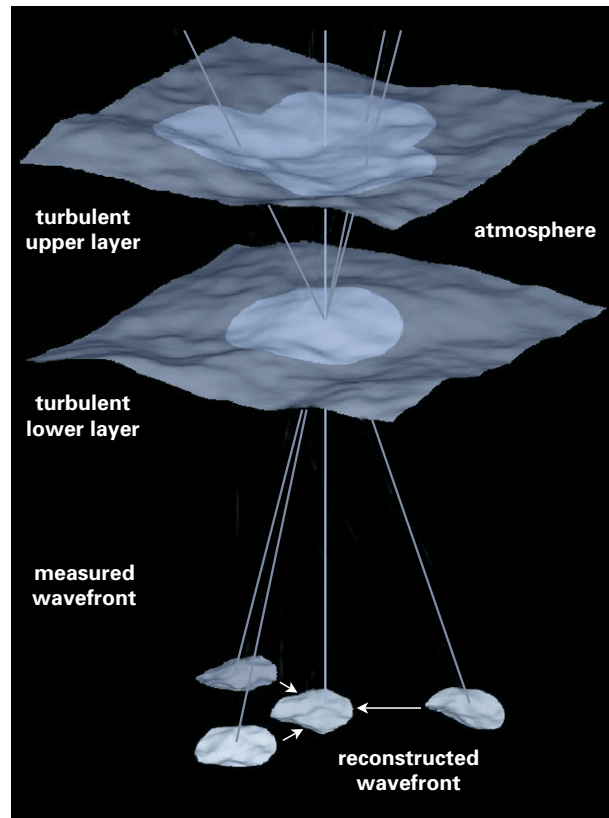


**Fig. III.3:** Disturbance of light rays coming from several directions in two atmospheric layers. From the measured wavefronts, the wavefront in the center, where the astronomical object is located, can be calculated.

For diffraction-limited imaging, the LBT yields spatial resolution of 0".031 at 1.23  $\mu\text{m}$ , 0".041 at 1.65  $\mu\text{m}$ , and 0".056 at 2.2  $\mu\text{m}$ . The cameras need to be exchanged in order to obtain the highest image quality for all seeing-limited imaging modes. Altogether three cameras are planned with respective resolutions of 0".015, 0".12, and 0".25 per pixel. The detector will be an infrared array with 2048  $\times$  2048 pixels.

LUCIFER will be used in the near infrared mainly for observing faint objects, including, for example, young galaxies at high redshifts. Astronomers also expect major progress in the spectroscopy of brown dwarfs, that is, very faint red stars. Dusty disks around young stars and in the cores of active galaxies are also given high priority.

The beam combiner is being designed and constructed at the MPIA, with the collaboration of the Osservatorio Astrofisico di Arcetri and the Universität Köln. A team at

the Institute, together with colleagues from Arcetri, is developing the adaptive optics system. A first Concept Design Review took place in November 2001, and the final concept should be completed by mid-2002.

One of the most ambitious instruments on the LBT will be the LINC Fizeau-interferometer, which coherently combines the light arriving from both primary mirrors (Fig. III.4), allowing unprecedented spatial resolution. Together with the enormous light-gathering power of both mirrors, this will make the LBT the most powerful telescope in the world. An instrument like this has never been built before and therefore requires an extremely demanding optical design. MPIA, forming a consortium with colleagues from the Universität Köln and Arcetri in Italy, is developing the optics of the beam combiner.

With LINC, interferometry at wavelengths between 0.6  $\mu\text{m}$  and 2.4  $\mu\text{m}$  will be possible. This entire range will be covered by two different detectors. For visible light, a CCD with pixel sizes of 9 to 12  $\mu\text{m}$  will be used. For the near infrared between 1  $\mu\text{m}$  and 2.4  $\mu\text{m}$ , an infrared array with 2048  $\times$  2048 pixels is foreseen.

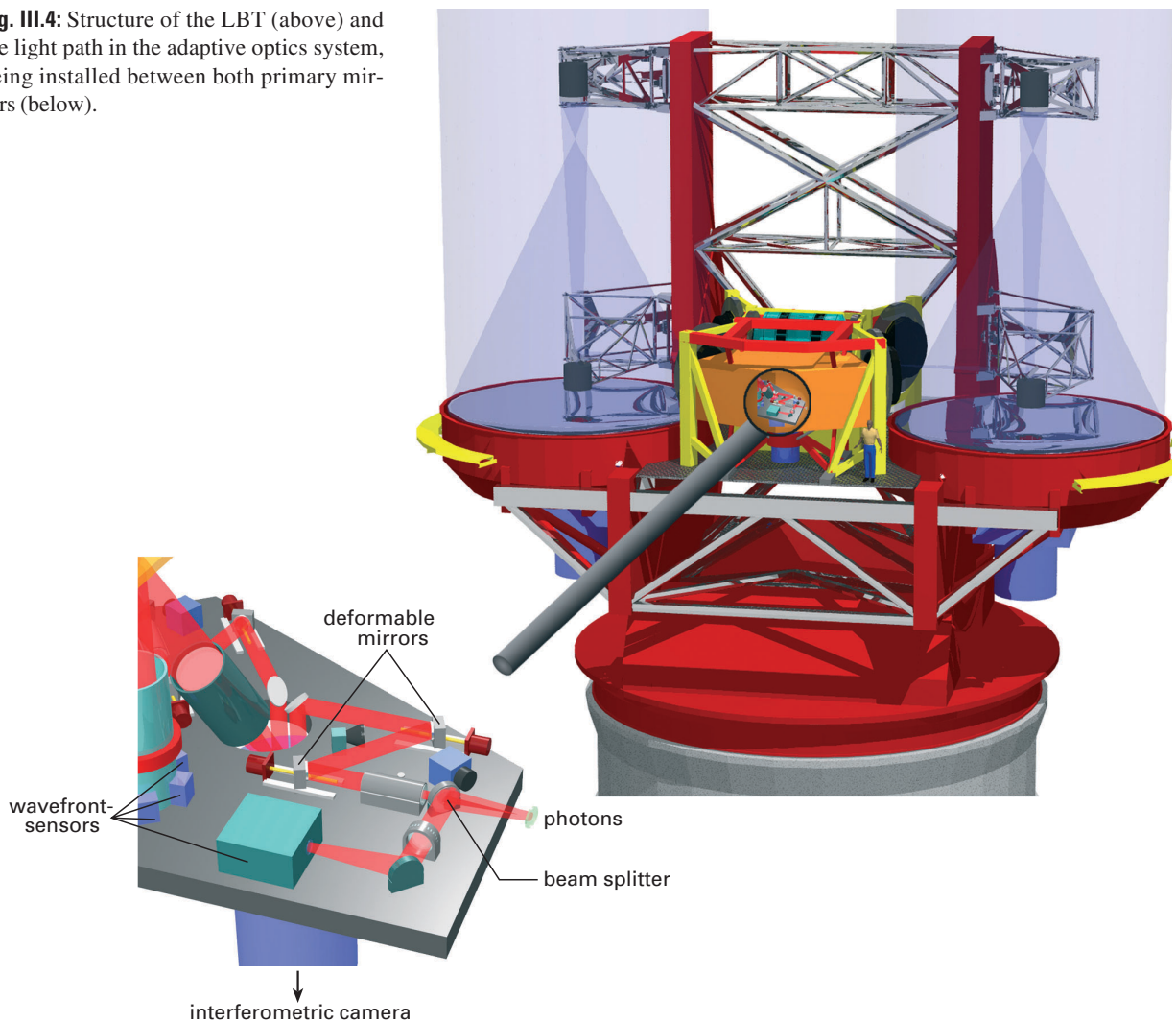
The interferometer will be operated together with an adaptive optics system which will correct, depending on the wavelength, a field of view between 20" (at 2  $\mu\text{m}$  wavelength) and 5" (at 0.7  $\mu\text{m}$ ). The ultimate resolution of LINC also depends on wavelength, lying between 0".02 (at 2  $\mu\text{m}$ ) and 0".006 (at 0.7  $\mu\text{m}$ ).

LINC will be developed in two stages. First, interferometry with only one natural guide star; in a second stage (NIRVANA), multiconjugate adaptive optics.

Astronomical observations will focus on compact objects, forming a long list ranging from the spatial extension of supernovae to the structure of protostellar disks to the search for extrasolar planets.

*(Tom Herbst, R. Lenzen, R. Ragazzoni, H.-W. Rix, R.-R. Rohloff, D. Andersen, H. Baumeister, P. Bizenberger, B. Grimm, W. Laun, Ch. Leinert)*

**Fig. III.4:** Structure of the LBT (above) and the light path in the adaptive optics system, being installed between both primary mirrors (below).



### OMEGA 2000 – a Wide Field Infrared Camera for Calar Alto

In future, essential science will continue to come from wide field surveys. This trend is increasingly taken into account by the Institute. First, a wide field camera for the 2.2 m telescope on La Silla was built in collaboration with ESO (cf. Annual Report 1998, p.33). In 2000, MPIA decided to build a new wide field infrared camera, named OMEGA 2000, for Calar Alto.

The development of new cameras depends critically on the availability of infrared detectors. Recently, arrays with  $2048 \times 2048$  pixels have become available. These are sensitive up to a wavelength of  $2.4 \mu\text{m}$ , and have a quantum efficiency of about 60 % between 0.8 and  $2.4 \mu\text{m}$ .

To keep Calar Alto at the forefront of infrared astronomy, MPIA decided to develop and build the new OMEGA 2000 camera for the near infrared. It will be similar to OMEGA -prime, but its field of view will be five times larger with a size of  $15' \times 15'$ , corresponding to a quarter of the size of the full moon. The instrument will be used at the prime focus of the 3.5 m telescope, where it will have an image scale of  $0''.45$  per pixel.

In the year under report, all important components were manufactured or delivered. First cooling tests have been passed successfully (Fig. III.5). Commissioning at the telescope is currently planned for early 2003. At that time, the new camera will replace the previous workhorse OMEGA-prime.

*(H.-J. Röser, C. Bailer-Jones, M. Alter, H. Baumeister, A. Böhm, B. Grimm, W. Laun, U. Mall, R.-R. Rohloff, C. Storz, K. Zimmermann)*

### LAICA – the Wide Field Camera for Calar Alto

As the third wide field instrument, the Large Area Imager for Calar Alto, LAICA for short, was built. It will work at the prime focus of the 3.5 m telescope, yielding an aberration-free field of 44 arc minutes (corresponding to 115 mm). In its focal plane, a mosaic of four CCDs is mounted, each having  $4096 \times 4096$  pixels. The image scale will be  $0''.225$  per pixel (cf. Annual Report 1999, p. 33).

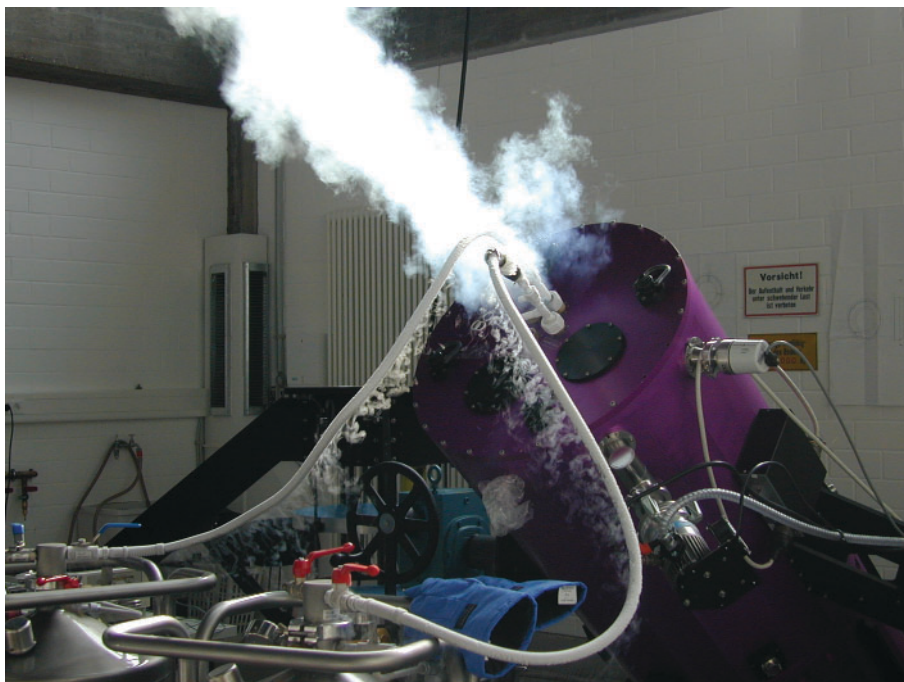
For production reasons, the CCDs cannot be joined without gaps. Therefore, a gap of about 50 mm width is left between them. It is therefore not possible to image a contiguous area of the sky in one shot. This can be accomplished without major effort by taking three more shots at different positions, thereby filling the gaps. A set of four images covers a contiguous field of one square degree, corresponding to about five times the area of the full moon.

In addition, two smaller CCDs are integrated into the focal plane for guiding purposes. With their help, image rotations, which may occur in longer exposures, can also be noted and corrected. In summer 2001, this guiding system was successfully tested at the telescope.

For the time being, two filter sets are planned. The filter mounting resembles the magazine of a slide projector, and contains 20 filters, which are taken out by a robot arm and placed in the light path.

Construction of LAICA started in early 1999. On 20 May 2001, it saw first light (Fig. III.6). However, further

**Fig. III.5:** OMEGA 2000: a) cooling tests in the laboratory



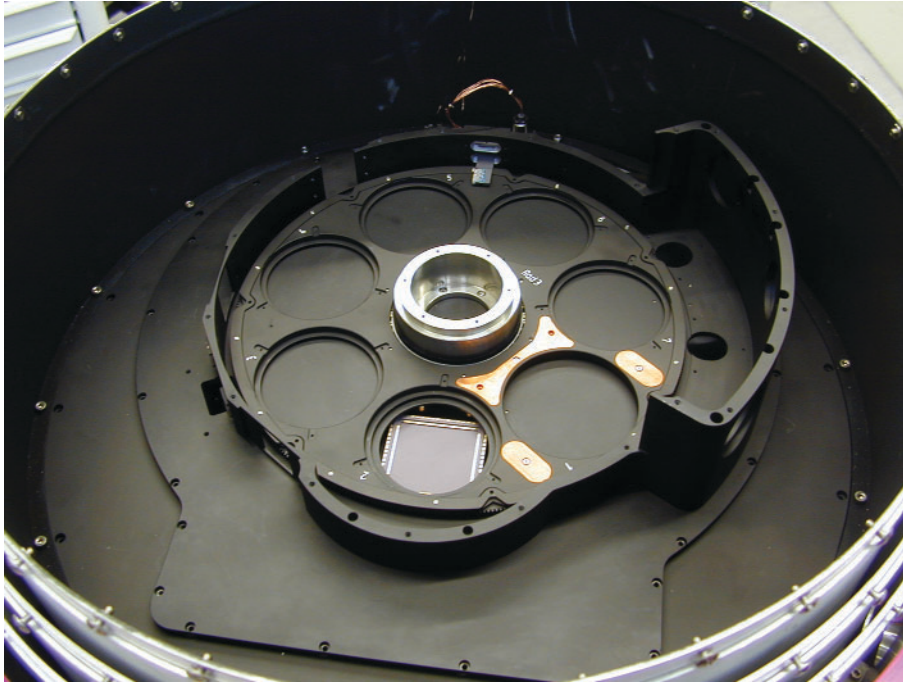


**Fig. III.5:** OMEGA 2000: **b)** view of the interior showing the filter wheel.

optimizations were needed to improve the image quality. In April 2002, Calar Alto was able to offer LAICA to guest observers on a “shared risk” basis, meaning that the observer has to be prepared for the camera not being available at short notice because of urgent tests. The Institute’s team expects the camera to start regular work at the telescope in 2002.

*(J. Fried, H. Baumeister, W. Benesch, F. Briegel, U. Graser, B. Grimm, K. Marien, R.-R. Rohloff, H. Unser, K. Zimmermann)*

#### **MIDI – an Infrared Interferometer for the VLT**

In the near future, the VLT will also operate as an interferometer. For this purpose, the light paths of two or more telescopes will be combined and coherently superimposed in a common image plane. An interferometer of this kind has the spatial resolution of a telescope with a mirror as wide as the separation of the interferometrically coupled telescopes. Two of the VLT telescopes, 130 m

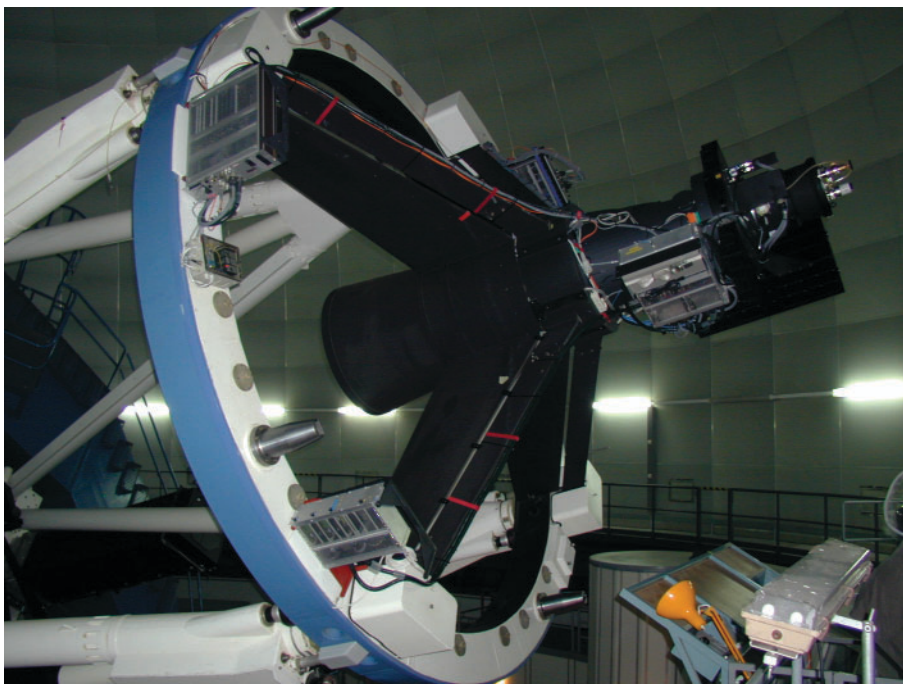


**Fig. III.6:** LAICA on the front ring of the 3.5m telescope on Calar Alto.

apart, will achieve a resolution of a few thousandths of an arc second in the near-infrared range.

One of the three VLT interferometric instruments, named MIDI, is being developed and built under the leadership of MPIA. Also involved are colleagues from the Netherlands and France, as well as from the Kiepenheuer-Institut in Freiburg and the Thüringer Landessternwarte Tautenburg. MIDI is intended to allow interferometry with two telescopes at wavelengths between  $8\ \mu\text{m}$  and  $13\ \mu\text{m}$ , signifying a huge step forward in astrophysical research as far as spatial resolution is concerned. MIDI is expected to achieve a resolution of about  $0''.002$  within a field about  $2''$  across. The detector consists of an array with  $320 \times 240$  pixels, each pixel having a size of  $50\ \mu\text{m}$ . Observations in different wavelength ranges are made possible by ten filters.

Interferometry at these wavelengths puts heavy demands on the technology. Two problems are of central importance: Light waves arriving from both telescopes must be combined in the instrument with a phase coincidence as precise as about  $1\ \mu\text{m}$ . In order to suppress thermal background radiation, large parts of the instrument have

to be cooled. The detector will be the coldest part with a temperature of 4 to 8 K. The cold section of the optics will be around 40 K, while the outer radiation shielding for the cooling system will be at 77 K.

The difference in path lengths of the light beams arriving from the two telescopes is mainly geometric, and will already have been compensated for the most part, before the beams enter the instrument. In addition, the path difference changes during the observation due to the rotation of the celestial sphere. This problem is resolved by an optical system moving on a cart in a tunnel below the telescope (a so-called delay line). The light beams arriving from the telescopes are reflected by this system and their different path lengths are compensated by shifting the cart. Inside MIDI, the residual difference in path lengths is compensated by means of movable piezo-electrically driven mirrors. A beam splitter combines the beams to create the interference image.

In March 2001, the final design review for the optics, mechanics and electronics was formally declared complete by ESO, and in November, the same took place for the software. Simultaneously, construction and testing of the

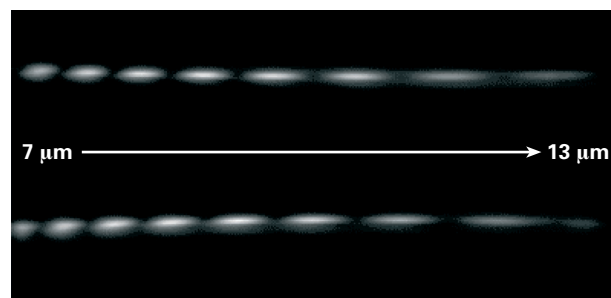
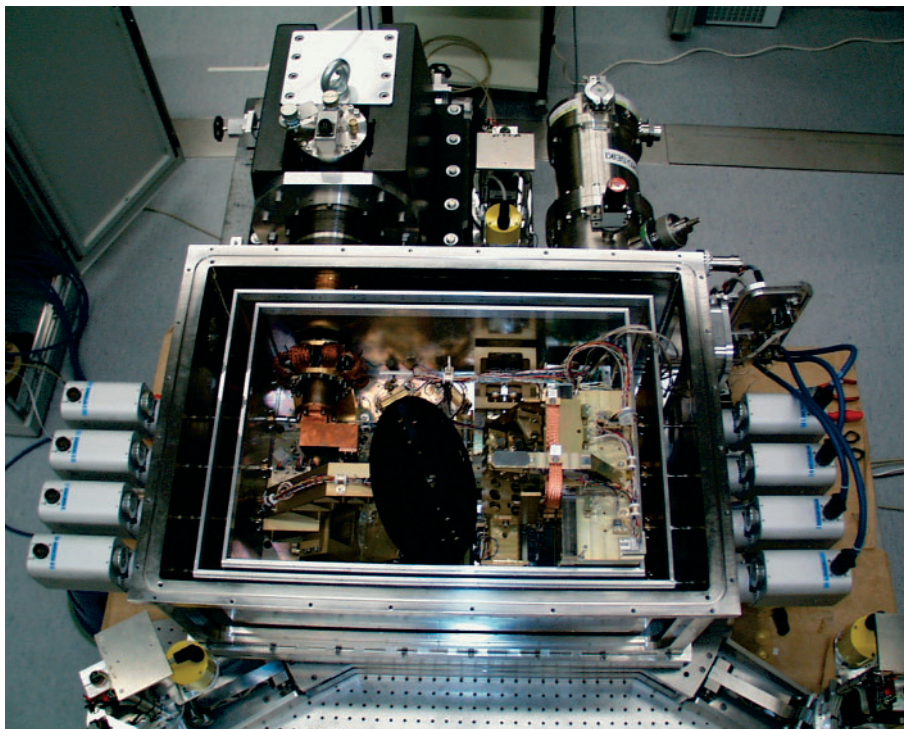


**Fig. III.7:** **a)** View of the interior of MIDI. The inner part of the optics is cooled by means of a closed cycle cooler (rear left at the instrument). Of the optical components, the filter wheel (black) is the most noticeable. **b)** Result of tests using a laboratory light source: interference pattern for wavelengths of  $7\ \mu\text{m}$  (left) to  $13\ \mu\text{m}$  (right).

instrument proceeded in the laboratory in Heidelberg (Fig. III.7a). In May, the partner institute ASTRON in Dwingeloo delivered the central piece of the device, the “cooled optics”. This component had to be adjusted optically and gradually fine-tuned with the mechanics. By the end of the year, first interferometric measurements could be made using an artificial star set up in the laboratory (Fig. III.7b).

MIDI will arrive in Chile in October 2002. First light at the 8 m telescopes is expected in 2002. Later, experiments at the 1.8 m auxiliary telescopes will follow. If all proceeds according to plans, MIDI will be put into regular operation at the end of 2003.

The team will be granted a total of 30 observing nights on the VLT, distributed over several years, and about three times as many nights at the auxiliary telescope. MIDI will focus on active galactic nuclei (black holes), young stars, extrasolar planets, circumstellar dust envelopes, protostellar and protoplanetary disks as well as binary stars.

*(Ch. Leinert, U. Graser, A. Böhm, O. Chesneau, B. Grimm, T. Herbst, W. Laun, R. Lenzen, S. Ligori, R. Mathar, K. Meisenheimer, U. Neumann, E. Pitz, F. Przygodda, R.-R. Rohloff, P. Schuller, C. Storz, K. Wagner, W. Morr)*

---

### **PACS – the Infrared Camera for HERSCHEL (formerly FIRST)**

In 2007, the European Space Agency (ESA) plans to launch the HERSCHEL far-infrared telescope (formerly called Far-Infrared and Submillimeter Space Telescope, FIRST) as its fourth major “cornerstone” mission. HERSCHEL will be provided with a passively cooled 3.5 m mirror and three scientific instruments covering the wavelength range from 60  $\mu\text{m}$  to 700  $\mu\text{m}$ . These are being built by international science consortia. One central issue of the research program will be the observation of protostellar dust clouds and protoplanetary disks. The far-infrared and submillimeter emission of very distant young galaxies will also be detectable. MPIA is participating in the construction of one of the instruments, named PACS (Photoconductor Array Camera and Spectrometer). The PACS project is conducted under the leadership of MPE.

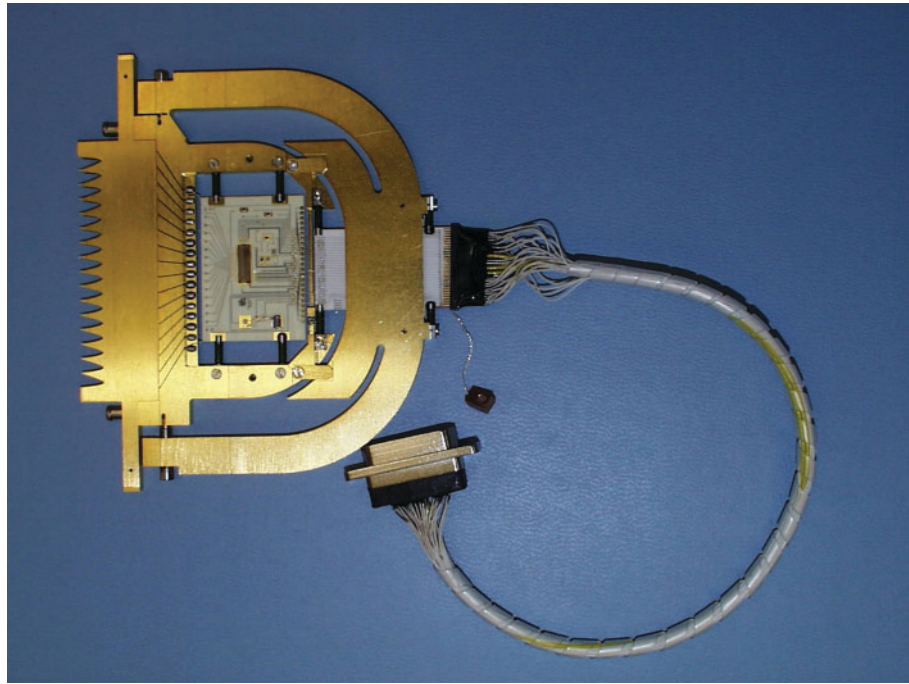
PACS is designed for photometric and spectrometric studies in the wavelength range between 60  $\mu\text{m}$  and 210  $\mu\text{m}$  (Fig. III.8). MPIA will make major contributions to the development of the cameras and pre-amplifiers, as well as to the focal plane chopper and the data center. Based on experience with ISO, the Institute will participate in the detailed planning of the structure of the HERSCHEL ground segment and in particular of the control center for PACS. The Institute will also be responsible for all aspects of the calibration of PACS before and during the flight.

The Carl Zeiss Company in Oberkochen was selected to manufacture the flight model of the chopper, based on the prototype developed at MPIA. A chopper is used for the following purpose: During satellite-borne infrared observations, a more or less strong confusing background signal can occur, caused by thermal emission of the telescope and the sun shield. In order to eliminate this signal, the object examined and an adjacent “empty” sky section are measured alternately. The empty section gives the background, which is subtracted later from the actual exposure. The alternating observation of two sky sections is achieved by putting a mirror into the light path, which tips (“chops”) to and fro up to ten times a second, with high optical and mechanical precision.

For the chopper, all mechanical components of the lifetime model as well as parts for the test sets were manufactured at MPIA’s workshops and then delivered to Zeiss. The flexural pivots of the chopper, which are exposed to great load during the launch of the rocket and the following three-year operation phase, are qualified for their application in space by additional durability tests at the “Fraunhofer-Labor für Betriebsfestigkeit”.

As a major contribution to PACS, the Institute has compiled the specifications of the cryo-harness. This includes the definition of all 1148 cables together with the cold interface connectors and all of the electrical parameters.

**Fig. III.8:** One of the detector arrays for the PACS infrared camera with  $16 \times 25$  pixels. To the left, the entrance openings of the light collecting cavities; in the middle, the cold readout electronics, surrounded by the stress module which exerts pressure onto the 16 Ge:Ga detectors. (Image: ANTEC, Kelkheim).



This document is an important basis for the thermal concept of the instrument.

*(D. Lemke, V. Galperine, U. Grözinger, R. Hofferbert, U. Klaas, R. Vavrek, H. Baumeister, A. Böhm)*



## IV Scientific Work

### IV.1 Galactic Astronomy

---

#### Evolutionary Stages of Bok Globules

**Due to gravitation, gas and dust have accumulated at different places in the Milky Way to large, dense clouds, forming potential star formation regions. The sizes of these nebulae range from less than a light year to several hundred light years. The smallest among them are called Bok globules. Last year, two of these compact dust clouds have been studied in detail at the Institute. One of the smallest known globules, Barnard 68, is in a physically interesting state of equilibrium between gravity and internal gas pressure. The second globule, CB 34, is already more evolved, having reached a stage of intense star formation.**

Bok globules are isolated, dense clouds of dust, silhouetted as dark spots against a starry background. As early as in the 1940s, the Dutch astronomer Bart Bok studied many of these nebulae and produced a first catalogue. Bok's conjecture at that time that stars may form in the interior of the globules, were confirmed only recently. The total number of globules within the Milky Way is now estimated to be about 100 000, their sizes ranging between some tenths and a few light years, their masses between about one and a hundred solar masses.

These compact nebulae could have formed in different ways: Either, a small condensation of matter forms accidentally and grows by attracting matter from its surroundings, or globules are the remains of a former, much larger dust cloud which has been dispersed by intense UV-radiation and particle winds from young stars.

#### Barnard 68 – a Globule on the Verge of Collapsing?

Barnard 68 (B 68) is one of the nearest and also smallest known globules. In its neighborhood, there are three more globules and the large Ophiuchus cloud complex. It is assumed, therefore, that B 68 and the nearby globules are leftovers of an originally much larger cloud.

The properties of these dense clouds can hardly be studied in visible light because they are opaque in this spectral range. In 2001, ESO astronomers had observed the cloud in the near infrared, taking advantage of the fact that electromagnetic radiation of increasing wavelength can pass through the dust more and more easily. At wave-

lengths up to 2.2  $\mu\text{m}$ , the globule starts to get transparent and background stars start shining through (Fig. IV.1). In the near infrared, altogether more than 1000 stars were identified. They shine through the globule from the back, thus allowing to measure the attenuation of the light (the degree of extinction) from which important variables of state can be derived. As it turned out, the extinction in visible light amounts to 35 magnitudes at the center of the cloud, corresponding to an attenuation of light by a factor of  $10^{14}$ . Moreover, no significant condensations were found in the interior of the cloud, meaning that nowhere star formation has set in yet.

For follow-up studies, it was important to know that the entire cloud is in a state of equilibrium, that is, the inward tug of gravitation is balanced approximately by the kinetic gas pressure directed outward. Presumably, gravity will dominate in the near future, causing the cloud to contract until a star may form in the center. A cloud being in a state of equilibrium like B 68 is called a Bonnor-Ebert sphere. Astronomically, this state is of special interest because it is defined physically in clear and simple terms: The structure of the cloud is completely determined by the kinetic temperature and central density of the gas.

Astronomers of the Institute, together with colleagues of the University of Helsinki and ESO, have observed B 68 at 1.36 mm and 2.7 mm wavelengths, using the Swedish-ESO Submillimetre Telescope (SEST) on La Silla, Chile. In this wavelength range, three lines of the isotopic molecules  $^{13}\text{CO}$  and  $\text{C}^{18}\text{O}$  are found from which the CO abundance can be determined. After molecular hydrogen, CO is the second most common molecule in the interiors of dust clouds and therefore particularly well suited for detailed studies.

Two approaches were chosen by the astronomers to calculate the density and distribution of the CO gas from these data: In the first model, a constant excitation temperature for the observed line transitions of the CO molecules was assumed. In the second model, excitation conditions within the globule were simulated, based on a Bonnor-Ebert sphere in an external radiation field.

Fig. IV.2 shows the column density of  $\text{C}^{18}\text{O}$ . (Column density is measured over all particles per area unit along the line of sight).  $\text{C}^{18}\text{O}$  is a rare molecule, whose lines do not get saturated even at the high density of B 68. Therefore, the measured  $\text{C}^{18}\text{O}$  line profile of B 68 should be similar to the extinction profile measured before (with a constant dust/gas ratio). But that is not the case, as is il-

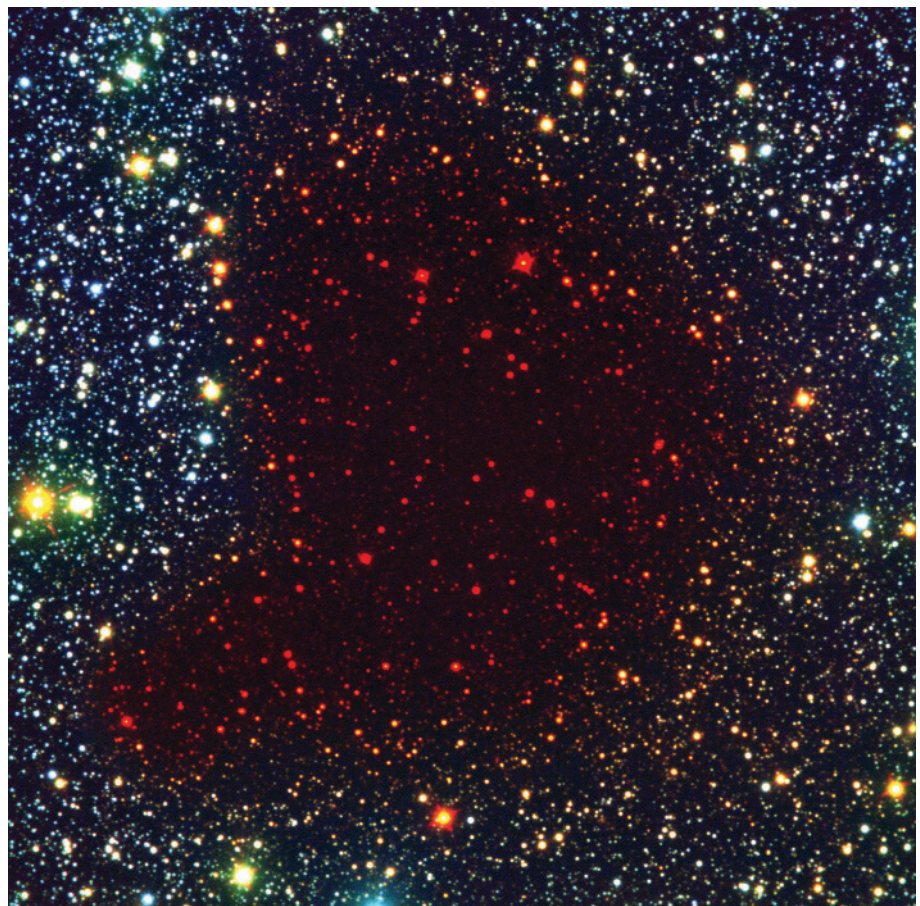


**Fig. IV.1:** The Bok globule B 68, imaged through several color filters using the ESO Very Large Telescope and the ESO New Technology Telescope. **Left:** In visible light and in the near infrared, the cloud is opaque. **Right:** At 2.2  $\mu\text{m}$  wavelength (K filter), many background stars appear. (Image: ESO)

lustrated in Figure IV.3. In the central region, the column density is only higher by a factor of three or four than in the outer reaches. The infrared observations by the ESO astronomers, however, had shown a much steeper increase of the extinction from the outer regions to the inner ones.

This behavior can be explained most easily by the fact that with increasing density of the dust an increasing fraction of the CO gas is freezing out onto dust grains. (This process, which is of great importance to the interstellar medium, has been studied by astronomers of MPIA, using the ISO Infrared Observatory; see following chapter on “Interstellar icy dust grains”.) Thereby an increasing fraction disappears from the gas phase and can no longer be detected. A kind of steady state has been assumed for B

68 – a state of equilibrium between the freezing out of the CO gas onto solid particles (adsorption) and the re-vaporization (desorption) due to the heating of individual particles by, e.g., cosmic rays. Adsorption and desorption rates depend on the size of the dust particles, the gas and dust temperatures, and the external radiation to which the dust grains are exposed. From the observational data, astronomers were able to determine the ratio of adsorption to desorption rate within certain limits.

The numerical simulations of the second approach, which does no longer assume constant line excitation, confirm the results of the first approach, namely that the freezing out of the CO gas is crucial for the observed abundance distribution and that the kinetic temperature of the gas within the cloud is 8 Kelvin. This value yielded a distance to B 68 of 80 pc (260 light years), which is significantly nearer than thought before.

From this new distance, other interesting values for B 68 were derived. The globule is only 0.04 pc (0.13 light years) in diameter. Transferred to our solar system, B 68 would fill the volume around the Sun approximately to the inner edge of the Oort cloud. The gas pressure at the edge of the globule is  $1.7 \times 10^{-12}$  Pa. This value is in good agreement with the independently determined gas pressure of the surroundings enclosing the globule. The central density of B 68 is  $2.6 \times 10^5 \text{ cm}^{-3}$ , while its total mass amounts to only 0.7 solar masses. Thus, B 68 is the lowest mass and nearest Bok globule known so far.

Detailed analysis of the observational data allowed a quantitative determination of the adsorption and desorption of the CO gas. The “depletion factor” could be represented as a function of the gas particle density and of the adsorption and desorption coefficients, determining its radial course within the globule. In the center of the cloud, only 0.5 to 5 percent of all CO molecules are in the gas phase. A much larger fraction is frozen out onto dust grains.

In May 2002, astronomers of the Institute and of the University of Helsinki will observe the globule using the 100 m radio telescope at Effelsberg. Studies of the spectral lines of the ammonia molecule, which can be found in the densest parts of interstellar clouds, will provide exact values for the kinetic temperature and the density (instead of the column density measured before) of the gas in the central region of B 68. If the results are found to be in agreement with the predictions based on the CO observations, this would be not only a remarkable confirmation of a state of hydrostatic equilibrium, but it would make B 68 the globule with the most exactly known values of density, mass, and distance and thus a model object for subsequent studies of the initial state of the gas within clouds before the onset of star formation.

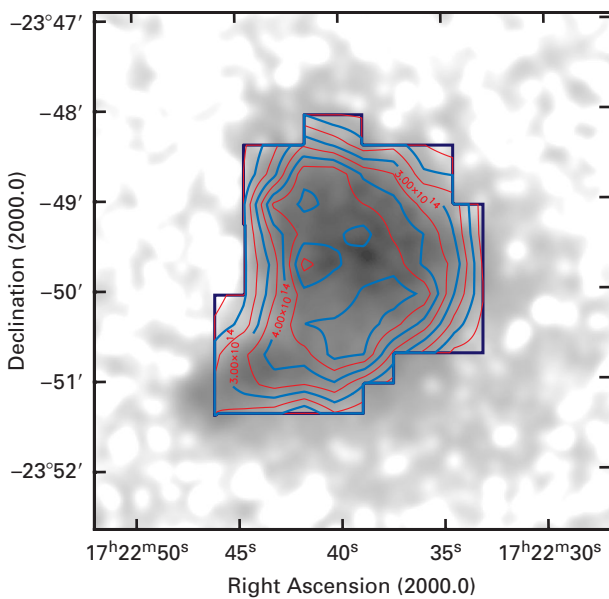


**Fig. IV.2:** Map of the column density of  $\text{C}^{18}\text{O}$  in B 68, derived from the observed molecular lines. Contour lines give the density in terms of particles per square centimeter.

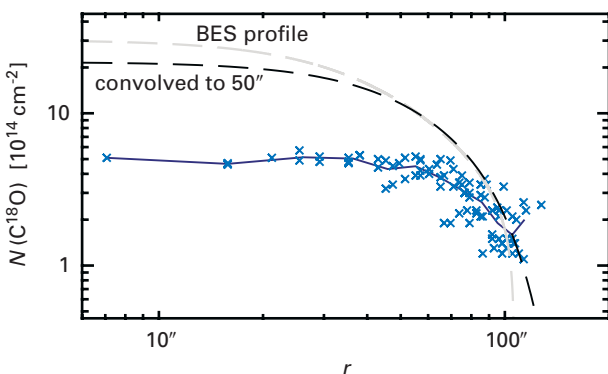


**Fig. IV.3:** Radial distribution of the  $\text{C}^{18}\text{O}$  column density (crosses) of B 68. For comparison, both dashed lines mark the density profile of an ideal Bonnor-Ebert sphere. The depletion of the CO gas in the central region can be recognized.

### Active Star Formation within CB 34

In collaboration with colleagues from the Max Planck Institute for Radio Astronomy in Bonn, from Northern Ireland and from Hawaii, astronomers of the MPIA studied the Bok globule CB 34, which is roughly 1500 pc (5000 light years) away. In certain respects, it is the exact opposite of B 68. With a diameter of about 0.75 pc (2.5 light years), it is 20 times as large and 250 times as massive as B 68. Above all, numerous new stars are forming within CB 34, making it an ideal object for studies of a globule in an advanced evolutionary state.

The astronomers observed CB 34 in the near infrared using the Calar Alto 3.5 m telescope with the Omega Prime camera built at the Institute. This way, it was possible to study excited molecular hydrogen at a wavelength of 2.12  $\mu\text{m}$ , which is an indicator of energetic, turbulent processes within the interstellar medium. Moreover, the globule was observed in the millimeter region using the IRAM telescope in Spain. In this wavelength range, lines of CO and  $\text{HCO}^+$  gas are found which provide information about the density distribution in the interior of the cloud.

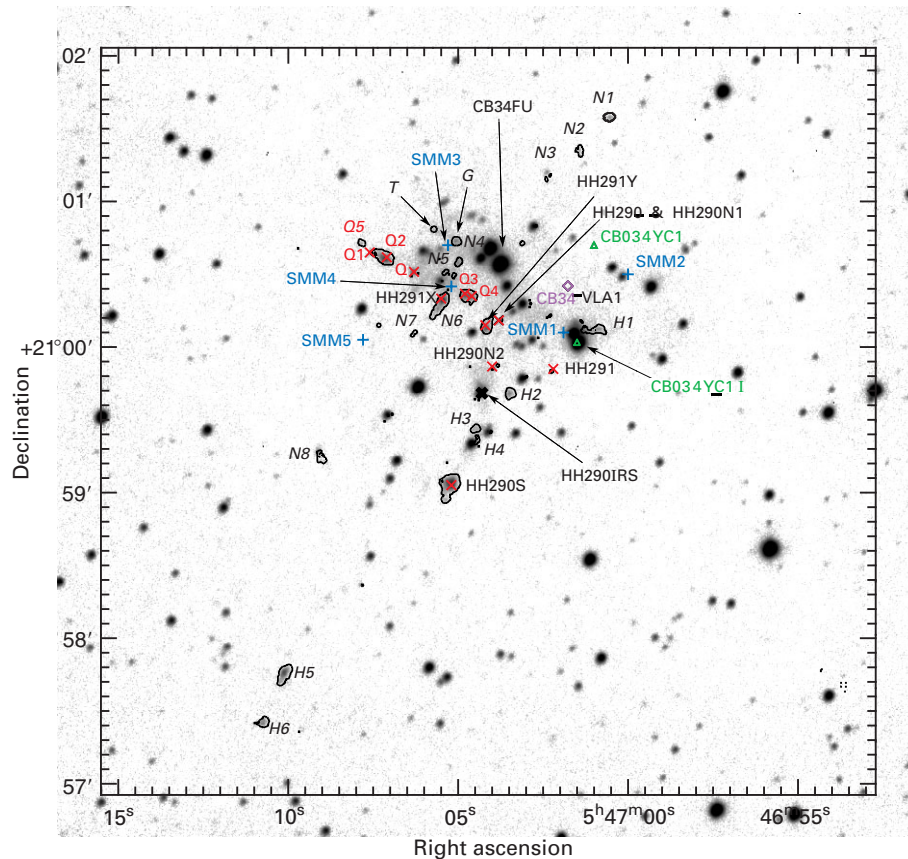
During earlier studies of CB 34 in different wavelength regions, excited gas had already been found, *e.g.* in Herbig-Haro (HH) objects, which indicated the presence of intense particle winds from young stars. Now, the new, very deep near infrared images revealed several  $\text{H}_2$  regi-

ons (H, N, and Q series, Fig. IV.4), which had been unknown so far. They mark three narrow gas outflows, so-called jets, emerging from young stars. Two of these jets were discovered in the course of this observing project. Jets from young stars are known since about 20 years. Astronomers at MPIA were involved in its discovery and have contributed significantly to its explanation (cf. Annual Report 1998, p. 54).

The  $\text{H}_2$  knots of the H, N, and Q series, respectively, are lying on a line marking the collimated outflows (Fig. IV.5). The  $\text{H}_2$  emission is probably produced by shock excitation of the gas within the fast particle stream. Here, temperatures up to 3000 K are generated, exciting the molecules to emit at the characteristic wavelength of 2.12  $\mu\text{m}$ . The projected sizes of the jets are 1.6 pc (5.2 light years) for H1-H6, 1.4 pc (4.6 ly) for N1-N8 and 1.2 pc (3.9 ly) for Q5-Q4-HH290N1. The fact that the putative ends of the outflows do not show bow shocks, as they are typically found in jets, suggests that the outflows are extending even further into the interstellar medium.

Assuming a typical velocity of 100 km/s for the jets yields a (dynamical) age of about 13 000 years – a value also found in other jets and hence typical for this phenomenon. The sources of the jets cannot be recognized clearly. The submillimeter observations, however, show

**Fig. IV.4:** The central region of CB 34 in the light of molecular hydrogen,  $\text{H}_2$ . Newly found condensations are marked with the letters H1 – H6, N1 – N6, G, T and Q5.



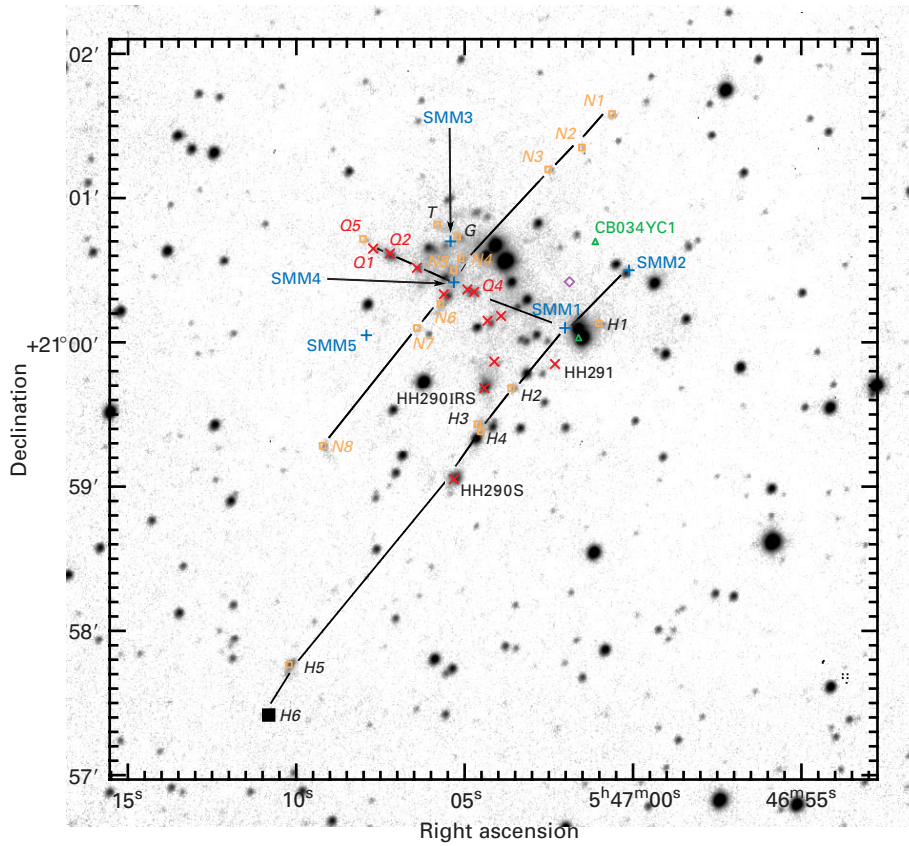
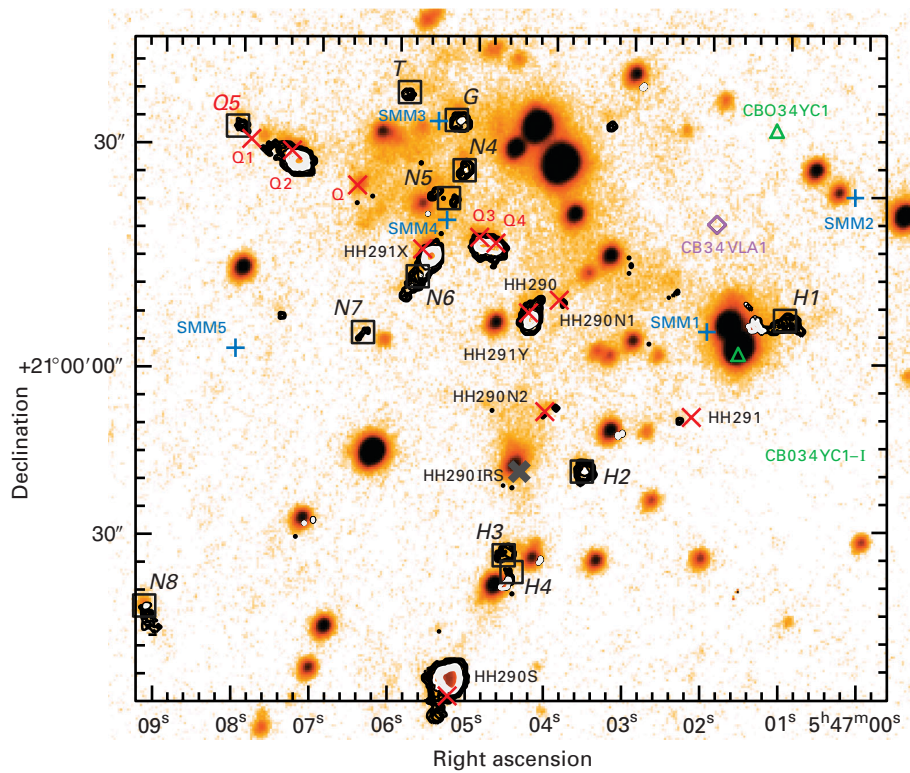


Fig. IV.5: Schematic map of the H<sub>2</sub> knots marking three jets.

Fig. IV.6: The central region of CB 34.



some condensations of the  $\text{HCO}^+$  gas, which are denoted by SMM in Figures IV.5 and IV.6. SMM1 is 10 arc seconds across corresponding to 0.08 pc (0.25 light years) and has a submillimeter luminosity of 40 solar luminosities while SMM4 emits 20 solar luminosities. In each of these condensations probably several protostars are hidden. Two of these objects in SMM1 are possibly responsible for the H and Q jets. The SMM4 submillimeter source is located roughly in the center of the N jet and may be the source of this outflow. This assumption is supported by the presence of the Herbig-Haro object HH291X in the proximity of SMM4 (Fig. IV.6). As it is generally known, HH objects are luminous, shock excited gas condensations within jets.

For a long time, an outflow of CO gas is also known in CB 34. Using the IRAM telescope, astronomers could study the distribution of the CO gas in great detail. A bipolar structure was found with the source SMM1 apparently sitting in its center.

Infrared observations support the assumption that star formation in CB 34 has occurred in several phases. More than 20 protostars reddened by dust have been detected in the cloud's central region. The other stars lying further out appear to be older. This fact is in agreement with the observations of the  $\text{H}_2$  and CO gas. The different outflows emanating from young stars are concentrated in the central region of the globule where they cause strong turbulences of the interstellar gas.

A clue to the timescale of star formation history in this globule is provided by a main sequence star, called CB34FU, which is about one million years old. Astronomers assume two phases of star formation: One million years ago, the first stars formed in many places within the cloud. Particle winds and shock waves produced by these stars then compressed the gas in the central region, initiating a second wave of star formation. And these objects are now the sources of the jets.

### Origin of CB 34

How did the globule form? About 15 arc minutes away, there is another globule called CB 33. Both clouds are connected loosely by diffuse matter (Fig. IV.7a). At a greater distance, a large cloud complex containing young, hot O and B stars is located near the Gemini association. There is the possibility that the two small globules originally have been part of the large Gemini cloud. But then the globules had to be at least ten million years old, which is in contradiction to the latest findings.

Another discovery, however, could explain the origin of the globules. A deep infrared image benefiting from the large field of view of the OMEGA-PRIME camera revealed a diffuse luminous halo around CB 34 (Fig. IV.7b). Several explanations for this emission are conceivable: scattered light from the protostars, or fluorescent radiation from molecular hydrogen excited by UV emission of a

nearby hot star. But neither these nor other processes considered by the astronomers can explain the halo emission around CB 34 and CB 33.

But there is another fascinating possibility: When two hydrogen atoms combine on the surface of a dust grain to form molecular hydrogen, infrared radiation is emitted. If the atomic hydrogen in the halo around the globules has a density of  $10^4 \text{ cm}^{-3}$ , the estimated formation rate of molecular hydrogen is sufficient to explain the observed intensity of the near-infrared emission in the halo. If this interpretation is correct, it would suggest a model in which the globules have formed from a cloud of atomic hydrogen by cooling and collapse. This scenario will be tested by subsequent observations.

(Roland Gredel)

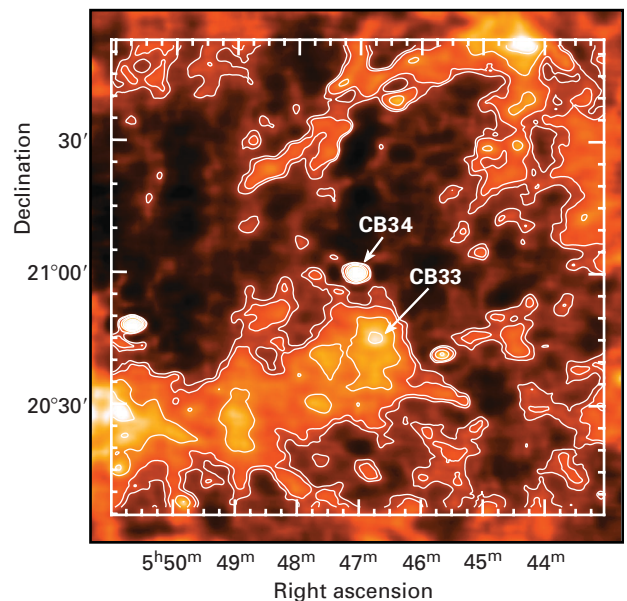


**Fig. IV.7: a)** This IRAS image taken at 100  $\mu\text{m}$  wavelength shows the two globules CB 34 and CB 33 (IPAC/CalTech);

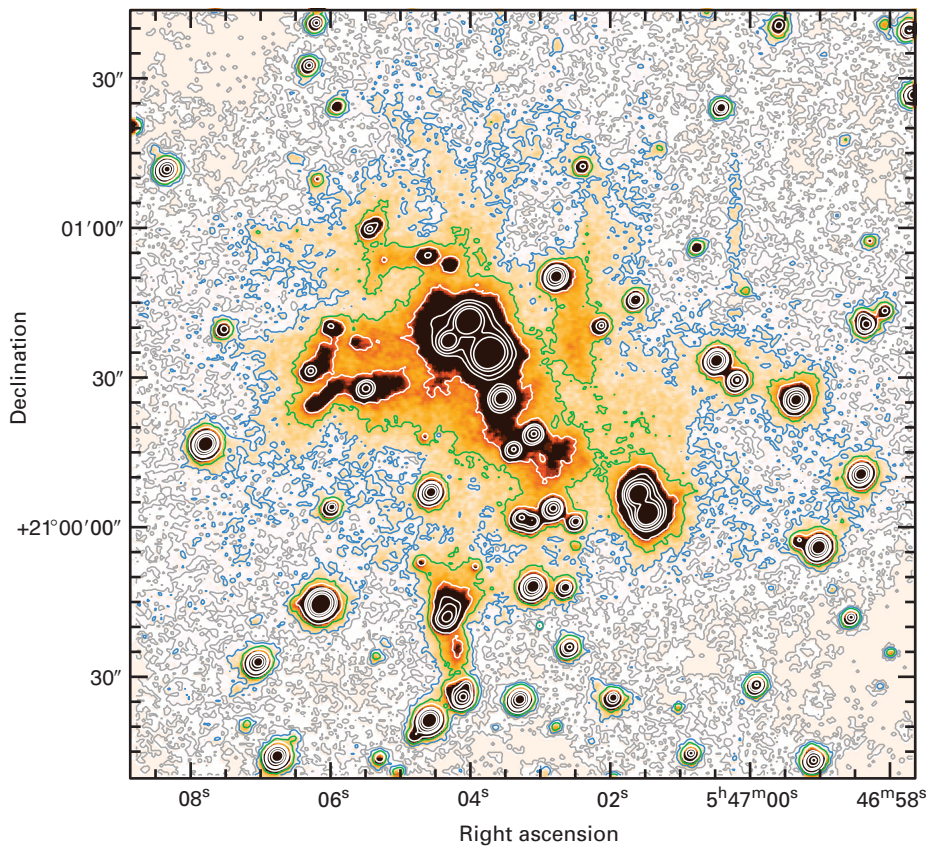


**Fig. IV.7: b) b)** In this image obtained with OMEGA-PRIME, the halo gas and its large-scale distribution can be recognized. CB 34 is located at  $21^{\circ}00'30''$  declination and  $5^{\text{h}}47^{\text{m}}05^{\text{s}}$  right ascension.

very efficiently heat released in the star formation process, radiating it back into space in the longer-wavelength range. This way, they cool down hot regions and allow matter to contract further and finally form stars and planets.

## Interstellar Icy Dust Grains

**With a mass fraction of about one percent, interstellar dust constitutes the smallest portion of the total amount of interstellar matter. Nevertheless, it is of great importance to many processes, especially to the formation of stars and planets. Since a long time astronomers believe that the majority of solid particles in the interior of dense dust clouds consists of a silicate core surrounded by a mantle of frozen molecular gases. While these gases are essential for the chemical evolution of interstellar clouds, they are extremely difficult to detect. Together with colleagues from the Universitätssternwarte Jena, astronomers of the Institute were able to identify ammonia, methanol and methane ices using the European ISO space observatory.**

Stars and planets form in dense interstellar clouds of gas and dust. Especially in the radio and infrared spectral range, roughly one hundred different species of molecules were detected in the gas phase. The molecules play an important role in star formation. For instance, they absorb

## Core-mantle Model of Dust Grains

The great variety of molecules, some of which consist of more than ten atoms, suggests a complicated network of chemical reactions within the molecular and dust clouds. Here, the surfaces of tiny dust particles play an important role serving as catalysts for many chemical reactions. The most abundant molecule in the gas phase is molecular hydrogen ( $\text{H}_2$ ). It cannot form, however, by combining two freely moving hydrogen atoms, for during its formation process, the molecule has to release energy, and this is not possible under the extreme conditions (low particle densities and temperatures) prevailing within molecular clouds. This is where interstellar dust comes in.

Hydrogen atoms can be adsorbed onto the particle surfaces and wander about them. If they meet another hydrogen atom in doing so, both can combine to form an  $\text{H}_2$  molecule. Part of the heat, which is liberated during the reaction, is absorbed by the grain while another part can be transformed into kinetic energy enabling the molecule to leave the grain and move into space, into the gas phase.

For other elements like carbon, oxygen and nitrogen, dust is important, too. These elements already form smaller molecules like carbon monoxide (CO) or ammonia (NH<sub>3</sub>) in the gas phase. Subsequently, such molecules can freeze out onto the surfaces of dust grains in reactions deep inside the dust clouds, forming larger molecules, which are highly improbable to form in the gas phase.

Actually, at temperatures around 10 K, all gases should be frozen out completely onto the grains within some ten to a hundred thousand years. The fact that they are yet detected in the gas phase, therefore suggests that molecules are constantly evaporating from the grain surfaces, energized, *e.g.*, by UV emission of hot, young stars.

Observational results and theoretical considerations indicate a core-mantle model for the structure of the dust particles. Accordingly, a typical grain comprises a core made of silicates and carbonaceous materials surrounded by an icy mantle. The latter results from a balance between molecules evaporating and freezing out.

While molecules in the gas phase can be detected relatively easily in the interior of dust clouds, observation of ices on the grains is still in its infancy. The ices can be identified by their chemical “finger prints”. If the molecules bound within the ice crystals are exposed to external electromagnetic radiation, certain wavelength ranges are absorbed, their energy causing stretching, deformation and inversion vibrations of the atomic components. The attenuation of radiation in these wavelength regions can be observed as typical absorption bands. The external radiation is produced by young stars, which are deeply embedded within the dust clouds.

So far, only the most abundant compounds like H<sub>2</sub>O, CO and – since the ISO observations – CO<sub>2</sub> could be clearly identified. The main absorption bands of ice molecules are in the infrared region where spectroscopy from the ground is only possible in limited wavelength regions, due to absorption of atmospheric water vapor. Molecular bands of different species can overlap, thus complicating identification. To assign absorption bands to a specific molecule, their wavelengths have to be determined by laboratory experiments. Such measurements are very difficult and can be carried out only by a few laboratories, *e.g.* that of the University of Leiden.

### Detection of Icy Dust Using ISOPHOT

The European ISO Infrared Space Observatory opened a new era for studies of the chemical composition of dust particles. It had several spectrometers on board, which completely covered the wavelength region crucial for studying these ices and which had sufficient sensitivity. One of these spectrometers, the spectrometer channel of the ISOPHOT instrument developed and built under the leadership of the MPIA, was especially designed for studies of dust. It consisted of two grating spectrometers covering

the wavelength ranges from 2.5 μm to 4.9 μm and from 5.8 μm to 11.6 μm.

Using this instrument, astronomers of the Universitätssternwarte Jena and of the MPIA had been able as early as 1996 to detect CO<sub>2</sub> ice for the first time in two molecular clouds apart from water ice. In addition to the low-resolution spectroscopy with ISOPHOT, the Short Wavelength Spectrometer (SWS) on ISO for the first time allowed high-resolution spectroscopy from 2.4 μm to 45 μm wavelength. This instrument, however, was not sensitive enough for faint objects and required significantly longer exposure times than ISOPHOT. So, in the end, less objects could be studied using SWS.

Now the astronomers of the Universitätssternwarte Jena worked together with their colleagues at the MPIA to detect also solid ammonia (NH<sub>3</sub>), methane (CH<sub>4</sub>) and methanol (CH<sub>3</sub>OH). Ammonia is of particular importance within the chemical network because it is a basic building block for more complex nitrogen compounds. Although it freezes out at temperatures around 195 K, it has not yet been clearly detected as an ice. For their recent analysis, the astronomers used data of the ISOPHOT spectrophotometer as well as of the Short Wavelength Spectrometer to test the analysis procedure against two data sets obtained by independently calibrated instruments.

Measurements taken with both instruments were available for altogether ten dust clouds containing young stars. Comparison of both data sets showed a good agreement for each object. Minor differences could be attributed to differing sizes of the entrance slits of both instruments, resulting in slightly different sizes of the sky fields, which have been spectroscopically observed.

Solid ammonia (NH<sub>3</sub>) has three strong molecular bands in the infrared region: at 2.95 μm, 6.16 μm, and 9.0 μm. Earlier attempts to detect the molecule concentrated on the shortest wavelength. But this characteristic signature overlaps with a band of water ice.

The astronomers at MPIA searched their data for the NH<sub>3</sub> absorption at 9.0 μm. Laboratory studies predict an absorption extending from 8.6 μm to 9.4 μm, with a maximum at 9.0 μm. To extract this spectral feature, a superimposed absorption of silicate particles had to be subtracted. This absorption band is significantly stronger and extends over a broader wavelength range from 8.0 μm to 12.0 μm. Since the profile of the silicate band varies with the local conditions, no standard procedure could be used for the subtraction. Moreover, there is no way to model the actual silicate profile by means of laboratory data. Therefore, the silicate absorption feature in the range of the NH<sub>3</sub> absorption from 8.6 μm to 9.4 μm was approximated by fitting a polynomial. Its coefficients were determined by means of the spectral shape in the adjacent wavelength ranges (8.2 μm to 8.6 μm and 9.4 μm to 9.8 μm, respectively), which is only influenced by the silicate profile. The measured spectrum was related to this interpolated silicate profile.

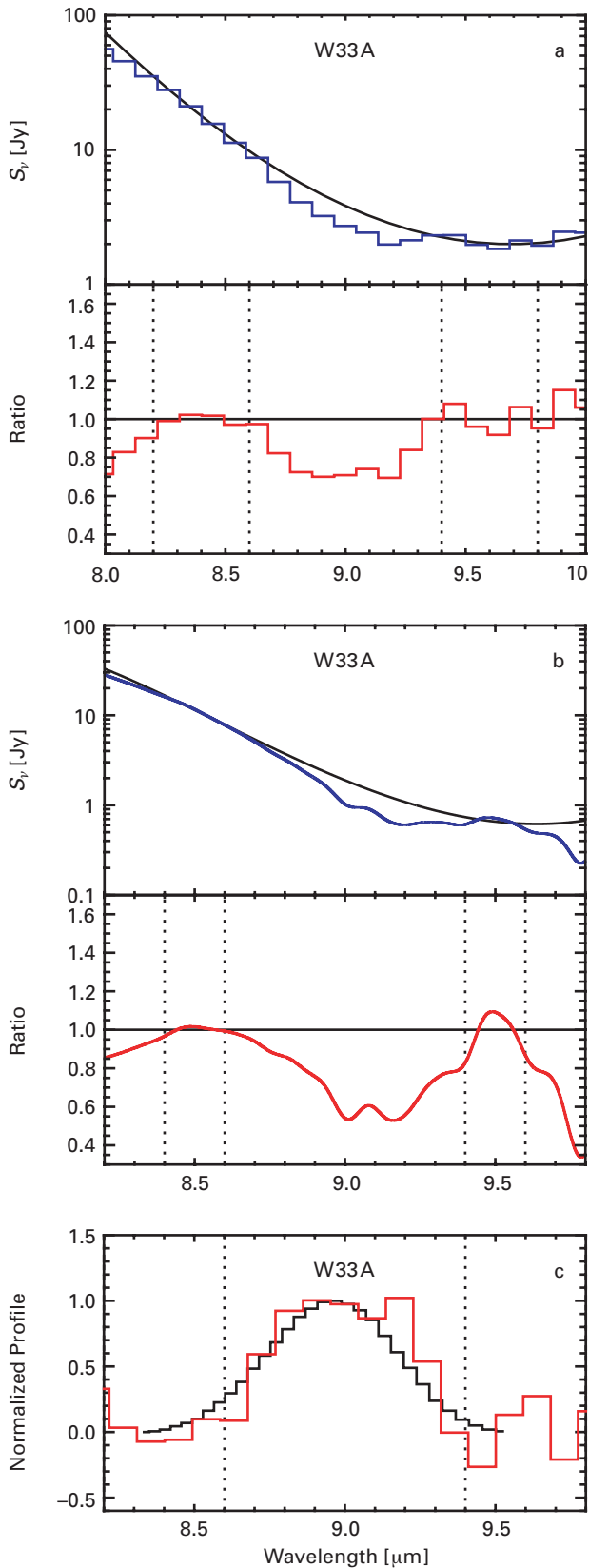


**Fig. IV.8:** Spectrum of the dark cloud W33A, taken with ISOPHOT (a) and with SWS (b). The strong decrease towards longer wavelengths is caused by the deep silicate absorption. The upper frame shows the fitting of the polynomial, the lower frame shows the ratio of the measured spectrum and the polynomial

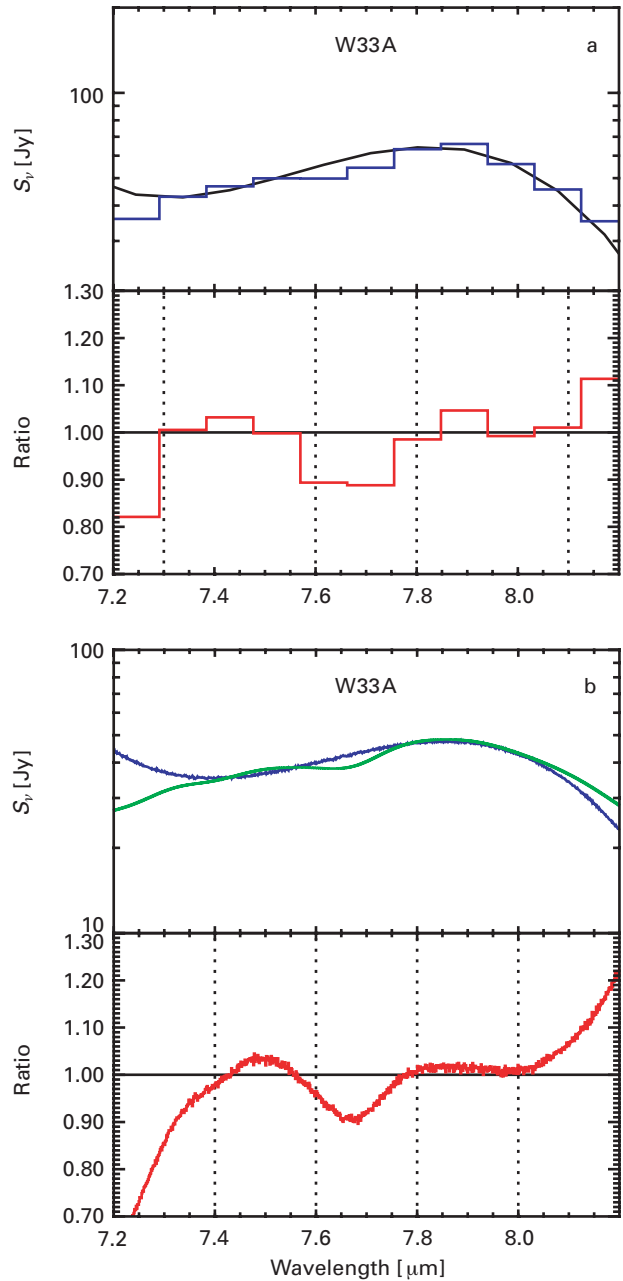


**Fig. IV.9:** Spectra of W33A in the region of the  $\text{CH}_4$  absorption around  $7.7 \mu\text{m}$ , obtained with ISOPHOT (a) and SWS (b).

fit. The  $\text{NH}_3$  absorption around  $9.0 \mu\text{m}$  wavelength is clearly evident. The pairs of dashed vertical lines indicate the ranges from which the polynomial coefficients were determined. (c) Comparison of the profile normalized to the minimum with a laboratory spectrum.



**Fig. IV.10:** Cep A, one of the molecular clouds studied, imaged in the near infrared. (2MASS)

After this procedure, the ammonia band showed up in the ISOPHOT data as well as in the SWS data of four objects. The line occurs most prominently in the dark cloud W33A (Fig. IV.8), which contains a deeply embedded young star. W33A is the 33<sup>rd</sup> object on a list of 82 bright radio sources compiled by the Dutch astronomer G. Westerhout in 1957. “A” designates a substructure found later with better spatial resolution.

Using the same procedure, the astronomers looked for the spectral signatures of methane ( $\text{CH}_4$ ) and methanol ( $\text{CH}_3\text{OH}$ ). A  $\text{CH}_4$  absorption is expected at  $7.7 \mu\text{m}$ . It was clearly detected in W33A again (Fig. IV.9) and in NGC 7538 IRS9. Traces of it were found in two other clouds named AFGL 2591 and Cep A (Fig. IV.10). The signature of  $\text{CH}_3\text{OH}$  at  $9.7 \mu\text{m}$  was also detected in W33A (Fig. IV.11), in Cep A, and in one other object.

The spectrum of W33A also shows a strong absorption band of water ice. From the depths of the bands, the ratios of the abundances of the ices can be determined. The analysis shows that there is about 10 % to 20 %  $\text{NH}_3$  compared to  $\text{H}_2\text{O}$ . This result is in agreement with the laboratory spectral analysis of icy grains with similar composition. For W33A, other research teams already had found the relative abundance of  $\text{CO}_2$  and  $\text{CO}$  to  $\text{H}_2\text{O}$  to be 10 %, respectively. Thus, at least for this star forming region rather robust values are available. They are of great importance for the further understanding of star formation processes.

Thus, the team from Jena and MPIA was able to show the spectral resolution of ISOPHOT to be high enough to identify the typical molecular bands of interstellar ices. The astronomers now plan to apply their newly developed method to other dust clouds whose data are stored within the ISO archive.

*(U. Klaas, D. Lemke)*

---

### Formation of Binary Stars: New Answers and New Questions

**Most stars are members of binary or multiple systems. For G stars, e.g., – which include our Sun – the ratio of single to double to triple to quadruple stars in the solar neighborhood is 57 : 38 : 4 : 1, that is, not even 40 % of all stars are “loners”. Today, everything seems to indicate that multiple systems already form during the star formation phase. So, obviously physical quantities like the distribution of the orbital periods or the mass ratios of the stars must include information about the star formation process. These quantities have been analyzed at the Institute in a theoretical and an observational study.**

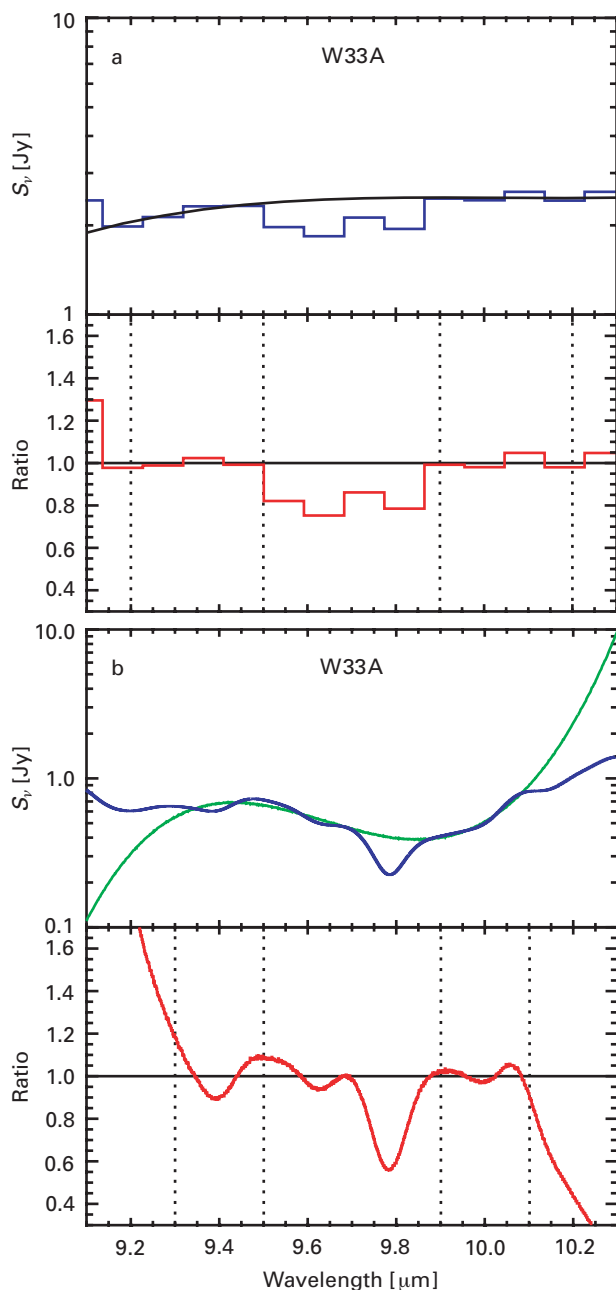


**Fig. IV.11:** Spectra of W33A in the region of the  $\text{CH}_3\text{OH}$  absorption around  $9.7 \mu\text{m}$ , obtained with ISOPHOT (a) and SWS (b).

During the past years, formation and evolution of binary systems as well as their properties have been studied in various ways at the MPIA. These include numerical simulations (Annual Report 1997, p. 59) as well as high-resolution observations (Annual Report 1998, p. 47). The latter led to the surprising finding that the proportion of multiple systems in the star forming regions in Taurus-Auriga and Lupus is significantly higher than for main-sequence stars. Astronomers at the MPIA were able to show that in Taurus-Auriga about twice as many young stars are bound to one or more stellar partners than in the later

main sequence stage. A conceivable explanation could be that young multiple systems rip off members from one another gravitationally during close encounters. The probability for such a process is higher in young stars than in old ones as in early evolutionary stages they are closer together in their parent cloud than in later stages. Moreover, it is assumed that physical conditions during star formation, like the temperature of the surrounding interstellar cloud, influence the number of multiple systems formed.

In the year under report, astronomers at the MPIA together with colleagues from the Thüringer Landessternwarte Tautenburg carried out near infrared speckle observations to obtain the masses and mass ratios for the components of young binary systems. The goal was a comparison of the results with numerical model calculations.

Young stars in the star formation region of Taurus-Auriga were observed with the 3.5 m telescope on the Calar Alto using the MAGIC infrared camera built at the MPIA. In addition, observations of star-forming regions in the southern sky were made using the ESO New Technology Telescope on La Silla, Chile. As in most young binaries the components are separated by less than one arc second, high-resolution speckle techniques had to be used. Here, typically one thousand single images of 0.1 seconds exposure time each were taken and then superimposed to make one composite image. Thereby the blurring of the images caused by atmospheric turbulences (“seeing”) can be overcome. The measurements were taken at  $2.2 \mu\text{m}$  wavelength where also stars are to be seen whose visible light is heavily obscured by dust extinction.

The total sample comprises 119 stars, the projected separations of the components of binary systems being at least 20 AU. The star formation regions are 450 light years (Taurus-Auriga) to 620 light years (Lupus) away from Earth. For all objects, spatially resolved photometric measurements in three near-infrared wavelengths were obtained.

Before analyzing the data, they had to be “de-reddened”, that is, corrected for the extinction effect of the interstellar dust. Then the data were plotted in a color-magnitude diagram together with theoretical evolutionary tracks. Here some of the systems fell out of the theoretically possible region (Fig. IV.12), presumably because of the presence of stellar dust disks which are common in young stars. These disks generate an additional strong extinction, which could not be corrected for. Therefore, these stars were excluded from further analysis.

For the remaining stars, luminosities and spectral types were determined. The latter is especially difficult to obtain as only spectra of the combined light of each binary system are available, but not of each single component. Therefore, astronomers assumed that the optical primary component of each system dominates the spectrum. On this supposition and the very plausible assumption that both stars in a binary system are coeval, the spectral types of the companions could also be derived.

Given these data, it was possible to place the stars into a Hertzsprung-Russell diagram containing theoretical evolutionary tracks and to determine the masses of the components. Unfortunately, the results depend strongly on the assumed evolutionary model for pre-main sequence stars. Furthermore, the sample is incomplete below about 0.5 solar masses. For these reasons, it was not possible to show if and where the mass function of the components has a maximum and how it continues towards substellar objects.

The mass ratio of both components, however, is of great importance for the intended comparison with predictions of numerical models for the formation of binary systems. A few years ago, such models had shown that during their formation both components of a young binary system continue to accrete matter from their surroundings. Consequently, the mass ratio of both components should approach unity. But as is shown in Fig. IV.13, there seems to be no preference of binaries having components of equal masses. Further observations are needed to explain this disagreement. Progress will depend significantly on the development of more reliable evolutionary models for pre-main-sequence stars and binary systems.

### Evolution of Orbital Periods

Apart from the mass ratio, the orbital period is one of the characteristic quantities of binary systems. For main-sequence binaries, periods are ranging from about one day to one thousand years. This broad distribution is astonishing because binary stars form from gas clouds of very similar radii and masses. Therefore, the characteristic properties of binaries should also exhibit only a small scatter.

Theoreticians at the Institute posed the question if this very broad distribution already arises during the formation phase of binaries or if it was created by later influences. Maybe gravitational interactions during close encounters of proto-binary systems within the dust cloud widen the initial narrow period distribution. This possibility was considered because numerical simulations of the formation of binary systems do not produce the wide range of periods. In particular, these calculations do not lead to systems with periods shorter than about one thousand days. This was the motivation for simulating the gravitational influence on orbital periods within a star cluster using N-body calculations.

In four different models one hundred respectively one thousand binary systems were treated. In particular, the models differed in the values of the initial densities ranging from one to nine stars per cubic parsec. The components of the systems were chosen randomly from the stellar mass function. In three of the models the stellar mas-

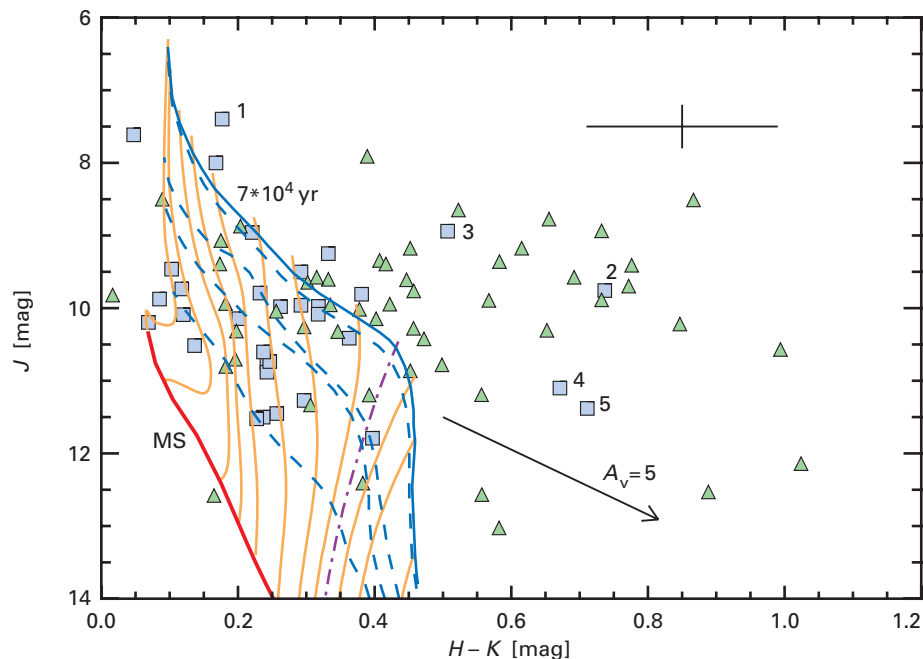


**Fig. IV.12:** Color-magnitude diagram for the components of young binary systems together with the theoretical evolutionary tracks for stars of different masses. Theoretically, only positions

between the two thick solid lines are possible. Stars outside this region are probably surrounded by dense disks or envelopes of gas and dust reddening the stellar light.

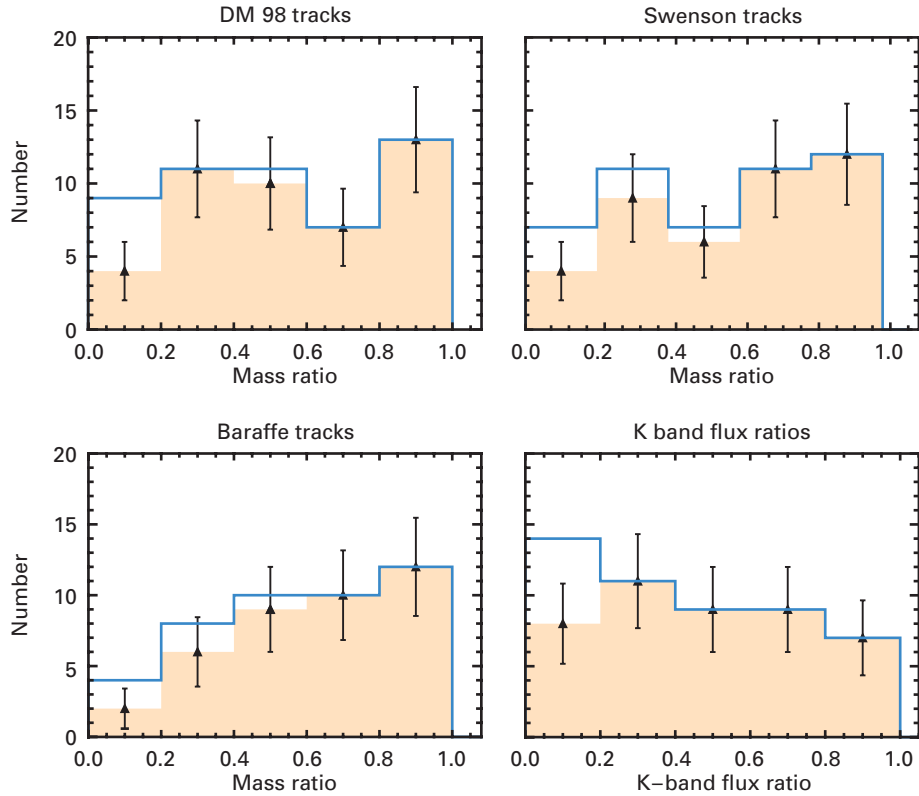


**Fig. IV.13:** Mass ratios of the components of binary systems. The histograms are based on three different stellar evolutionary models used to derive the masses.

ses varied between 0.1 and 50 solar masses while the fourth one only contained low-mass stars of 0.08 to 1.1 solar masses. The initial periods were distributed uniformly between 90 and 900 years. All systems had orbits with an eccentricity of 0.75; but as it turned out later, this value did not have much influence on the results.

Then the models were left to the effects of gravitation, their evolution being followed. In the course of time, some of the binary systems, preferably the wide ones, were disrupted. In some cases, even companions were exchan-

ged. On the whole, the distribution of orbital periods widened due to the gravitational interactions. But none of the models even nearly reached such a broad distribution as observed in nature (Fig. IV.14). The same is true for the eccentricities.

So these simulations demonstrate that the broad distribution of orbital periods already arises during the formation process of binary systems. Now it is the task of the theoreticians to find the cause of this phenomenon.

*(Ch. Leinert, T. Herbst, A. Burkert)*

### Early Chemical Evolution of the Milky Way System

**The oldest stars in the halo of the Milky Way System contain a significantly lower fraction of heavy elements than our Sun. This reflects the chemical evolution of our Galaxy whose interstellar medium has been enriched with heavy elements over the past billions of years. Surprisingly, however, the abundance of different elements varies considerably within the population of old**

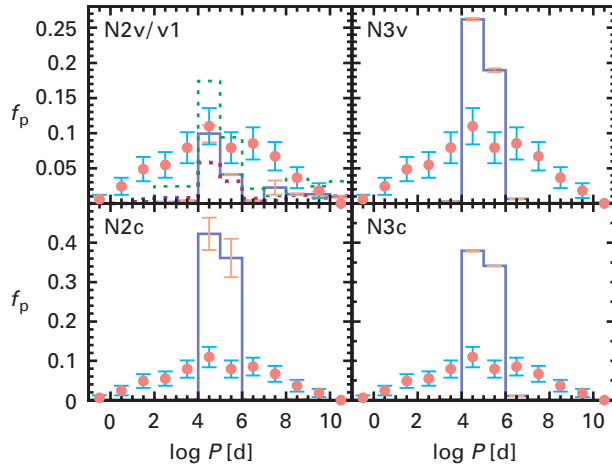


**Fig. IV.14:** Final distribution of orbital periods obtained in the four simulations: The observed distributions (dotted lines) are significantly broader than the theoretical ones (histograms).

**stars. The theory group at the MPIA has calculated a model to simulate the inhomogeneous chemical enrichment of the interstellar medium and compared the results with observational data. Interesting predictions were made that can be tested by further observations.**

The simplest models of the formation and evolution of our Galaxy predict a trend in the abundances of heavy elements (generally called “metals” by astronomers). Accordingly, the Galaxy formed from matter consisting almost solely of hydrogen and helium. This cloud slowly contracted, forming the first stars. Massive stars produced the first heavy elements in their interiors and dispersed them into the interstellar medium by stellar winds or supernova explosions. Meanwhile, the cloud continued to collapse, thereby forming the Galactic disk. The interstellar matter in the disk, out of which the new stellar generation was created, was already enriched with heavy elements then. Consequently, a star’s metallicity is a measure of the age and evolutionary stage of the Galaxy.

If that simple scenario were true a gradient should exist, the percentage of heavy elements in stars within the Milky Way System increasing from outside to inside, *i.e.*, from the halo to the center.

A lot of observational results, however, now show that the evolution of the Galaxy could not have been that straightforward. Therefore, astronomers now generally believe that big disk galaxies have been formed in a hierarchical process. In this picture, the Galaxy did not form out of a single big cloud but grew bigger over billions of years by the merger of several smaller protogalaxies.

Generally, inhomogeneities in the interstellar medium must have been of great importance. This is proved by spectroscopic observations of old stars in the Galactic halo using the abundance of iron in the stellar atmospheres as a measure of the stars’ age. As it turned out, very old stars with about the same very low abundance of iron exhibit strongly varying fractions of other heavy elements like europium, barium and strontium. An extreme example is a star called CS 22892-052. While its abundance of iron is only about one thousandth of the solar value, the proportions of some other heavy elements are 40 times higher than in the Sun. These findings can only be explained if the interstellar gas of the early Galaxy had been enriched inhomogeneously with metals.

## A Model of the Chemical and Dynamical Evolution of the Halo

There have been numerous attempts to simulate an inhomogeneous chemical evolution of the Galaxy assuming that stars enriched their surroundings locally with heavy elements and that these small regions mixed only slowly. This mixing process is difficult to simulate, as various other dynamical processes have to be taken into account simultaneously. Theoreticians at the Institute together with colleagues from the Arcetri Observatory, Florence, have computed a chemo-dynamical model of the early Galaxy considering a number of essential processes.

The model starts from individual gas clouds of different sizes. Each cloud is assumed initially to be spherical and chemically homogeneous and to host independent episodes of star formation. As these newly formed stars later release heavy elements into their surroundings, the chemical composition of the cloud gas changes over time. At the same time, these clouds are moving under the influence of gravitation and some of them sink down into the Galactic disk. Furthermore, they can coalesce with each other as well as fragment into smaller units, thus modifying the initial distributions of size and mass. The frequency ratio between fragmenting and coalescing clouds with star formation does not follow from the model itself but is a free parameter. Different cases were simulated and the number of G stars forming this way was compared with the observed population in the halo. The best agreement was obtained by assuming the coalescence rate being on average twice as high as the fragmentation rate. This value was later taken as standard.

The simulations included 10 000 clouds with a total of 50 billion solar masses. Individual cloud masses initially covered a range from 1000 to ten million solar masses. Star formation only set in if a cloud exceeded a critical value of 10 000 solar masses. During each star formation episode three percent of the gas was converted into stars. At the same time, the intervals between successive star formation episodes were determined to be 20 million years. This way, a star formation rate of 1.5 solar masses per years was obtained. At the end of the simulation spanning one billion years stars with a total mass of some billion solar masses had formed from the gas in the halo.

The mass spectrum of the newly formed stars essentially determines how much heavy elements are created and ejected into the interstellar medium. The astronomers chose the standard Salpeter mass function with a maximum stellar mass of 120 solar masses.

The main goal of the simulation was to follow the evolution of europium and barium in relation to iron because good observational data are available for these elements. These metals are ejected into the interstellar medium by supernova explosions of type II within one billion years. For barium, winds from lower-mass stars in their later gi-

ant stage have to be considered, too. Production rates of elements in a supernova explosion are not known exactly but lie between several  $10^{-7}$  solar masses for europium and several  $10^{-6}$  solar masses for barium.

## Evolution of Metal Abundances

These parameters given, the model followed the evolution of the abundances of iron, europium, and barium within each cloud over time. Doing this, the effect of mergers between clouds with different star formation episodes became evident. Figure IV.15 shows the abundance of iron during one billion years. For comparison, a theoretical relation between age and abundance was also plotted which, however, does not take into account the mergers of clouds of different chemical composition described above.

Figure IV.15 clearly shows that the well-defined relation between age and element abundance has to be replaced by a statistical analysis of the observed data. One can notice, *e.g.*, that after some ten million years the spread in the iron abundance (in terms of the ratio of iron to hydrogen: Fe/H) ranges between  $10^{-6}$  and  $10^{-2}$ . It takes about one hundred million years for the clouds to mix up and thereby homogenize the chemical composition of the gas, the value for the iron abundance converging to about 10-2. Nevertheless, it is still possible for a star of Population II to have higher iron abundance than one of Population I.

Furthermore, the enrichment of the halo gas with europium was modeled. Figure IV.16 shows the europium abundance as a function of the corresponding Fe/H ratio instead of time. Here, too, one can recognize a wide scatter of the values compared to the simple model. The first small Eu concentrations occur after the first supernova explosions of stars of eight to ten solar masses and correspond to values of  $\text{Fe}/\text{H} = 10^{-5}$ . The model even produces clouds, which are enriched in europium having a ratio  $\text{Fe}/\text{H} = 10^{-5}$  but have formed later than clouds with a higher Fe/H ratio.

These results demonstrate that the determination of stellar ages based on element abundances is possible only with great uncertainties or on a statistical basis. Moreover, the results explain the broad variation of observed element abundances. To compare these observational data with the model predictions, the abundance ratios Eu/Fe and Ba/Fe were plotted as a function of Fe/H (Fig. IV.17a). Clearly, the wide spread is reproduced. Only for high values of the iron abundance ( $\text{Fe}/\text{H} = 0.1$ ) the model does not provide any values. This result can be modified by assuming higher star formation efficiency within the clouds, converting 30 % of the gas into stars (Fig. IV.17b). This model has the advantage of showing the effects of different parameters like star formation rate or production rate of the elements in supernovae on the enrichment history of the halo.

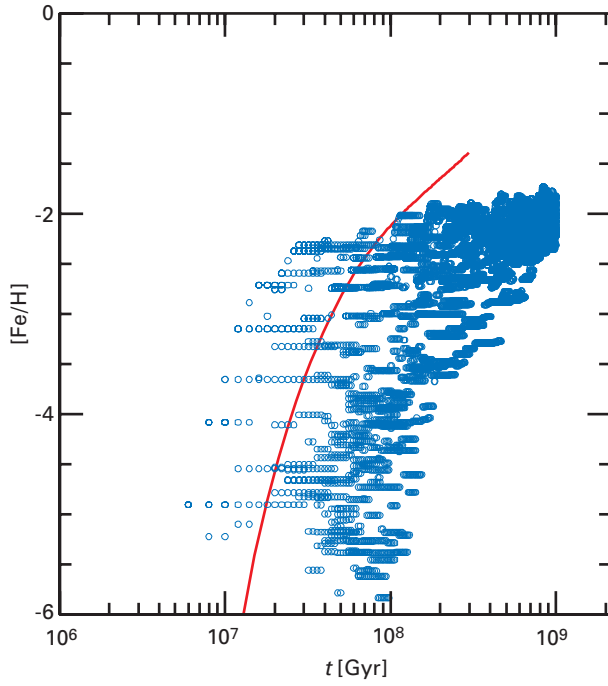


**Fig. IV.15:** Evolution of the abundance of iron during one billion years. Points represent the values of the numerical model while the solid line is based on the results of a chemical evolution model without mergers of gas clouds.

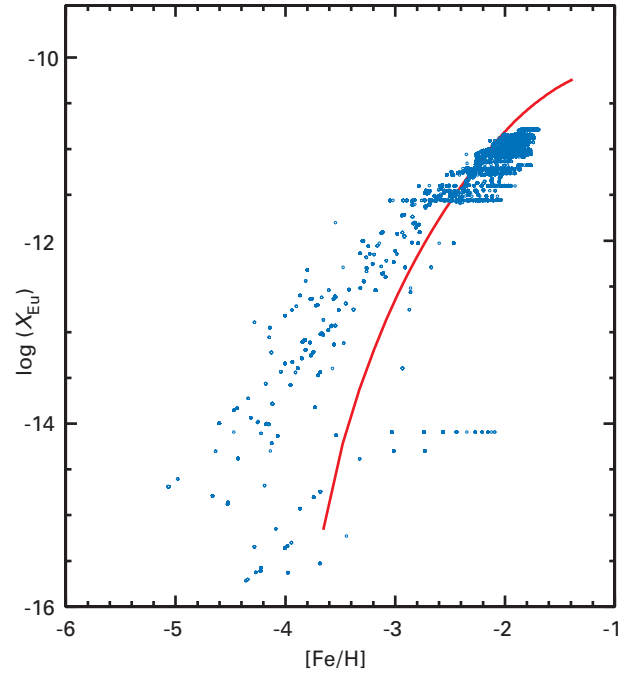


**Fig. IV.16:** Enrichment of europium as a function of the abundance of iron.

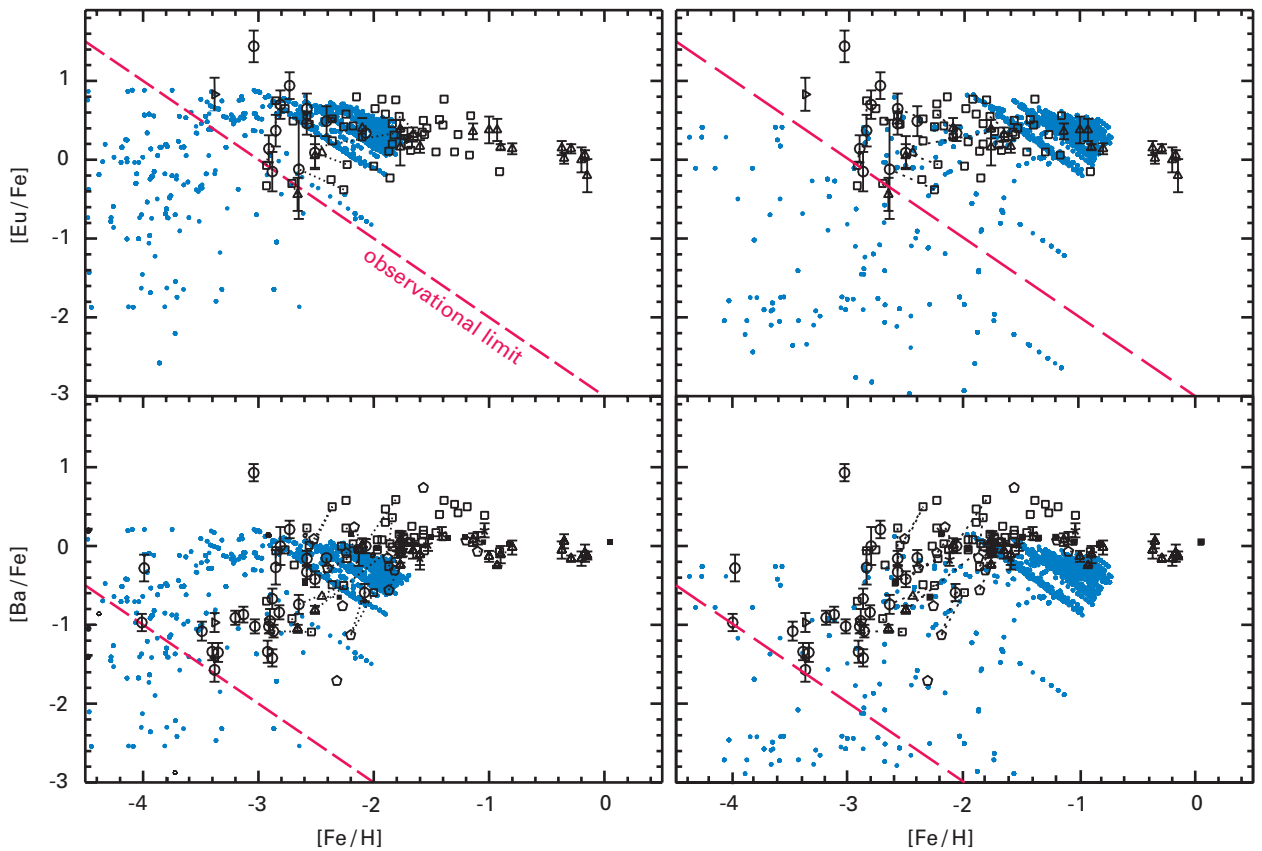


**Fig. IV.17: a)** Computed abundance ratios (small open circles) compared with observational data. Beneath the dashed line, no measurements are possible yet.

**b)** As a), but with a star formation efficiency ten times as high.

The model makes two more interesting predictions. For one thing, there should be a large number of stars with smaller Eu/Fe and Ba/Fe ratios than have been observed until now, lying beneath the dashed line. For another thing, the model predicts the existence of stars with  $\text{Fe}/\text{H} < 10^{-4}$  for the halo. They, too, have not been found yet.

Maybe these predictions of the model can be tested soon using instruments with a higher sensitivity than available today. In the future, this model will allow to compute also the evolution of further elements, which are forming in other stars, like red giants, for instance.

*(C. Travaglio, A. Burkert)*

## IV.2 Extragalactic Astronomy

### The Deepest Infrared Image – an Inventory of Stellar Masses in High Redshift Galaxies

**One of the most urgent tasks of astrophysics is to understand the formation and evolution of galaxies. Modern observational techniques have made it possible only recently to study a large number of galaxies out to large distances. Astronomers of the Institute together with colleagues from the Netherlands have started a galaxy survey in the southern sky. In the course of this Faint Infrared Extragalactic Survey (FIRES), images of the HUBBLE Space Telescope in visible light are combined with new near-infrared images obtained with the Very Large Telescope (VLT) of the European Southern Observatory (ESO). Up to now, these are the deepest and best images in this wavelength region. The goal is, among other things, to determine the magnitude distribution, sizes and shapes of galaxies over a wide redshift range and the evolution of their stellar masses. First results confirm the strategy of the method and have already revealed a number of interesting facts.**

Modern theories of the formation and evolution of galaxies start from a so-called hierarchical scenario. At first, galactic “building blocks” of dark matter, gas and stars were forming, growing only by dynamical merger processes into the present-day large galaxies. But it is still unknown at which epochs, respectively redshifts, these mergers between protogalactic fragments reached a maximum. And it is also unclear yet which effects these processes, accelerated by dark matter, had on star formation. It appears that cosmic star formation is declining today. But it is unclear at which epoch it had set in - maybe at a redshift around  $z = 6$  or earlier. One of the research goals is to find out at which time the rate of cosmic star formation was at its peak: When did the majority of present-day stars form?

Previous galaxy surveys did confirm the hierarchical scenario qualitatively but nevertheless this field of research is still at its beginning. In the future, galaxy surveys will provide significant new insights.

### The Faint Infrared Extragalactic Survey (FIRES)

Those surveys can be conducted in various ways, the kind of astronomical findings depending essentially on the wavelength region in which the survey is carried out. Structure, morphology and luminosity of (proto)galaxies depend on the observed wavelength since characteristic emission features of a galaxy are shifted towards longer

wavelengths with increasing distance because of the expansion of the Universe: The light which astronomers are receiving now from a galaxy lying at  $z = 1.5$  had been emitted when the Universe was about one quarter of its present age. The intense UV radiation of young hot stars in such a distant galaxy has been shifted from the original UV wavelength of about 200 nm to 500 nm which is in the visible spectral range. Thus, a sky survey conducted in visible light will be sensitive mainly for UV emission, which can originate only from galaxies with high star formation rates. But these galaxies in particular are frequently affected by strong dust extinction making them appear much fainter than they really are.

An infrared galaxy survey, in contrast, promises several major improvements. Most of the total mass of every stellar population is contained in stars whose emission maximum lies in the range of visible light, which is then redshifted into the infrared. So one has to observe this wavelength region in order to determine the evolution of stellar masses within galaxies. The goal of FIRES is to observe as many galaxies as possible over a wide redshift range at identical rest-frame wavelengths. The rest-frame wavelength is the unshifted wavelength of the radiation emitted at the locations of the respective galaxies. Moreover, galaxies with high star formation rates can be detected in the infrared region by their UV emission out to a redshift of  $z = 10$ .

FIRES is an observing project conducted by astronomers from Heidelberg, Leiden (Netherlands) and Garching at the ESO Very Large Telescope in Chile. Several fields in the southern sky for which very deep optical images of the HUBBLE Space Telescope are available were observed in the near infrared. In particular, the HUBBLE Deep Field South (HDF-S) was imaged during two observing runs in 1999 and 2000 in three filter bands with 100 hours exposure time. These images were taken with the ISAAC instrument at the VLT. In combination with the HUBBLE image of the HDF-S obtained in four filter bands these data represent the worldwide deepest image of a sky field in seven filter bands covering a wavelength range from 0.3  $\mu\text{m}$  to 2.2  $\mu\text{m}$  (Fig. IV.18). The K-band image (2.2  $\mu\text{m}$ ) is the deepest ever taken at this wavelength. Furthermore, three excellent images of the galaxy cluster MS 1054-03 were obtained in the course of FIRES at 1.25  $\mu\text{m}$ , 1.65  $\mu\text{m}$ , and 2.2  $\mu\text{m}$  wavelength.

From these data the redshifts of the galaxies were estimated using a photometric technique. In this method, the fluxes in the measured filter bands are compared with model templates of different galaxy types including several elliptical, spiral and irregular galaxies with extremely high star formation rates (starburst galaxies). Figure IV.19 exemplifies this technique.

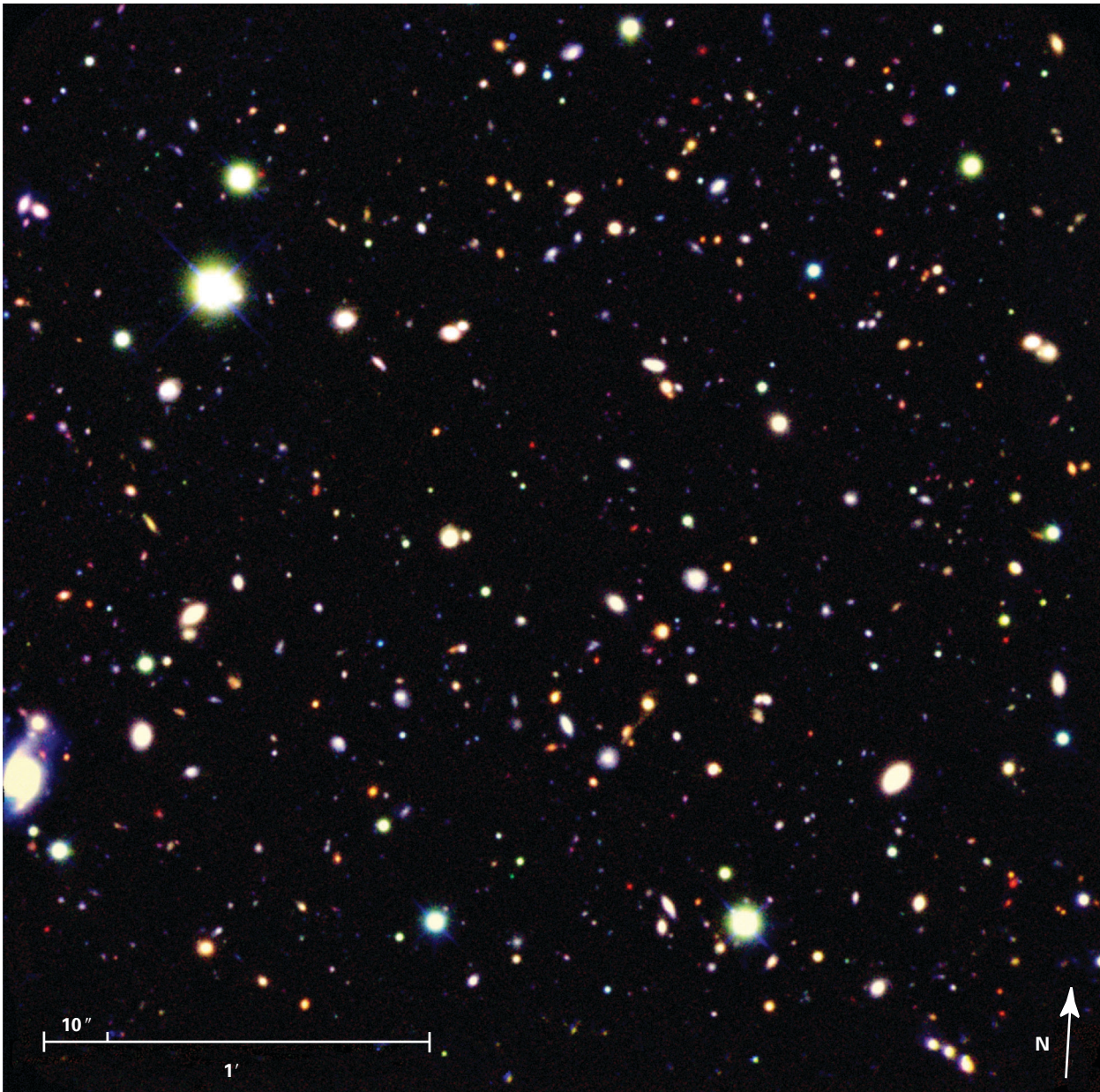


**Fig. IV. 18:** The HUBBLE deep Field South imaged with ISAAC at the VLT. The figure shows a superposition of the three images at 1.25, 1.65, and 2.2  $\mu\text{m}$ .

In order to test the accuracy of this technique some galaxies in the field were studied spectroscopically using FORS 1 at the VLT. The result was very encouraging: the photometrically obtained redshifts  $z$  of the galaxies with magnitudes down to 23.5 mag at 2.2  $\mu\text{m}$  wavelength showed an error of  $\Delta z/(1+z) = \pm 0.07$ . The entire galaxy catalogue in the HDF-S comprises 136 objects, which were selected for the first time on the basis of their near-infrared magnitude.

### Bright and Massive Galaxies in the Early Universe

The distribution of the redshift values is obtained immediately from the data (Fig. IV.20). It shows a prominent peak at  $z = 0.5$  and a broad enhancement up to  $z = 1.4$ . (At a redshift of  $z = 0.5$  the respective galaxy is seen in a state when the Universe was about half its present age.) Further analysis shows that this redshift interval mostly contains bright galaxies.

The evolution of the luminosity as a function of redshift can also be determined from the data. Figure IV.21 shows the result for luminosities in the blue spectral range. A remarkably large number of galaxies with luminosities higher than  $5 \times 10^{10}$  solar luminosities are found beyond  $z = 2$ . This number is very large compared to the results of galaxy surveys of the nearby Universe. It could be explained if the galaxies in the early Universe were ab-

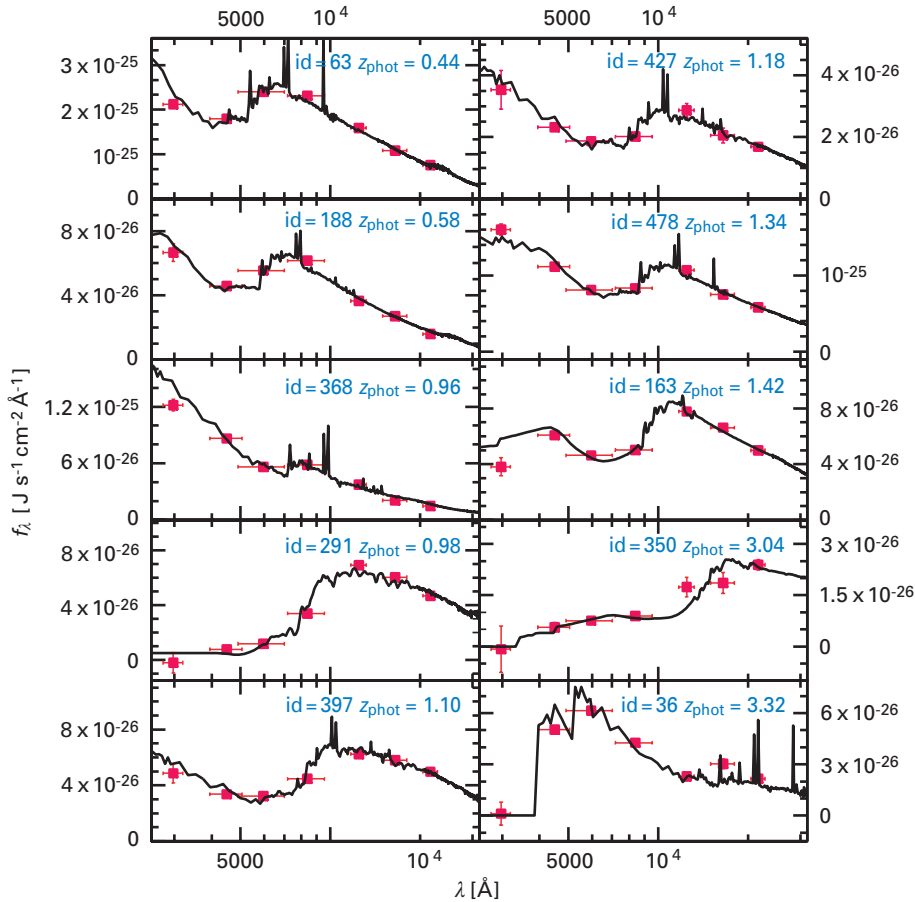


**Fig. IV.19:** Comparison of photometric data (squares) with templates of different galaxy types at different redshifts  $z$ .

out three times as luminous as today because of their high star formation rates. Detailed studies of these bright galaxies will provide information about processes, which took place when the Universe was only 15 to 20% of its present age.

### An Extraordinary Large Disk Galaxy at $z = 3$

Hierarchical models of galaxy formation predict all galaxies in the early Universe being small and compact. Large galactic disks should form only comparatively late at redshifts smaller than  $z = 1$  by the infall of matter. Surprisingly, the astronomers discovered an unusually large galaxy with a size of about 1.7 arc seconds at a high redshift of  $z = 2.793$  (Fig. IV.22). Depending on the adopted cosmological model, this value corresponds to a real diameter between 20 000 and 30 000 light years. At these high redshifts, optical images are dominated by the emission of hot, young stars. In the visible range, a ring-like structure is seen in this galaxy, quite similar to the large star formation regions in local galaxies like M 31 or M 81. At increasing wavelengths, this ring gradually vanishes giving way to a rather uniform, more compact brightness distribution. In the near infrared, the galaxy looks

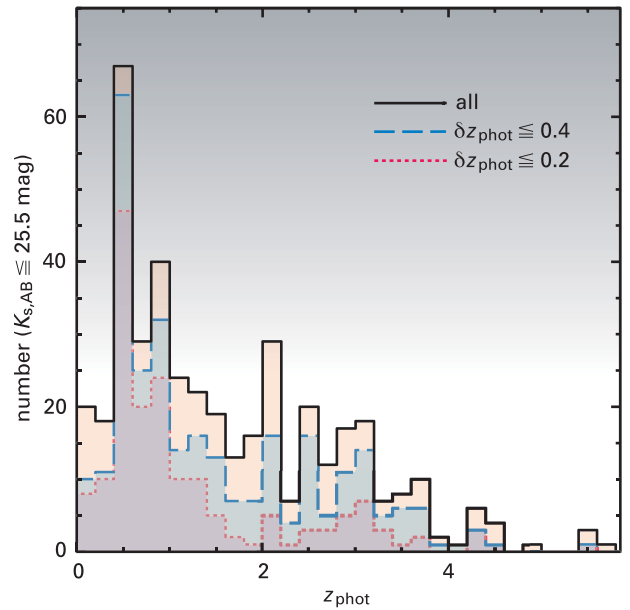


**Fig. IV.20:** Redshift distribution of 132 galaxies down to a magnitude limit of 23.5 mag at 2.2  $\mu\text{m}$  wavelength.

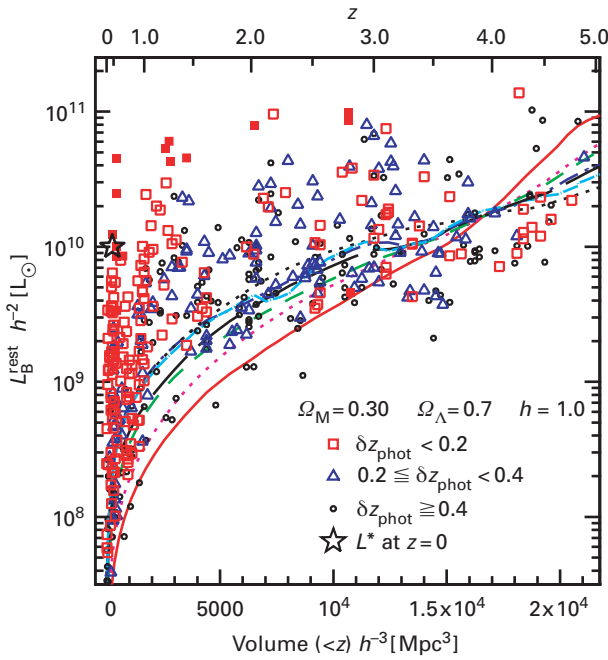


**Fig. IV.21:** Evolution of the luminosities in the blue spectral range as a function of redshift, compared to hierarchical models of galaxy formation. The lower scale gives the volume observed up to the respective redshift  $z$ .

symmetrical with a central brightening resembling the galactic bulge of present-day spiral galaxies.

The central condensation seen in the near infrared and the ring-like structure argue against the picture of two merging galaxies suggested by the hierarchical scenario. In principle, vast dust clouds could explain the wavelength-dependent morphology since optical radiation is obscured more heavily than infrared emission. But there is another attractive explanation. The central condensation in the infrared could originate from an old stellar population while the more ring-like emission in the optical

comes from young stars. So, do we see here a large spiral galaxy in the early Universe with an old core and a young disk population?

This scenario and the unusual size of the disk are in disagreement with most of the theoretical models of hierarchical galaxy evolution. According to them, the size of the predecessors of the present-day galaxies should be smaller than the disk observed here by a factor of ten. Future studies will have to search for other large disks in the early Universe because a single case can be easily explained by unusual circumstances.

**Old Galaxies at  $z = 2$ ?**

After classifying the galaxies their colors in the respective rest frames could be obtained from the data at hand. It was noted that a great number of red systems with high luminosities existed at all distance ranges. Although their fraction is somewhat smaller than that of blue bright galaxies, they are thought to have much higher mass-to-light ratios ( $M/L$ ). Therefore, they should contribute considerably to the total stellar mass encountered within a given redshift interval.

Using theoretical models, it was attempted to construct a time-dependent  $M/L$  ratio and to determine from it the stellar masses contained in galaxies. In the present-day Universe, one finds  $M/L \approx 2$  for spiral and  $M/L \approx 5$  for elliptical galaxies. It is demonstrated in Figure IV.23, that at all redshifts red galaxies are the most massive ones. Such a result can only be obtained with infrared data. Nevertheless, dust and other effects will still have to be considered here, too. The present result is to be understood as a first approach to this problem.

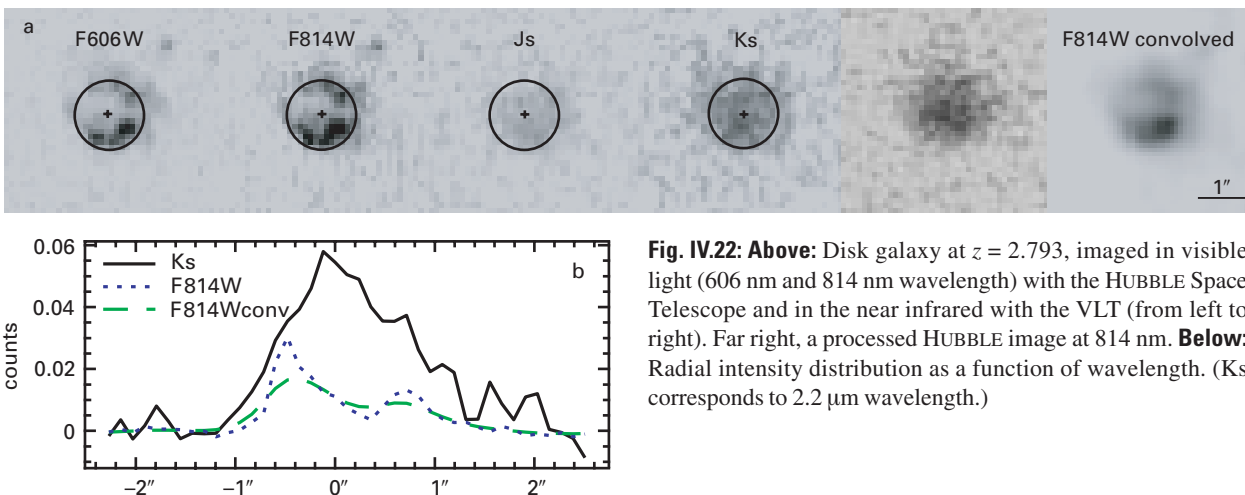


**Fig. IV.22:** Above: Disk galaxy at  $z = 2.793$ , imaged in visible light (606 nm and 814 nm wavelength) with the HUBBLE Space Telescope and in the near infrared with the VLT (from left to right). Far right, a processed HUBBLE image at 814 nm. Below: Radial intensity distribution as a function of wavelength. (Ks corresponds to 2.2  $\mu\text{m}$  wavelength.)

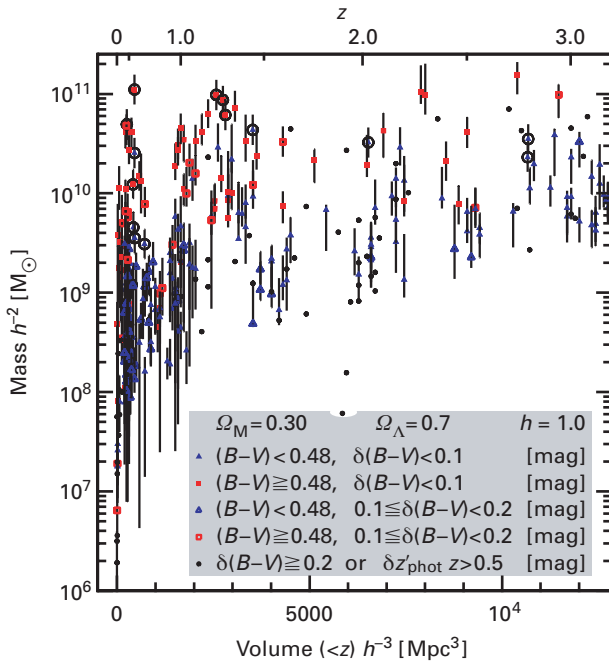


**Fig. IV.23:** Evolution of the stellar mass in galaxies as a function of redshift. Squares mark red galaxies, triangles blue ones. Circled symbols represent galaxies with spectroscopically measured redshifts.

### Limits and Future Tasks

In the future, more galaxy surveys of this kind will be conducted. Telescopes with high light-gathering power and sensitive cameras with large fields of view are available since recently. Future surveys should tackle mainly two questions: How do large-scale structures in the galaxy distribution (galaxy superclusters) and strong dust extinction within the galaxies affect the results?

Concerning the first question, one has to realize that up to a redshift of  $z = 1$  FIRES covers a volume corresponding to only two thirds of a typical galaxy supercluster. Between  $z = 2$  and  $z = 3.5$  it corresponds to about four times the volume. In the near range up to  $z = 1$ , random galaxy clustering or voids can therefore falsify the statistical result.

This shortcoming is being eliminated in a first approach by observing the region of the galaxy cluster MS 1054-03 covering about four times the area of the HDF-S. Moreover, the new Advanced Camera for Surveys aboard the HUBBLE Space Telescope is suited for surveys of this kind. The wide field camera OMEGA 2000 which is currently being built at MPIA and which will be installed at the Calar Alto 3.5 m telescope is also perfectly suited for near infrared surveys (cf. Chapter II).

(Gregory Rudnick, Hans-Walter Rix)

### Dust in Galaxy Clusters

In 1997, astronomers at the Institute caused a stir announcing the discovery of dust in the Coma cluster of galaxies (cf. Annual Report 1997, p. 26). Actually, it had been the first direct detection of intergalactic dust and was accomplished by analyzing the far-infrared data of the ISO space telescope. Last year, the same team inspected the data of five other galaxy clusters. But this time they did not discover any dust. Obviously, the Coma cluster is an exceptional case. This new result is in disagreement with a twenty years old controversial theory stating that hot gas in galaxy clusters cools down in so-called cooling flows and condenses into dust. But it confirms latest observations with the European XMM-NEWTON X-ray telescope, which also seem to disprove the theory of cooling flows.

The space between galaxies in clusters is not completely empty as images taken in visible light might suggest. Rather, there exists a very finely distributed hot gas at temperatures of several million kelvins. Because of its high temperature it emits only in the X-ray region. This intergalactic gas has an average density of about a thousand atoms per cubic meter - roughly a thousand times lower than the density of the diffuse interstellar gas in the Milky Way Galaxy.

In the 1980s, the discovery of intergalactic gas led to a theory which is controversial up to now: At that time, some astrophysicists concluded from the X-ray emission which is concentrated strongly towards the center of the cluster that the gas there should be very dense and cooler than in the outer regions. The cooling should increase in a process reinforcing itself and the gas should finally condense into a still unknown form - into stars, for instance, or into cold dense clouds containing dust. The condensation reduces the pressure at the center causing gas lying further out to flow inwards, cool down and condense, too. According to the inferred inward flow of gas the phenomenon was named "cooling flow".

From the data available at that time, astronomers estimated that in extreme cases more than one thousand new stars could form in the cooling flows this way each year - an incredibly high rate compared to an average spiral galaxy like the Milky Way where roughly one new star appears per year. Thus, this prognosticated process should profoundly affect the evolution of galaxy clusters.

This sensational theory, however, could never be confirmed beyond doubt. Only some vague evidence of dust was found, e.g., in studies of galaxies and quasars lying behind galaxy clusters. These studies indicated that the surface density of observable background galaxies decreases towards the center of a cluster lying in front of them. This could be explained by a homogeneous distribution of dust in the cluster, which would absorb the light

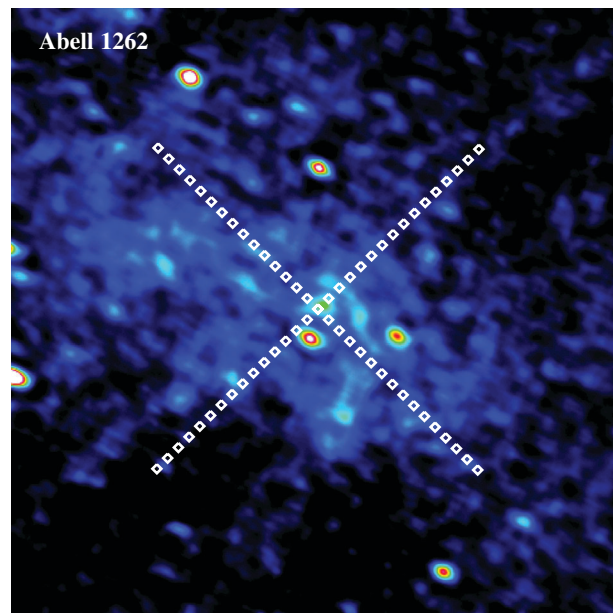
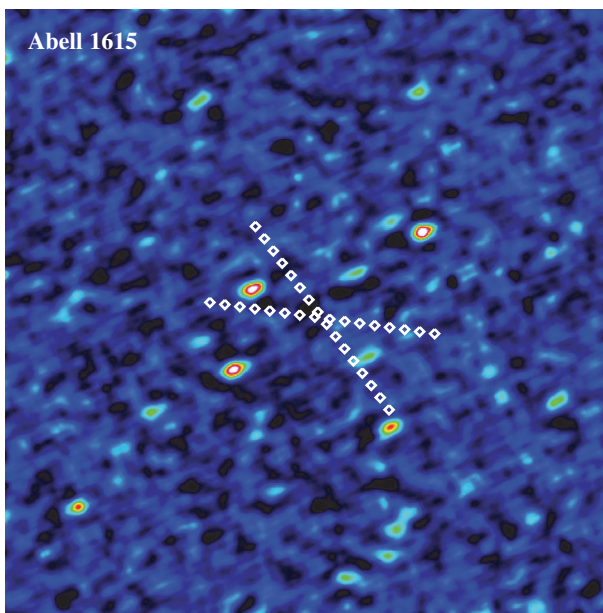
passing through the central region more strongly than that in the outer regions.

However, all studies of this kind were not convincing. The visual extinction at the central region of the Coma cluster was estimated to be less than 0.3 magnitudes. An investigation of more than 60 clusters in the infrared range using the IRAS satellite telescope and in the sub-millimeter range could not provide any evidence for the existence of diffuse intergalactic dust.

The ISOPHOT instrument built under the leadership of the MPIA offered an additional possibility to tackle the problem by observing galaxy clusters in the hitherto in-

Only then an almost symmetric intensity increase around the central region was noticed. This behavior is due to the radiation properties of the intergalactic dust in the Coma cluster, which differ from those of the Galactic cirrus in our own Milky Way System.

Furthermore, the analysis has to take into account the zodiacal light. Because of its rather high temperature, this diffuse dust in our solar system emits only very little in the far-infrared region beyond  $100\ \mu\text{m}$ . But if a localized patch of Galactic foreground cirrus happens to lie along the line of sight to a galaxy cluster, even the small contribution from the zodiacal light will cause the same charac-



accessible spectral range beyond  $100\ \mu\text{m}$  where very cold dust becomes apparent. In addition to the Coma cluster, the astronomers studied five other clusters selected according to special aspects. The Coma cluster is known to undergo merging with other smaller galaxy groups. It was suggested therefore that the dust has been swept from the intruding galaxies rather than having condensed from the intergalactic gas as claimed by the cooling-flow model. The other five clusters were selected under the aspect of a morphological variety as large as possible. They covered a redshift range between  $z = 0.023$  and  $0.076$ , corresponding to distances of about 650 to 2100 billion light years.

In 1997/1998, the five galaxy clusters were observed using ISOPHOT, the exposure times being between 50 and 100 minutes. Each cluster was scanned along two perpendicular axes measuring the intensities at  $120\ \mu\text{m}$  and  $185\ \mu\text{m}$  (Fig. IV.24).

In the analysis, the IR fluxes of the four detector pixels were first determined separately for each image and subsequently averaged. The study of the Coma cluster (Abell 1656) already had shown that dust only became apparent when intensity ratios at  $120\ \mu\text{m}$  and  $185\ \mu\text{m}$  were taken.

**Fig. IV.24:** Galaxy clusters Abell 1656 (Coma) and Abell 262, imaged with the IRAS infrared satellite at  $100\ \mu\text{m}$  wavelength. The crossed ISOPHOT scans are marked.

teristic modification of the  $120\ \mu\text{m}/185\ \mu\text{m}$  intensity ratio as the intergalactic dust in the galaxy cluster itself. From the differences between the  $120\ \mu\text{m}/185\ \mu\text{m}$  ratios with and without the contribution of zodiacal light the causer of a change in the  $120\ \mu\text{m}/185\ \mu\text{m}$  ratio can be identified. But if the properties of the intergalactic dust closely resemble that of the Galactic cirrus, there is no possibility to separate the two components even by subtraction of the zodiacal light.

All galaxy clusters were analyzed using this method. The Coma cluster again showed an almost symmetric run of intensity (Fig. IV.25). But such a run was not found for the other clusters as is illustrated by the cluster Abell 262. Here, the intensity ratios at  $120\ \mu\text{m}$  and  $185\ \mu\text{m}$  (Fig. IV.26 a) show a minimum around the central region. After subtraction of the zodiacal light component (Fig. 26 b), however, only a monotone incline is left which can be attributed to the Galactic cirrus.

The dust within the Coma cluster must differ in properties such as temperature, particle size and composition from the Galactic cirrus because otherwise both components could not be separated. These properties, however, are difficult to determine. From the data a minimum temperature of 30 K is derived. The interior of the cluster probably contains hardly more than 107 solar masses of cold dust. From this follows also a very low extinction of less than 0.1 magnitudes.

If any, only very small amounts of dust can be present in the other galaxy clusters. This confirms the assumption that intergalactic dust is of no relevance in most of the galaxy clusters. As mentioned before, there probably are special conditions prevailing in the Coma cluster. Currently, two scenarios for the origin of dust are discussed: Either dust is blown constantly from the galaxies into intergalactic space by stellar winds or it was swept from the galaxies during the merger of two galaxy clusters. The second scenario in particular could apply to the Coma cluster as various observations indicate that this

cluster has a rather low dynamical age and consists of two interpenetrating or merging clusters whose central galaxies once were NGC 4889 and NGC 4874, respectively.

This result is of cosmological significance, too, as it shows that intergalactic dust hardly affects the view of distant regions of the Universe. This is very important, *e.g.*, for various methods of measuring cosmological distances.

In particular, the results can be taken as a strong argument against the cooling-flow hypothesis. Recent X-ray observations with the European XMM-NEWTON space telescope seem to disagree with this theory, too, as they failed to detect cooling gas. This suggests the intergalactic gas to be continually heated. The heating could be achieved by energetic particle beams, or jets, which are spurting from the centers of active galaxies. This phenomenon is also investigated by astronomers at the MPIA (cf. the following section).

(Manfred Stickel, U. Klaas, D. Lemke)

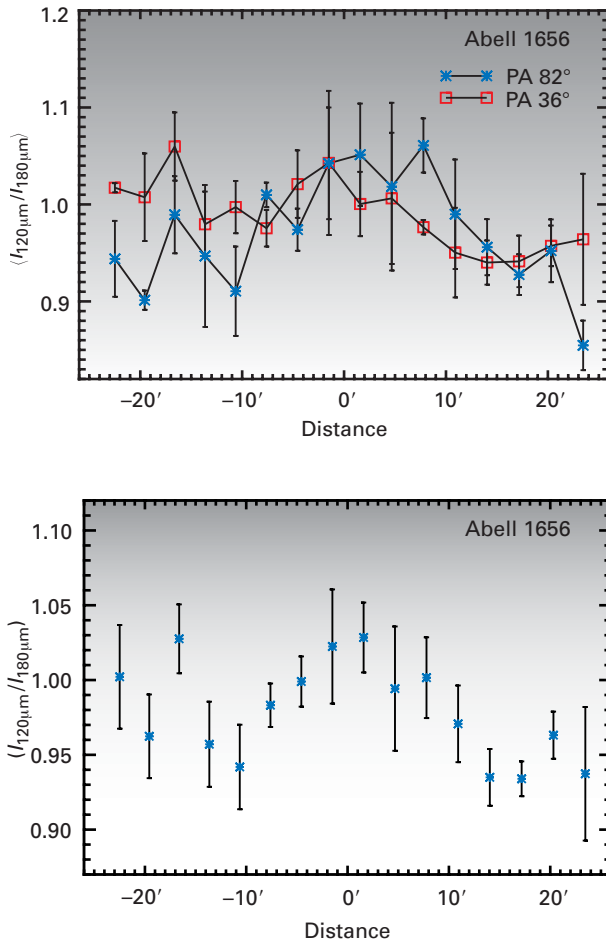


**Fig. IV.25:** **a)** Intensity ratios at 120  $\mu\text{m}$  and 185  $\mu\text{m}$  wavelength along both scans across the Coma cluster (Abell 1656) after subtraction of the zodiacal light; **b)** average of both scans shown in a).

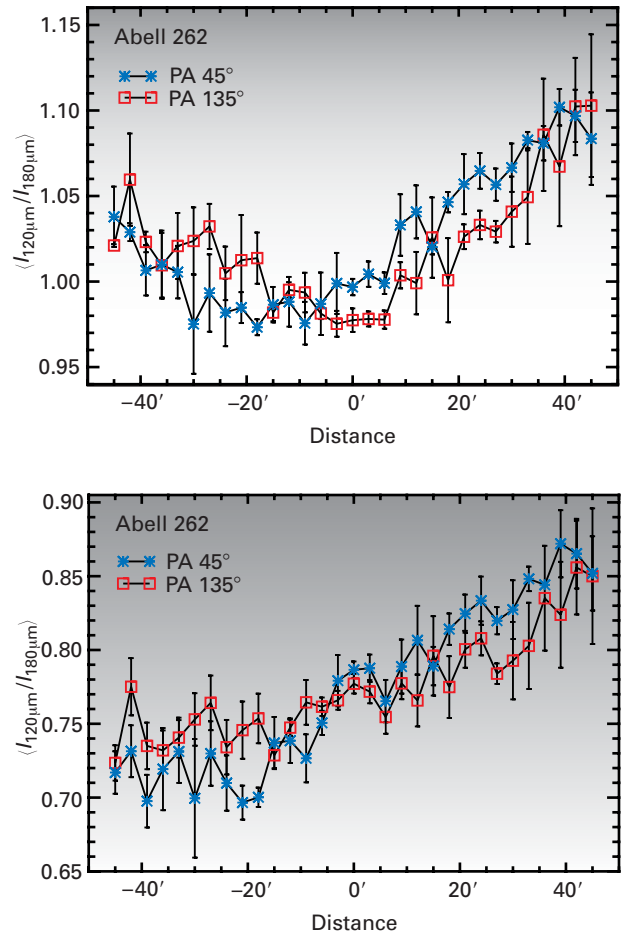


**Fig. IV.26:** **a)** Intensity ratios at 120  $\mu\text{m}$  and 185  $\mu\text{m}$  wavelength along both scans across the galaxy cluster Abell 262 after subtraction of the zodiacal light; **b)** average of both scans shown in a). The linear ascent can be attributed to the foreground Galactic cirrus.

## The Jet of the Quasar 3C 273

Numerous radio galaxies and quasars show an interesting phenomenon: one or two plasma beams, so-called jets, emanate from their central regions, sometimes stretching over several million light years into space and ending in extended radio lobes. Up to now, several hundred jets are known in the radio range. About fifteen jets are also observable in visible light, but only three of them are extended and bright enough to be studied spatially resolved, among them the jet of the quasar 3C 273. Astronomers at the MPIA have investigated this jet with high resolution using the HUBBLE Space Telescope for the optical and the Very Large Array for the radio range. The new data suggest that two particle populations with different energy distributions exist in the jet. These results raise new questions about the acceleration process of the jet particles.

The jet of 3C 273 can be optically detected over a distance from 11 to about 20 arc seconds from the quasar, corresponding to a projected length from the core of 123000 light years (adopting a Hubble constant of 65 km/(s Mpc)). On long exposures the jet appears as a series of bright knots with a diffuse medium in between (Fig. IV.27).

## Particle Acceleration and Synchrotron Emission

The jet originates at the center of the quasar where according to current theory a black hole resides. It is surrounded by a gaseous disk from which matter spirals into the black hole. In a hitherto unknown process, part of the gas is accelerated perpendicular to the disk probably by magnetic fields and confined into jets, which propagate into the intergalactic medium.

The observed jet emission is synchrotron radiation produced by charged particles moving with relativistic speeds in strong magnetic fields. The streaming particles in the jets probably are mostly electrons and maybe also their antiparticles, positrons. But in principle, a plasma consisting of electrons and protons cannot be excluded. As synchrotron emission produces a purely continuous spectrum without any absorption or emission lines the streaming velocity of the gas cannot be measured directly. Based on numerous findings, however, the jet gas is thought today to move outwards at almost the speed of light.

But it is still a puzzle how the particles within these jets are accelerated permanently to highly relativistic energies. Synchrotron radiation of a given frequency is emitted only by electrons with a given energy. A particle having a higher energy is radiating at a higher frequency. By emitting radiation, though, it loses energy and over the course of time it can be observed only at increasingly lower frequencies. After a few thousand years, an electron originally emitting optical or infrared synchrotron radiation has lost so much energy that it emits only in the radio range. So electrons radiating in the infrared or optical range certainly cannot travel the entire length of the jet of 3C 273 but have to be continuously re-accelerated at the location of their emission.

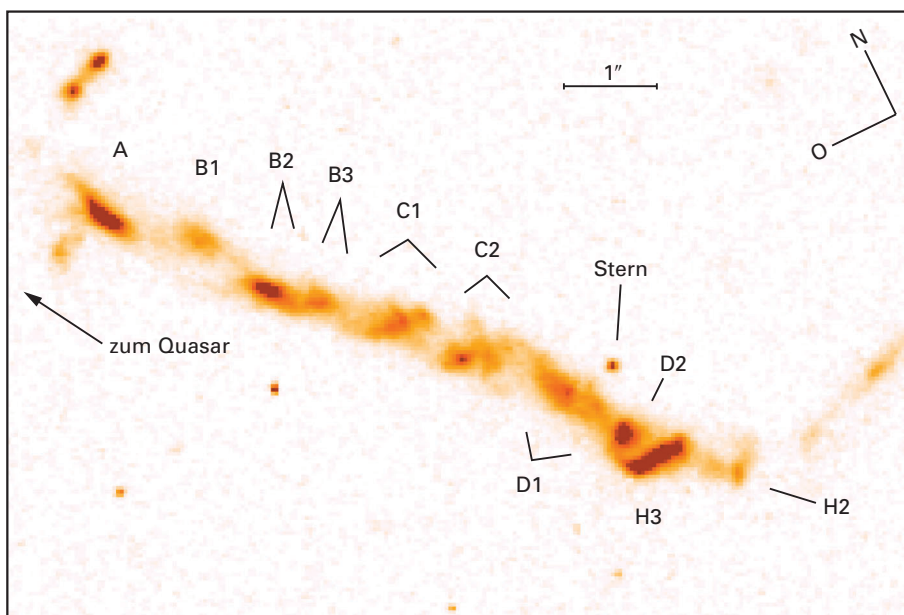


**Fig. IV.27:** The jet of 3C 273 imaged with the HUBBLE Space Telescope. The resolution here is limited by the pixel size of 0.05 arc seconds.

Since the 1980s, astronomers at the Institute are studying intensively extragalactic jets and have contributed significantly to the clarification of this phenomenon. So they were able in 1997 to obtain the first deep near-infrared image of the 3C 273 jet using the 3.5 m telescope on Calar Alto. Closing the gap between the optical and the radio range, the IR data were of great importance to the determination of the intensity run of the synchrotron emission (cf. Annual Report 1997, p. 64). From the data the astronomers had concluded that the particles are accelerated not only within the knots, as had been assumed for a long time, but also in the regions in between.

### Observations with the HUBBLE Space Telescope (HST) and the Very Large Array (VLA)

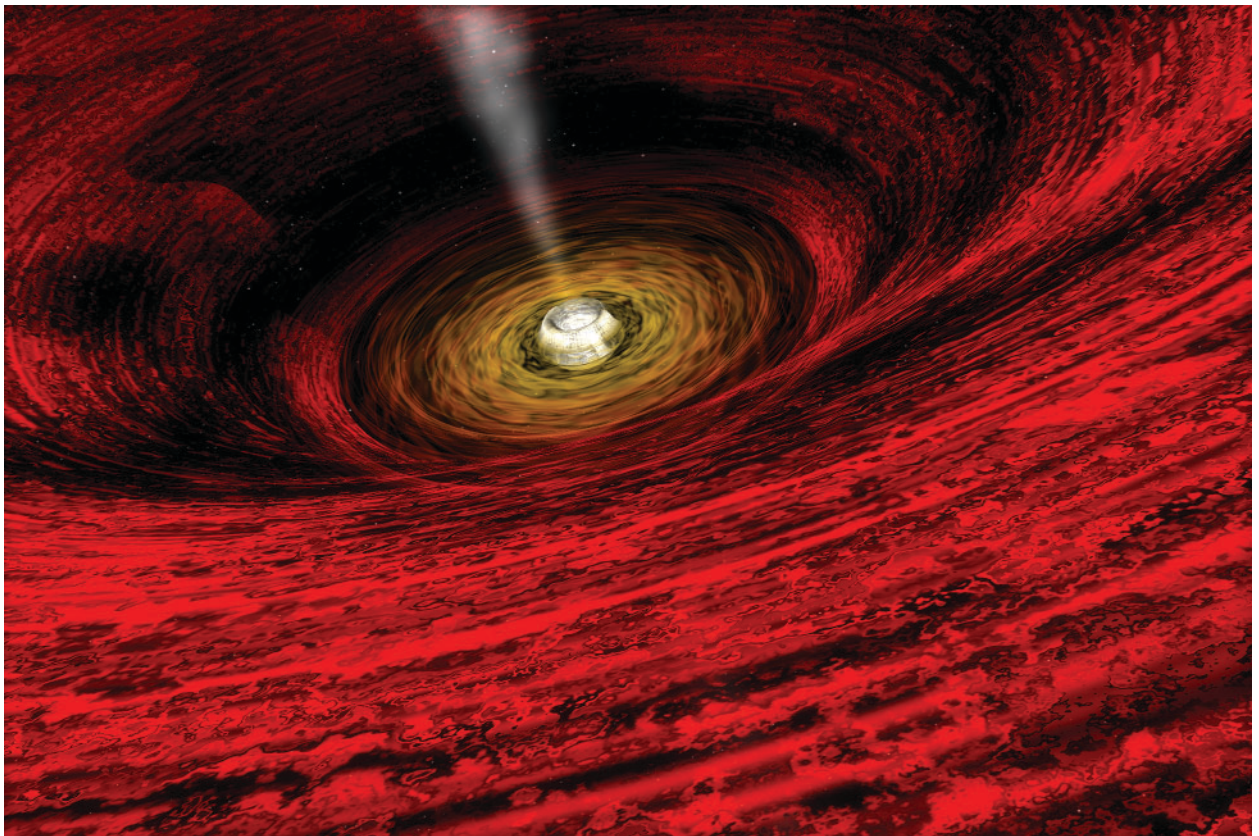
Together with colleagues from the USA and Great Britain, astronomers at MPIA observed the jet of 3C 273 using the Wide Field and Planetary Camera 2 onboard the HST. Exposure times were a little less than ten hours in the UV (301 nm wavelength) and almost three hours in the red (620 nm). During another ten hours observing time images at 1.6  $\mu\text{m}$  were obtained using the NICMOS infrared camera onboard the HST. New observations with the VLA at Socorro, New Mexico, constitute the second part of the data set. From the radio data images at 1.3 cm, 2 cm and 3.6 cm wavelengths were selected and subsequently superimposed with the HST data using a common

resolution of 0.3 arc seconds corresponding to 1800 light years at the location of the jet. This way, a homogeneous data set was obtained.

These new observations, being the most detailed and deepest images of this jet so far, reveal some interesting new details. In the optical images, e.g., criss-cross patterns in the knots can be discerned, particularly in the knots C1 and C2 (Fig. IV.28). These pattern could be an indication for a helical structure of the jet similar to the double helix of the DNA molecule. But it is also conceivable that the criss-cross structure is produced by the superposition of two shock waves within the flowing plasma.

From the combined VLA and HST data the spectral distribution of the synchrotron emission, that is, the intensity of the radiation as a function of frequency could be obtained over a very broad spectral range. The emitted spectrum first runs continuously and then drops steeply beyond a certain frequency. This means that there are hardly any electrons emitting synchrotron radiation above this cut-off frequency. Because of the relation between frequency and particle energy the maximum energy of the electrons can thus be determined.

**Fig. IV.28:** Computer simulation of a black hole surrounded by a disk with a jet emanating from its center.



Based on the new data the research team could determine the maximum particle energy spatially resolved and measure variations along the jet as well as across it (Fig. IV.29). Along the jet, the maximum particle energy is found to decrease generally with increasing distance to the quasar. The crucial fact is that the maximum energy is decreasing very slowly and almost continuously and that the variations of the maximum energy are less prominent than the brightness variations (with the exception of knots A-B, see Fig. IV.27).

This confirms the assumption that the electrons are re-accelerated within the entire jet rather than in the knots only. Further confirmation comes from estimates of the lifetime of the relativistic electrons. As mentioned above, these electrons lose so much energy by emitting synchrotron radiation that without continuous energy supply they would not be able to travel the distance of about 6500 light years between two knots and remain visible for the HST.

### Two Populations of Electrons

Recent observations with the CHANDRA X-ray space observatory show that more jets than thought up to now are emitting X-rays. For 3C 273, X-ray emission of the jet had already been detected with the ROSAT satellite and was now confirmed by CHANDRA (Fig. IV.30). How are the X-rays generated?

The optical and radio emission is established to be synchrotron radiation emitted by the same electron population. This has been proven by observations already published in 1991 by astronomers at the Institute. The X-rays, however, seem to be of different origin. Astronomers at MPIA suppose a second particle population to emit this highly energetic radiation, plus an additional significant fraction of the UV emission.

This assumption is made because the analysis showed the intensity of the jet emission in the high-frequency optical and in the UV range to exceed the theoretical values extrapolated from the low-frequency radio and infrared range. This is the first time that such a behavior is found in an extragalactic jet. It suggests that, in those two spectral ranges, the emission is not generated by the same electrons.

In a simple model, the astronomers were able to describe the “excess” of UV emission very well by extrapolating the X-ray data, at least for the three brightest knots of the jet. This suggests a common origin of both of these contributions. Thus the new data indicate a second electron population emitting synchrotron radiation in the UV and X-ray range.

However, there is another possible emission mechanism for the UV and X-ray radiation: the so-called Self-Compton-effect. In this process, the relativistic electrons collide with the photons of the synchrotron emission providing them with an additional energy and thus shifting

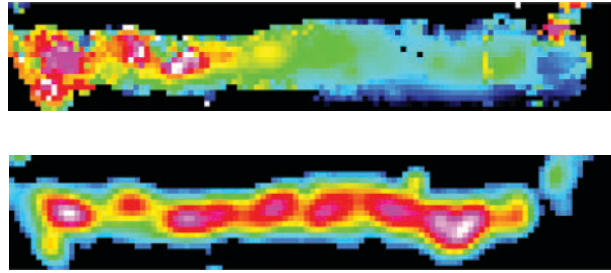


**Fig. IV.29:** a) Map of the maximum energy of the electrons in the jet. The maximum energy is decreasing from purple to red to green to blue; b) the image of the jet at 620 nm smoothed to 0.3 arc seconds is shown for comparison.

them into the UV and X-ray range. For this model to be in agreement with the observations, the entire jet would have to be highly relativistic and move almost along our line of sight.

Based on the available observational data, this issue cannot be settled yet. Further measurements in the optical, UV and X-ray region are needed to determine the run of the spectral index in greater detail. The best method would be to measure the polarization of the X-ray emission. Observations of this kind, however, will be possible only with future space observatories.

*(S. Jester, H.-J. Röser, K. Meisenheimer)*

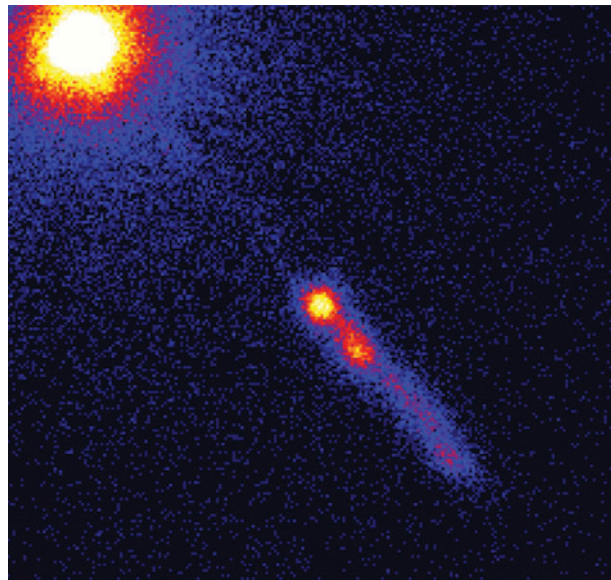


**Fig. IV.30:** X-ray image of the 3C 273 jet with the CHANDRA X-ray telescope. (NASA)

### Spiral Systems in Elliptical Galaxies

About 80 years ago, Edwin Hubble developed a classification scheme for galaxies, which basically is still in use today (Fig. IV.31). Accordingly, galaxies are broadly divided into three major types: elliptical, spiral and irregular. Hubble suspected at that time that his scheme might represent an evolutionary sequence running from the ellipticals to the spirals. This idea has been dismissed today. Instead, theoretical arguments as well as observational data increasingly suggest that elliptical galaxies form from mergers of spirals. Two years ago, the theory group at the Institute had already been able to confirm this hypothesis by numerical simulations (cf. Annual Report 1999, p. 67). In recent simulations, however, the theoreticians discovered an interesting phenomenon: In order to explain the observed stellar motions in elliptical galaxies, one has to assume a stellar population being arranged in a disk around the central region.

Elliptical and spiral galaxies clearly show different morphologies. In spirals, the stars are arranged in a disk with a more or less prominent spheroidal accumulation of stars at their centers, the so-called bulge. The spiral arms are varying in their distinctness. Elliptical galaxies are characterized by a tri-axial shape similar to a rugby-ball. The degree of oblateness depends on the viewing angle under which the system is seen. If one looks in the direction of the major axis the galaxy appears circular; at right angles to this direction, it is seen as highly elliptical.

Both galaxy types also differ significantly in their kinematics. The disks of spiral galaxies are dominated by the orbital motion of the stars around the center. Random stellar motion, the so-called velocity dispersion, is low, only about 10 % of the rotational velocity. For elliptical galaxies, in contrast, the situation is exactly inverted. Here, the stars move on irregular unorganized orbits and

the velocity dispersion often exceeds the rotational velocity.

Moreover, marked differences occur within the group of ellipticals. On one hand, there are systems which are rotating rather fast and whose isophotes (lines of equal brightness) deviate from the perfect elliptical shape, being more elongated (disky) and rather similar to the isophotes of disks. On the other hand, there are systems, which are rotating more slowly, showing angular (boxy) isophotes.

Astronomers at the Institute were able to explain this difference with the help of numerical simulations. According to them, elliptical galaxies with boxy isophotes form by mergers of two spiral galaxies of the same size while low-luminosity ellipticals with disky isophotes originate from mergers of a massive and a low-mass spiral galaxy.

While the photometric properties of elliptical galaxies could be explained very well within the merger scenario, questions concerning kinematic characteristics remained unsettled. Now, the theoreticians wanted to explain the observed velocity dispersions, too, by computing new simulations.

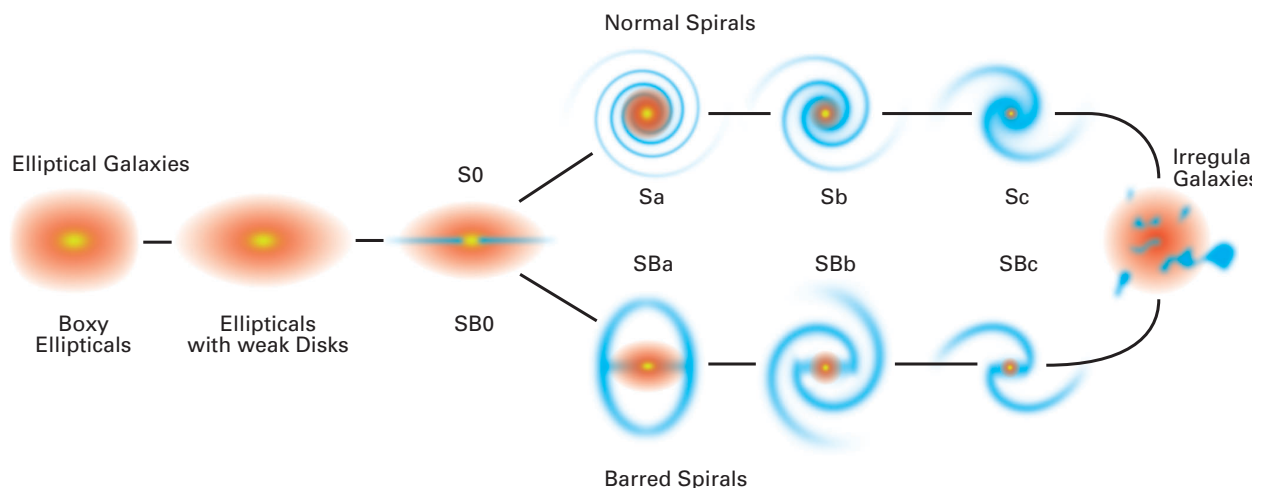
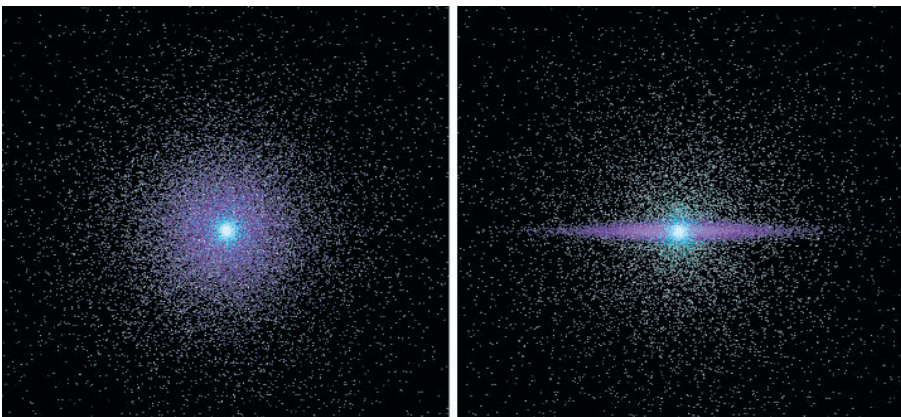


Fig. IV.31: Classification scheme for galaxies developed by Hubble.

### Simulations of the Kinematics

These computations, like the previous ones, distinguished two cases: the merger of two spiral galaxies of the same size and that of two spirals with a mass ratio of 3:1. The massive galaxies were represented by 200 000 test particles each, forming the central bulge (20 000 particles), a disk with exponentially decreasing density profile (60 000 particles) and a spherical halo of dark matter (120 000 particles) (Fig. IV.32). In the case of the 3:1 model the smaller galaxy was represented by one third of the particles.

The simulation only studied the dynamical behavior of the particles, that is, their gravitational interactions. More complex processes within a gaseous component (such as compression, heating, star formation etc.) were ignored. Moreover, the astronomers chose two different geometries for the motion of the merging galaxies in which two co- or counter-rotating disks approach one another on parabolic trajectories. Both disks are inclined by 30 and  $-30$  degrees respectively, to the orbital plane. As the team was able to show in a separate study, both geometries yield generally representative results. After the merger the simulation was carried on long enough for the newly formed system to reach a state of equilibrium (Fig. IV.33).



**Fig. IV.32:** Distribution of the test particles of a spiral galaxy at the beginning of a simulation.

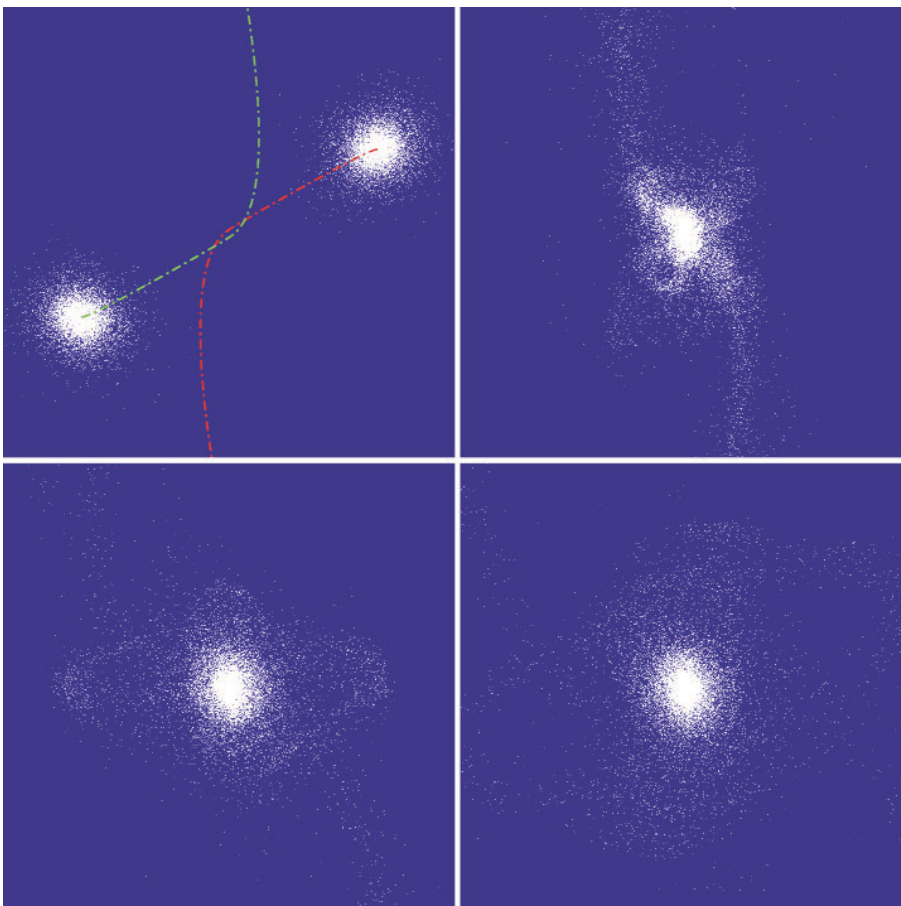


**Fig. IV.33:** Four stages of the merger of two spiral galaxies of the same size forming an elliptical galaxy. The dashed lines represent the trajectories of the galaxies.

Afterwards, the projected velocity dispersions were inferred from the model, as they would be measured with the telescope. Thus a comparison between the results of the model and actually measured data became possible. Finally, the particle velocities obtained for each measuring interval were fitted with a Gaussian function. This way, it was possible to compare quantitatively the results of the simulation with the observed data.

Fig. IV.34 shows the velocity normalized to the velocity dispersion ( $v/\sigma$ ) as a function of a quantity called  $H_3$ . A large (positive or negative) value of  $v/\sigma$  means a rapidly rotating (retrogradely or progradely) galaxy.  $H_3$  is a measure of the asymmetry of the Gaussian function. As can be noted clearly, the simulated values (dots) do not agree with values typical for elliptical galaxies (straight lines). This means that in a real elliptical galaxy there are more stars moving at high orbital velocities around the center than calculated in the model. Only model B, representing two counterrotating merging galaxies of the same size, is roughly in agreement with the observations. This case yields highly anisotropic elliptical galaxies without significant rotation.

Interestingly, the model values are in much better agreement with the observational values if a disk is assumed to exist in the central region of the elliptical galaxy. In further simulations taking into account such a disk, its mass and size were left as free parameters. Fig. IV.35 shows the effect of such a disk on the kinematics. Here, a thin central disk with 15% of the galaxy's mass and a radius corresponding to 1.25 times the half-light radius of the elliptical galaxy was added to the 3:1 model. If a more massive disk is chosen the theoretical values are in discrepancy with the observations.

Therefore the astronomers assume a disk-like component with a mass fraction of 10 to 20% to exist at the centers of almost all elliptical galaxies. Actually, several of such cases have been observed in the 1990s, particularly in rapidly rotating galaxies with diskly isophotes. It is still unclear yet how such disks can form. Maybe they are a result of the merger. The theoreticians at the Institute have tested this idea, too, by numerical simulations.

Up to then, they had not taken into account the complex interactions of the interstellar gas. In their new simulations the model was extended to include this component. It turned out now that during the merger large amounts of gas are expelled from the galaxy in form of long "tidal arms" as it is also seen, *e.g.*, in the famous case of the Antennae (Fig. IV.36). After the merging process within the central regions, part of this gas falls back into the newly formed galaxy accumulating there in a disk (Fig. IV.37). It seems altogether plausible that in the course of time new stars are forming in this interstellar medium creating a disk population as it is required by the simulations and already has been observed in some cases.

So the outlines of the formation of elliptical galaxies get clearer and clearer. Nevertheless, there are still several aspects, which have to be followed up. So at least some

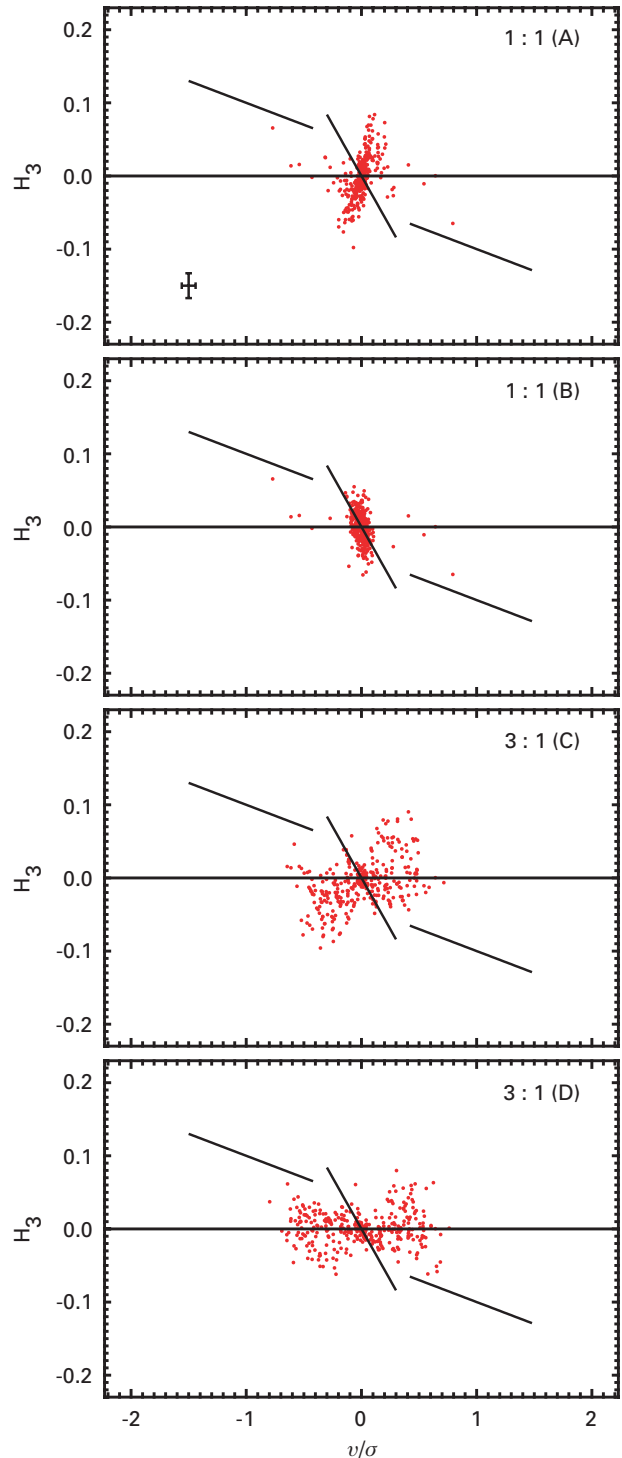


**Fig. IV.34:** Correlations of  $v/\sigma$  as a function of  $H_3$ . Each dot represents the value of the respective model viewed under 50 different viewing angles. Straight lines represent typical observational values.

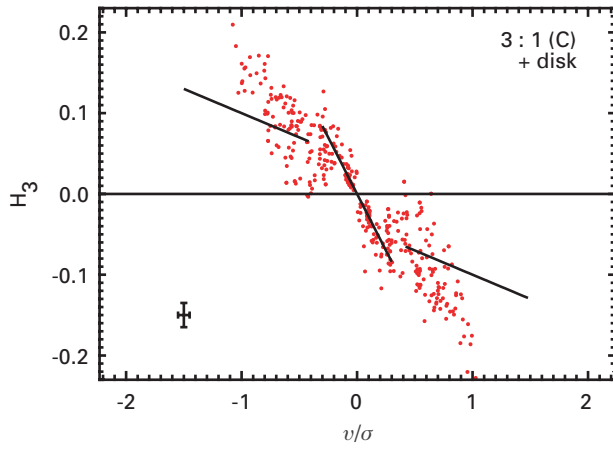
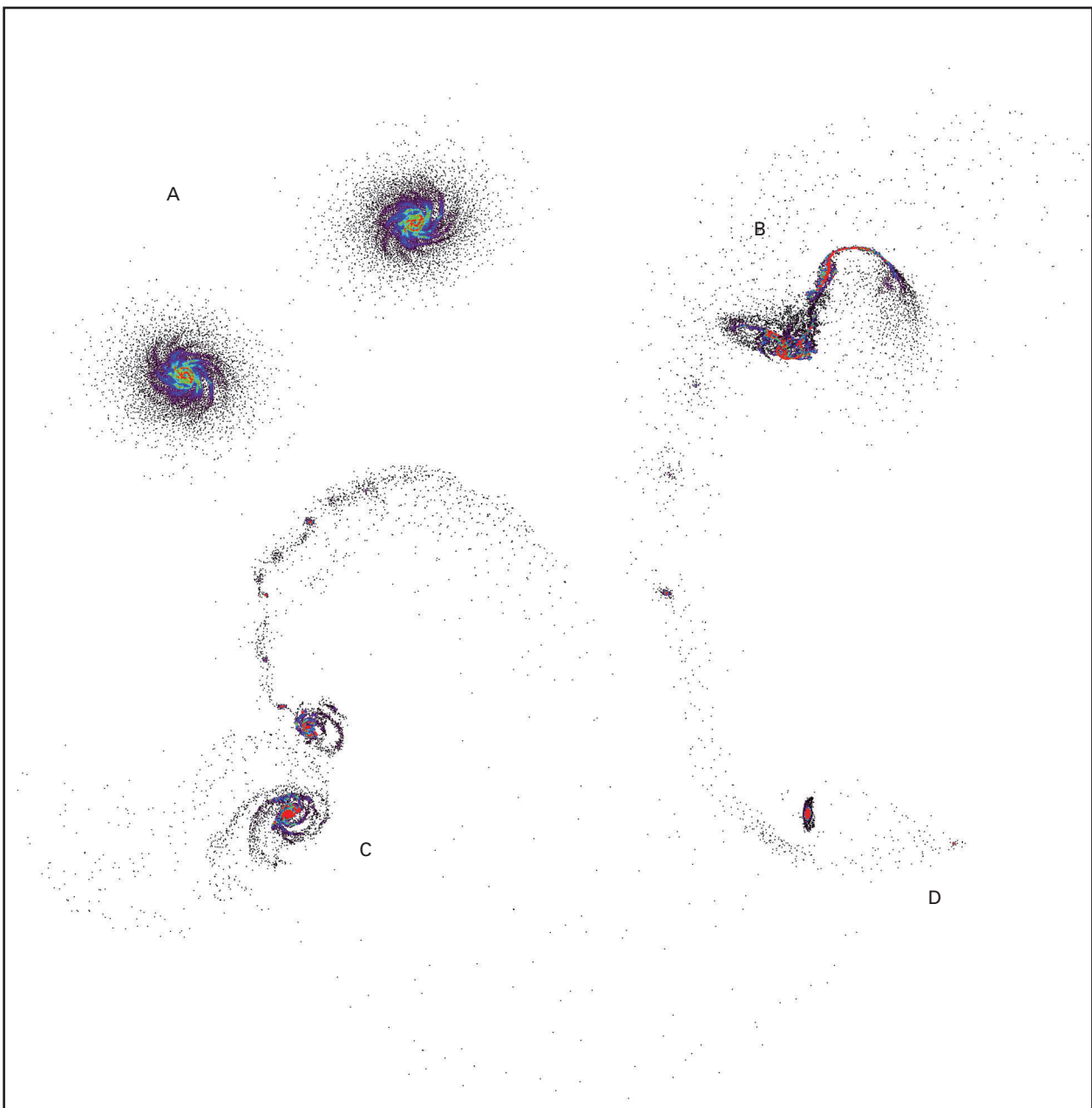


**Fig. IV.35:** Model C with an additional disk-like component.

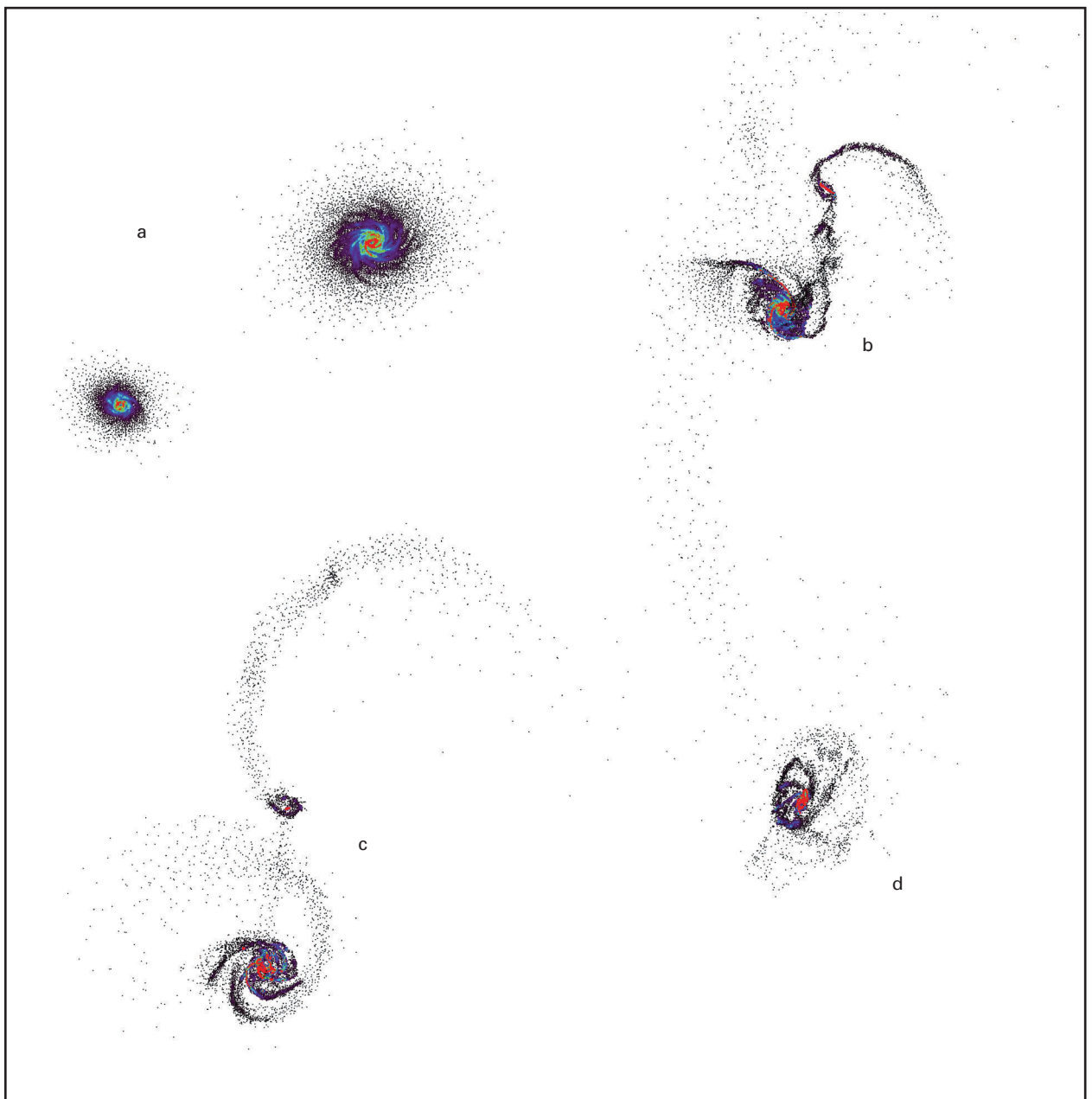
**Fig. IV.36:** Chronological steps of the merger of two spiral galaxies: A, B, C, D with mass ratios 1:1 and a, b, c, d with mass ratio 1 : 3. The figure illustrates the behavior of the gas particles.



elliptical galaxies contain black holes at their centers, which are surrounded by accretion disks. Here, *e.g.*, giant plasma beams are generated – jets extending up to several hundred million light years into the intergalactic medi-

um (cf. previous chapter on 3C 273). It would be interesting to know how these black holes form and how they affect the formation and evolution of elliptical galaxies.

*(Thorsten Naab, Andreas Burkert)*



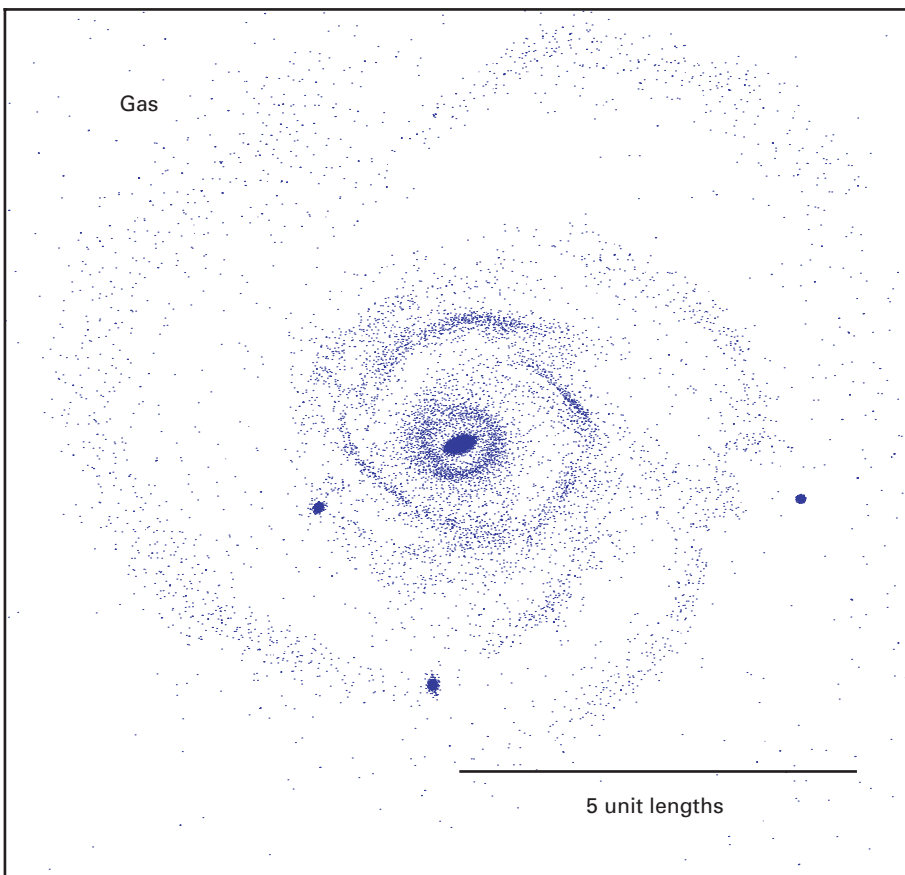
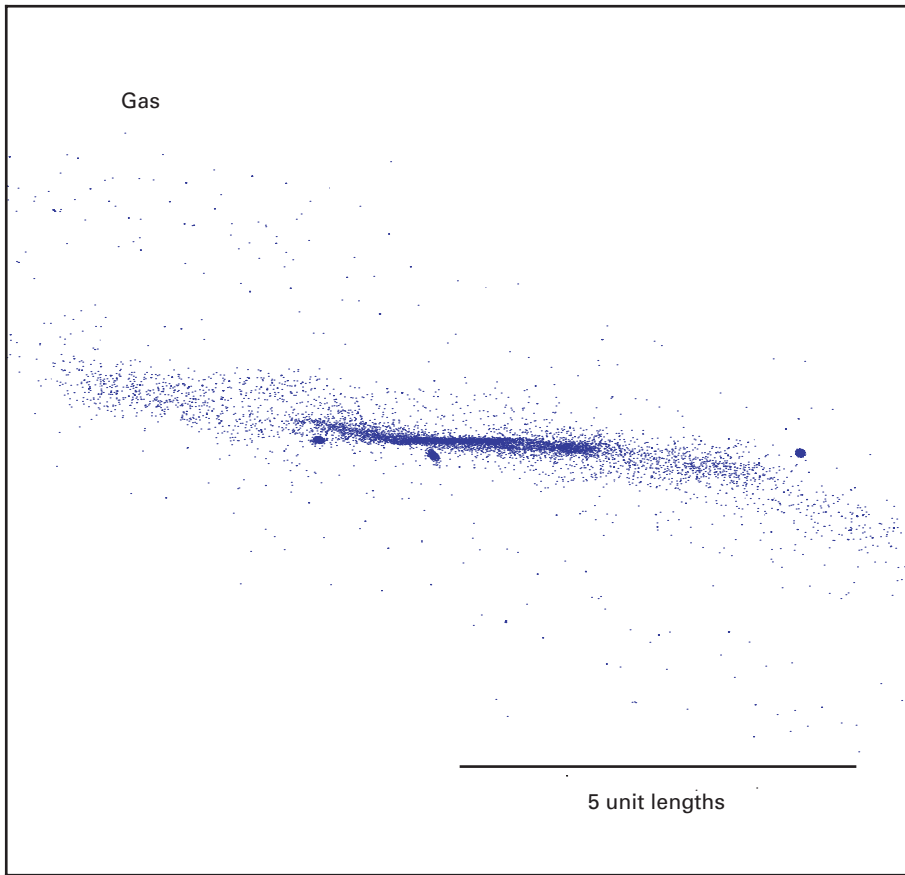


**Fig. IV.37:** Distribution of gas particles in a central disk at the end of the simulation, seen edge-on (left) and from above (right).

## Dark Matter and Galaxy Formation

**Since decades, dark matter is part of the cosmological standard model. According to our current knowledge, it alone contributes about one third of the total mass of the Universe. Although the nature of dark matter is still unknown theoreticians include it in their calculations, making assumptions about its interaction with “normal” matter. This concerns in particular galaxy formation in the early Universe. Theoreticians at the Institute together with colleagues from the MPI für Astrophysik in Garching and the Carnegie Institution in Washington, USA, found out that the present angular momentum of dwarf spiral galaxies cannot be explained by current theories of galaxy formation. This work illustrates again fundamental deficits in the understanding of dark matter and its role in the evolution of the Universe.**

Evidence of the existence of dark matter is found in various fields of astronomy: spiral galaxies are rotating so rapidly that they have to be surrounded by a halo of invisible matter holding together these stellar systems by gravitation. Galaxies in clusters are moving so fast that they have to be bound gravitationally by dark matter. And last not least, the formation of galaxies and clusters of galaxies from the very homogeneous primordial gas cannot be explained without the additional gravitational effect of dark matter.

Part of the dark matter probably consists of dark bodies, such as brown dwarfs, black holes and extremely faint stars which cannot be detected by present-day telescopes. The major part, however, has to be made up by hitherto unknown elementary particles. They must have the property to emit or absorb only very little electromagnetic radiation, if any, and to interact only gravitationally with ordinary baryonic matter.

### The Angular Momentum Content of the Halos and Disks

In simulations of galaxy formation under the influence of (non-baryonic) dark matter, the latter is therefore treated as a gas with only gravitational interactions. Such computations have led to the following picture: In an originally almost homogeneous mixture of dark and baryonic matter, the dark matter at first forms dense clumps, so-called dark halos with highly concentrated cores. Baryonic matter then accumulates in these “gravitational traps”, condensing in the central regions into galaxies. The so-formed galaxies are then still surrounded by a dark matter halo.

During this early stage, dark halos interact and merge with one another rather frequently. Moreover, on larger scales dense filaments form, intersecting in knots where mergers of dark halos occur particularly often. During

mergers and by tidal interactions angular momentum is transferred to the halos. Numerical computations show the intrinsic angular momentum distribution of dark halos to be universal. The assumption is made that in this stage dark matter and baryonic matter are still strongly coupled. If this were true, the baryonic gas and eventually the newly formed spiral galaxies, too, should have the same angular momentum distribution as the dark matter halos.

Although this scenario explains many observable characteristics of spiral galaxies, there are problems, too. First of all, simulations with (cold) dark matter yield disk galaxies that are at least an order of magnitude too small. This is a consequence of visible matter losing angular momentum to the dark matter when it is falling into the dark halos. But obviously it is in disagreement with the observations. The second problem concerns the actual density distribution of spiral galaxies. If angular momentum conservation is assumed to explain the observed size of the disks, according to the numerical computations, the actual density distribution of the disks should reflect the original angular momentum distribution of the protogalaxy.

Theoreticians at the Institute and their colleagues have tested this fundamental prediction of the theory. First, they calculated the specific angular momentum distribution of 14 dwarf spiral galaxies from their observed density distributions and rotation curves. Then these results were compared with the predictions of the cosmological simulations, assuming the infalling gas not to lose angular momentum. As it is shown in Figure IV.38, the theoretical distribution (solid curve) is in rather good agreement with the observed data if a mass-to-light ratio of unity to two is assumed for the galaxies (middle and right diagram). (The dimensionless parameter  $\lambda$  is calculated from the total angular momentum and the mass and energy of the halo.)

Surprisingly, a very strong correlation of the angular momentum parameter  $\lambda$  and the fraction of baryonic matter in the disk was found (Fig. IV.39), implying that the angular momentum distribution depends on the baryonic mass of the galaxies. Such a behavior, however, cannot be explained by the cosmological theory.

A striking disagreement with the theory was found mainly by analyzing the angular momentum distribution within the disk (Fig. IV.40). The hatched area marks the range of the angular momentum distribution within the respective disk while the solid line represents the angular momentum distribution in the halo. For one thing, it is noted that the hatched regions are always smaller than the total areas below the curves. This means the fraction of baryonic matter in the disks being smaller than the mean value in Universe. For another thing, the angular momentum distribution reaches higher values in the halo than in the disks, meaning that at the formation of the galaxies matter with the highest angular momentum is not incorporated in the disk.

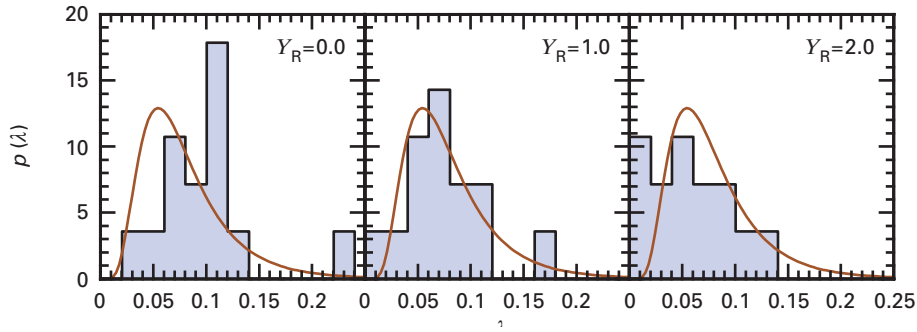


**Fig. IV.38:** Frequency distribution of the angular momentum parameter  $\lambda$  for mass-to-light ratios of 0, 1, and 2 (from left to right). The fraction of the total angular momentum contained in the disk is increasing with increasing  $\lambda$ . The essentially un-physical extreme case of  $\lambda = 0$  only means that the disks does not contribute at all to the total angular momentum.

The problem is, in a few words, that the average angular momentum over the entire disk is in rather good agreement with the predictions (Fig. IV.38), while the angular momentum distribution in the disk differs significantly from theory (Fig. IV.40).

This discrepancy between observation and theory could in principle result from a faulty analysis of the observational data. It is conceivable, *e.g.*, that part of the matter is in the form of undetectable brown dwarfs and very faint stars. This assumption, however, could be precluded by repeating the calculations of the angular momentum of galaxies using considerably higher mass-to-light ratios. These attempts led to no significant improvement. Another possibility would be that the outer regions of the galaxies were not detectable and thus an important fraction of the angular momentum was overlooked. But this option, too, was excluded by the theoreticians: gas beyond the observed maximum radius can contribute to the total angular momentum no more than half a percent. But how can the new results be interpreted in the framework of

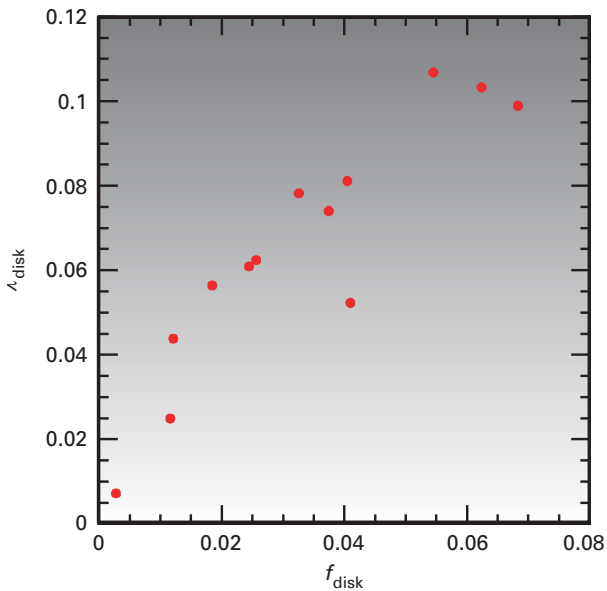
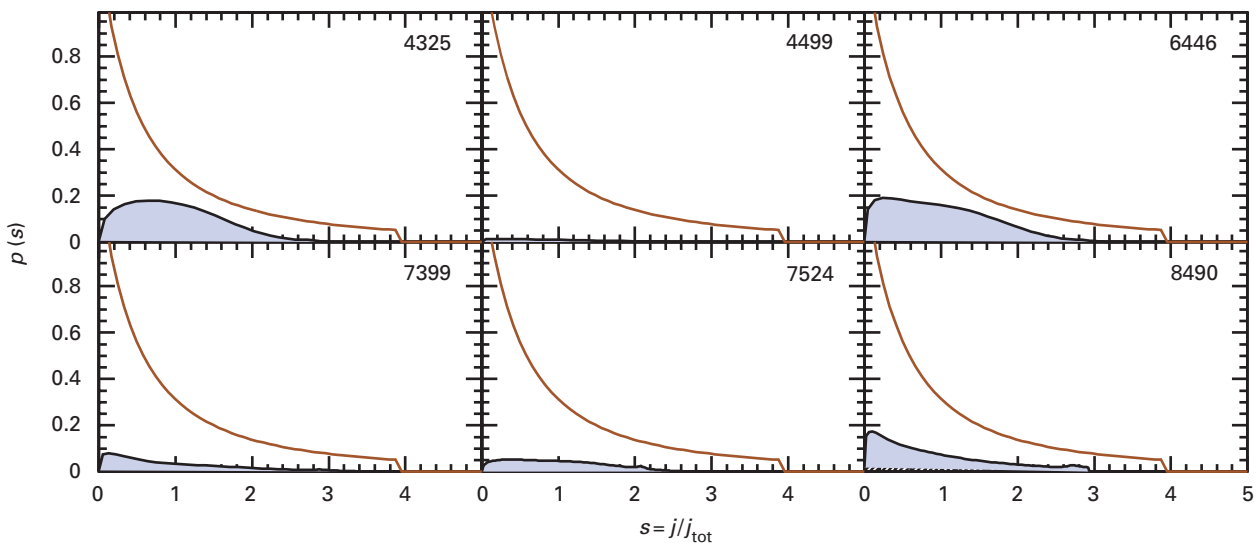


**Fig. IV.39:** Correlation between the angular momentum parameter  $\lambda$  and the fraction of baryonic matter in the disk.

**Fig. IV.40:** Frequency distribution of the angular momentum normalized to the total angular momentum. The hatched area marks the range of the angular momentum distribution within the respective disk while the solid line represents the angular momentum distribution in the halo.



an otherwise very successful cosmological standard scenario?

There are different ideas for a possible solution of the puzzle. First of all, dark matter could have different properties than assumed. The computations only consider cold dark matter, its particles having small kinetic energy. For several years, however, the possible existence of warm dark matter with higher kinetic energy is discussed, too. Future simulations will have to show whether this option can solve the angular momentum problem.

Still another possibility would be, that baryonic and dark matter have de-coupled in a very early stage of galaxy formation and that the angular momenta of the halo and the disk took a different evolution. However, the reason for such a behavior is not known. Obviously, the explanation of the angular momentum problem is an essential prerequisite for a complete understanding of galaxy formation.

(Andreas Burkert)

### The Far-Infrared Sky Background

**The importance of astronomical infrared observations will increase further in the future. The European space telescope HERSCHEL, which is currently being built (the MPIA is participating in its instrumental development) is just one example for this trend. Studies of faint objects in this spectral region, however, are confused by a widespread background radiation originating from sources within our planetary system and the Milky Way, but also from distant galaxies. Astronomers at the Institute together with colleagues from the University of Helsinki and the Konkoly Observatory in Hungary studied the infrared background using the ISOPHOT instrument aboard the ISO Infrared Observatory. They identified properties of this diffuse background radiation, which will be important for future infrared telescopes. Furthermore, they identified the faint signal of the extragalactic background radiation, which probably originates mainly from newly formed galaxies in the early Universe.**

ISO has peered through several luminous “curtains” lying at quite different distances to Earth (Fig. IV.41). Firstly, there is interplanetary dust within the solar system. At a temperature of 270 K it is relatively warm, so its thermal radiation in the mid-infrared is the strongest confusion noise in front of the faint background radiation. At much larger distances of hundreds or thousands of light-years, cool interstellar dust is spread out. Because of its wispy diffuse appearance it is also called cirrus. Intergalactic dust can be detected only in galaxy clusters and even there only very small concentrations have been found as studies at MPIA have shown (cf. the Chapter “Dust in galaxy clusters”)

The extragalactic infrared background was detected about ten years ago by the US-American COBE satellite.

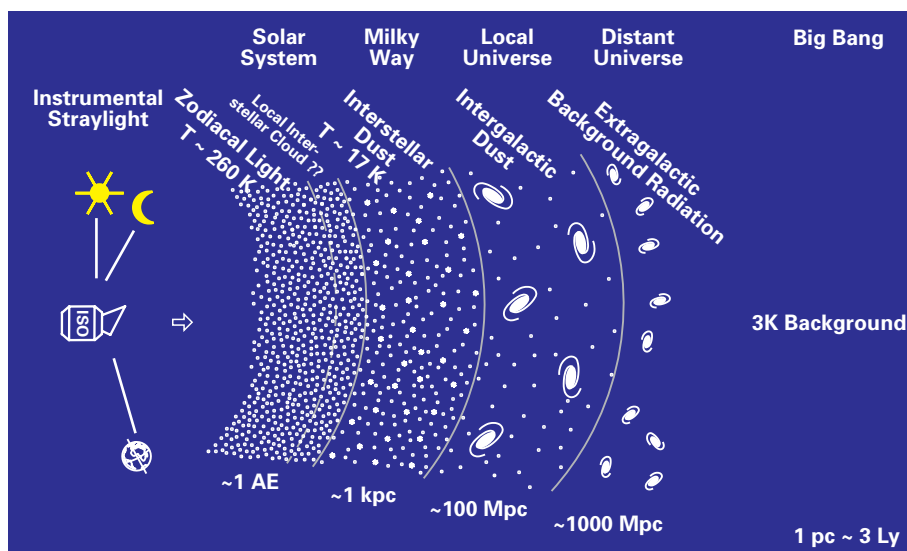


**Fig. IV.41:** Infrared observations of distant celestial objects look through different foreground layers. Dust emission in the planetary system as well as inside and outside the Milky Way always contributes to the recorded fluxes.

The DIRBE instrument onboard COBE, however, had a resolution of only 42 arc seconds and was incapable of detecting individual sources. Using ISOPHOT, astronomers at the Institute were also able to identify this weak radiation coming from young galaxies several billion light years away.

There is only one source lying at an even larger distance – that of the cosmic microwave background. It has its maximum in the millimeter range, though, and originates from a very early phase, only some hundred thousand years after the Big Bang. This emission has been mapped by COBE in great detail over the entire sky.

### Confusion noise – a fundamental problem in infrared astronomy

The different components of the infrared background are a fundamental problem for infrared astronomy as they are superimposed onto all observations and set an accuracy limit to intensity measurements of the radiation of cosmic objects. This infrared “confusion noise” can be determined as follows: During the observation of an object, images are taken in turn of the sky region containing the object (on target) and away from it (off target). The off-target image is used as a reference to determine the intensity of the sky background, which is mostly caused by the emission of galactic dust (cirrus). Subsequently, this background is subtracted from the on-target image (Fig. IV.42).

First studies of confusion noise have been conducted in the early 1990s on the basis of images taken by the IRAS infrared satellite. The spatial distribution of the background radiation had been found then to show something like a fractal pattern: Structures are similar on different scales. Based on IRAS data at 100  $\mu\text{m}$  wavelength and with additional theoretical assumptions, an analytic relation between confusion noise and telescope aperture (angular resolution), wavelength and the absolute background intensity was derived. It is quite plausible, for instance, that with increasing angular resolution of the telescope the diffraction-limited fields of view (airy disks) are getting smaller so that on-target and off-target fields can lie closer together. Thus, in this case the background can be de-

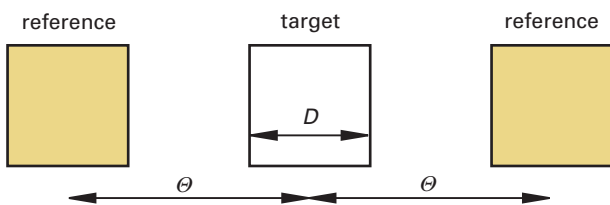


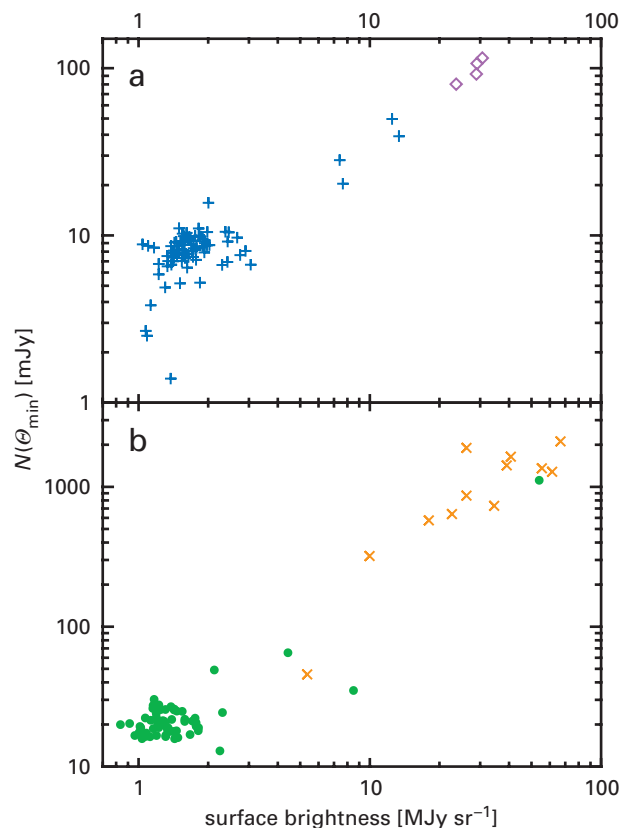
**Fig. IV.42:** Infrared images are taken in turn “on target” (middle) and “off target” as reference. The size of the measuring aperture  $D$  and the angle  $\alpha$  between the fields imaged are of great importance for the background noise.

termined with higher accuracy than at larger separations of on- and off-target fields. And it seems plausible, too, that a bright background, caused by a denser interstellar cloud, has more structure than a faint one and therefore increases the confusion noise.

With ISO, this partly theoretically deduced relation was to be tested for the first time on the basis of observational data and extended to longer wavelengths. For this purpose, astronomers at the Institute selected 175 maps with strongly varying background brightness from the ISO catalogue, which did not contain any obvious sources, such as stars, galaxies or nebulae. Firstly, the zodiacal light was subtracted from the data. Then the instrumental noise was analyzed in great detail and subtracted, too. The remaining signal was subject to a Fourier analysis providing the number of background structures as a function of their size. This size  $N$  is indeed increasing, as theoretically predicted, with increasing background intensity (according to a power law with an exponent of 1.5) (Fig. IV.43). That is true for wavelengths around 100  $\mu\text{m}$  (upper figure), as well as around 200  $\mu\text{m}$  (lower figure).

A direct comparison with the theoretical prediction is very informative. As Fig. IV.44 shows, the theoretical values are in very good agreement with the ISO data, at least in the region above about 10 mJy (the dashed line marks the run of identical values): Moreover, the analysis clearly showed that even in sky regions with very faint back-

**Fig. IV.43:** Confusion noise as a function of the brightness of the background.



ground radiation the instrument noise is below the confusion noise by a factor of two to three. Even at the maximum wavelength of 200  $\mu\text{m}$  the detector sensitivity was limited by fluctuations of the background rather than by instrumental effects. This is another proof of the quality of the ISO detectors, which had been developed by the Institute together with German and European companies.

So the studies of the background noise have confirmed to a large extent theoretical predictions which can now be used for future space telescopes of similar size, such as SIRTf (planned to be launched in 2003) and Astro-F (2005). This is crucial for the determination of the measuring accuracy of these telescopes. However, the relation between confusion noise and increasing angular resolution, that is increasing primary mirror, is still unknown as ISO and IRAS both had mirrors of the same size (60 cm). Predictions made for the HERSCHEL 3.5 m telescope therefore are still based on additional theoretical assumptions.

cosmological model of galaxy clustering, the astronomers were able to convert these values into absolute intensities. The obtained values of 14  $\text{nW m}^{-2} \text{sr}^{-1}$  for 90  $\mu\text{m}$  and an upper limit of 37  $\text{nW m}^{-2} \text{sr}^{-1}$  at 170  $\mu\text{m}$  are in agreement with the data measured by COBE. Two years ago, a lower limit to the background radiation was already obtained from galaxy counts with ISOPHOT. It is a factor of seven below the present upper limits.

This observation is notable in several respects. It represents an independent determination of the extragalactic background. But the goal is still to determine the absolute intensity without using a cosmological model. This can only be achieved if all foreground signals are subtracted correctly. The absolute intensity value is crucial for studies of the evolution of galaxies in the early Universe – a task that will be tackled by the team in the near future.

(C. Kiss, P. Ábrahám, U. Klaas, D. Lemke)

### Extragalactic Background Radiation

In Fig. IV.44, a discrepancy between the measured data and the predictions is obvious for very low intensities below about 10 mJy. In this region of faintest brightness the run of the measured noise is almost constant. Here, the fluctuations are no longer caused by the cirrus but by distant galaxies. Astronomers interpret this signal as extragalactic background radiation, which is – in contrast to the cirrus – distributed isotropically on the sky.

A detailed analysis of this emission provided relative fluctuation amplitudes of 7 mJy and 15 mJy at 90 and 170  $\mu\text{m}$ , respectively, with an accuracy of 30%. Using a cos-

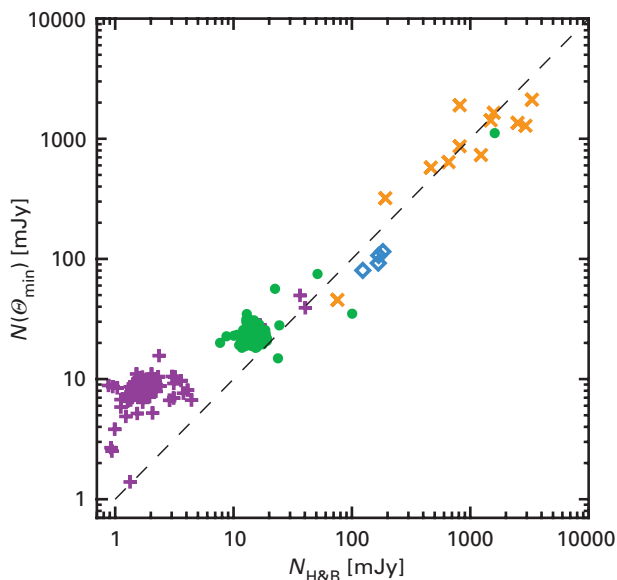


**Fig. IV.44:** Comparison of measured confusion noise (ordinate) with the theoretically predicted.

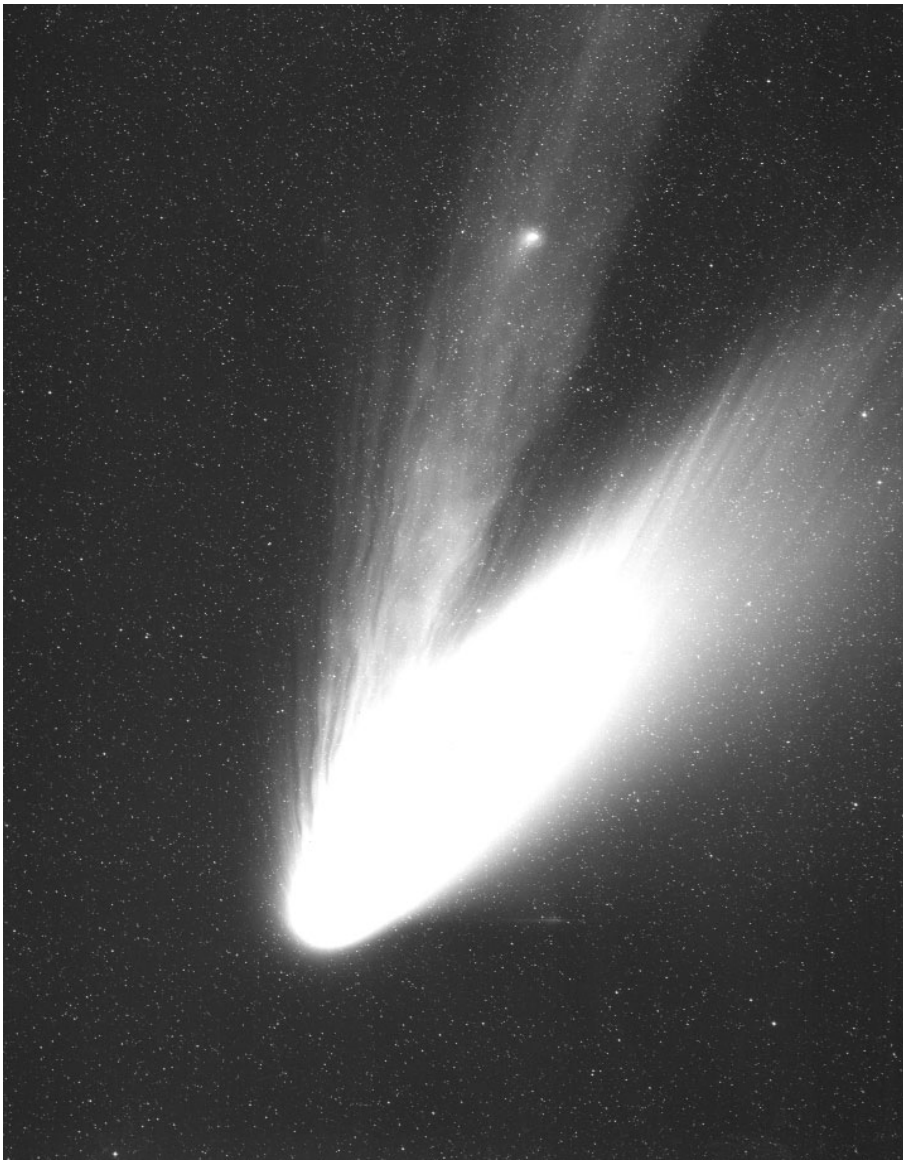
## IV.3 The Solar System

### Iso Observes Dust and Ice in Comet Hale-Bopp

In 1995, amateur astronomers Hale and Bopp discovered a new comet. In spring 1997, it reached a maximum brightness of  $-0.5$  mag, remaining brighter than 0 mag for more than seven weeks. Thus, comet C/1995 O1 (Hale-Bopp) was among the 20th century's brightest comets. Luckily, the European Iso Infrared Space Observatory was in operation when the comet appeared. So an international team of astronomers used the opportunity to observe the comet with Iso. Hale-Bopp was found to have unusual high dust production rates even at large distances to the Sun. In addition, infor-

mation on the properties and size distribution of the dust particles was gathered.

Fig. IV. 45: Comet Hale-Bopp in spring 1997.



At the time of its discovery in July 1995, Hale-Bopp still was at a very large distance of 7.15 AU from the Sun. On 1 April 1997, it passed perihelion and then moved back into the outer reaches of the solar system (Fig. IV.45). Hale-Bopp displayed a variety of spectacular phenomena such as jets and striae, the latter being very rare bright stripes in the tail which were observed on Calar Alto using the Schmidt telescope (cf. Annual Report 1997, p. 75). With a diameter of 40 to 70 km, the comet's nucleus was remarkably large.

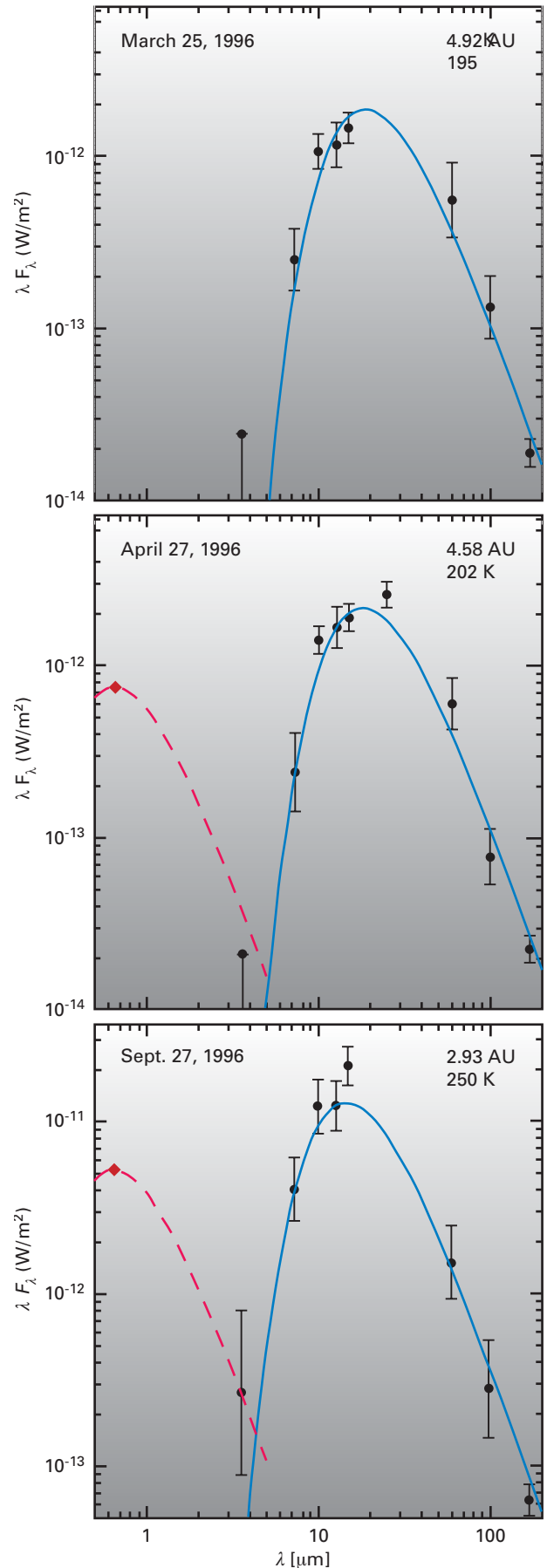
### Dust and Ice in the Coma of Hale-Bopp

Soon after its discovery, it became clear that this comet would get exceptionally bright. Thus, it was ideally suited to study its evolution also in the far infrared over a longer period of time. In this spectral range, emission of dust and ice is observable which provides information on various activity phases of comets and on the particles in the coma. Such observations also provide information on the structure of the nucleus.

It is known that, at large distances from the Sun, at first the volatile CO gas sublimates from the nucleus, dragging dust along with it. This way the coma forms. When approaching the Sun the comet gets warmer and warmer causing also water to sublimate from the nucleus with increasing rates until finally water dominates the gas production of the comet.

These phases of Hale-Bopp were observable from ISO in three observing "windows": March to May 1996 (4.9 to 4.6 AU heliocentric distance), September/October 1996 (2.9 to 2.8 AU) and December 1997/January 1998 (3.9 AU, after perihelion passage). During these periods, observations over the entire wavelength region from 3.6  $\mu\text{m}$  to 170  $\mu\text{m}$  were possible using the ISOPHOT instrument developed at the MPIA. This data set was completed by measurements of other instruments onboard ISO as well as by ground-based optical observations at 0.7  $\mu\text{m}$ . The multi-instrumental project was accomplished by a correspondingly large team of astronomers. In addition to researchers from three Max-Planck-Institutes (for Nuclear Physics and for Astronomy, both in Heidelberg, and for Aeronomy in Katlenburg-Lindau) astronomers from ESO, the USA, France, Great Britain and the Czech Republic were involved.

**Fig. IV.46:** Spectral energy distribution of the emission of comet Hale-Bopp at 4.92, 4.58 and 2.93 AU distance to the Sun. The increase of the color temperature from 195 to 250 K (solid line) is clearly visible. The dashed line represents the fraction of solar light with a blackbody temperature of 5700 K, which has been scattered by dust.



The project focused on the following questions:

- How does the thermal emission change as a function of the distance to the Sun?
- At which distance is it the water, and no longer CO, that dominates the coma?
- How do the dust properties change as a function of the distance to the Sun?

In a first step, the spectral energy distribution of the coma was determined as a function of heliocentric distance from carefully calibrated data. Fig. IV.46 shows three examples of these distributions for distances of 2.93 AU, 4.58 AU and 4.92 AU. In a first approximation, these data can be fitted with Planck curves of a blackbody to yield color temperatures. These temperatures, however, are not

identical with the physical temperature of the dust particles since the thermal emission of individual particles depends on their temperatures as well as on their emissivity. This in turn is a function of material and particle size. The dust coma contains grains of vastly different size, composition and temperature. The measured energy distribution in the infrared is the integral thermal emission of all these different particles: So the spectral energy distribution can be used to limit the properties of the particles.

The color temperatures obtained this way were compared to the temperature of a hypothetical rotating blackbody in equilibrium with the infalling solar radiation. Interestingly, the measured color temperature is about 50% higher than the blackbody temperature for all distances. This is the highest value ever measured, suggesting that the coma must contain particularly large numbers of small grains. At longer wavelengths of about a hundred times the particles' diameter, these grains are no longer able to emit their thermal energy efficiently and thus heat up more strongly than a blackbody.

The notably elevated color temperature even at the large distance of 4.9 AU was a great surprise. The astronomers had expected the dust grains to be bound in larger icy particles, which are dragged along with the sublimating CO gas into the coma. However, the data show that large amounts of free, fine dust must exist. At the same time, the shape of the Planck curve at large wavelengths indicates the presence of larger particles, too. So a dust population with a wide distribution of sizes seems to have existed in the coma. The presence of large amounts of dust is suggested by another observational fact: The spectral energy distributions are clearly elevated around 10 and 25  $\mu\text{m}$ . These features are attributed to silicates. It is the first time that these minerals have been detected in a comet's coma at such large heliocentric distances.

Comparison of the data showed the color temperature varying with the heliocentric distance ( $r$ ) as  $r^{-0.5}$  while the total emitted energy varies as  $r^{-3}$ . According to theory, the energy varies as  $r^{-4}$  if the dust production rate increases proportionally with the intensity of the infalling solar radiation. This behavior had been observed in many earlier comets, like comet Halley, for instance. Thus, the increase of the dust production rate in Hale-Bopp during its approach to the Sun was lower than in other comets, at least in the distance range between 4.6 and 2.8 AU. This is a consequence of the exceptionally high dust activity starting already at very large distances.

In order to investigate the properties of the coma particles, the spectral energy distribution was calculated for

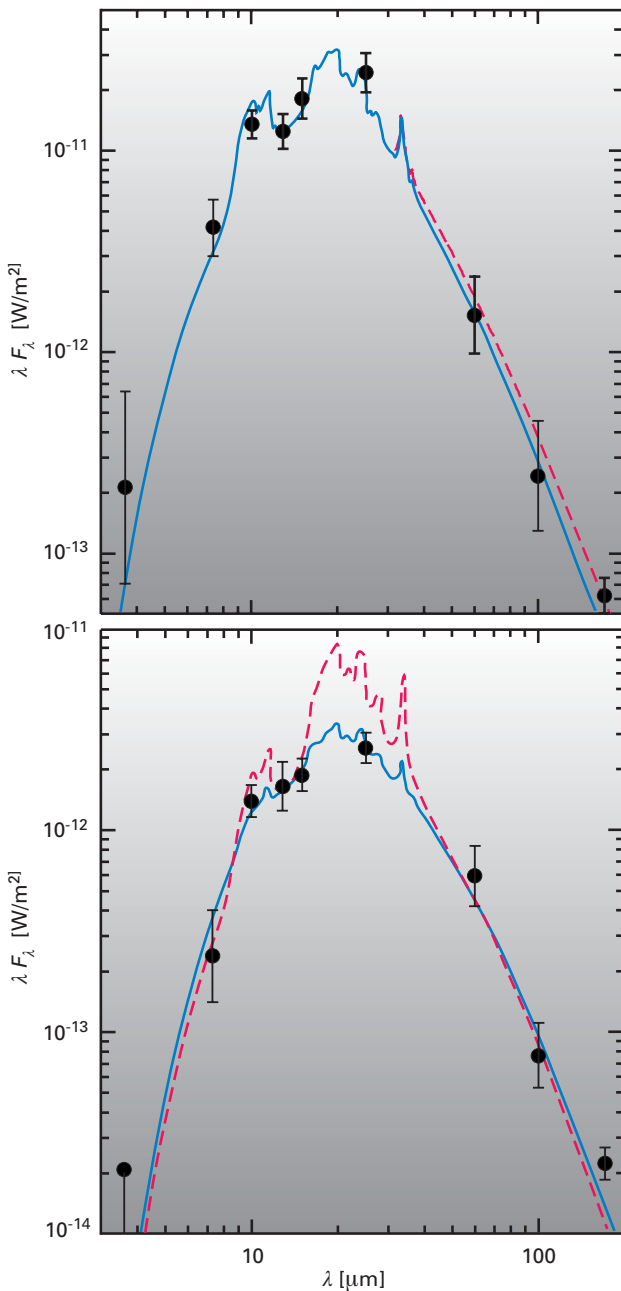


**Fig. IV.47:** Comparison of the dust model and the ISOPHOT data. At a heliocentric distance of 2.8 AU (**a**), both models with a somewhat different distribution of particle sizes are in good agreement with the data. At 4.6 AU (**b**), only a reduced silicate abundance (solid line) matches the data.

models of different dust compositions in order to find the best fit to the observed spectral shape. After some experimentation, a mixture of 75 % glassy pyroxene, 10 % glassy olivine and 15 % crystalline olivine (forsterite) was found to fit best. The size distribution of the grains is defined by three quantities whose values were determined by the fit to the measured data. These quantities are: a minimum radius of 0.1  $\mu\text{m}$ , a most common radius of 0.42  $\mu\text{m}$ , and an exponent  $N = 3.7$  which determines the shape of the distribution curve. A value of  $N < 4$  means that large particles contribute the major portion to the total dust mass.

Figure IV.47 shows this model to be in very good agreement with the data of 7 October 1996 (left) when Hale-Bopp was 2.8 AU away from the Sun. The values of 27 April (right), however, when Hale-Bopp still was at a distance of 4.6 AU, are discrepant from the model (dashed) which predicts a much too high silicate emission. While maintaining the size distribution, the discrepancy can be eliminated only by reducing the relative fraction of the silicate component by a factor of three.

Using the model, the dust production rate could be determined from the observed infrared fluxes. Unknown parameters in this calculation are the average density of the grains and their maximum size. Assuming values of 1  $\text{g}/\text{cm}^3$  for the density and 1 cm for the size, dust production rates of  $1.5 \times 10^5$  kg/s (at 2.8 AU) to  $5 \times 10^4$  kg/s (at 3.9 AU) to  $3 \times 10^4$  kg/s (at 4.6 AU) were obtained, yielding a dust-to-gas mass ratio of about six. These values are matching older sub-millimeter observations which had yielded a rate of  $2 \times 10^6$  kg/s at 1 AU. In particular, the exceptionally high rate at large distance was a surprise, as mentioned above. Thus, it will be interesting to discover other bright comets at large heliocentric distances and study them in detail.

Another interesting subject in comets are water ice particles. Previously, optical and UV observations had already yielded a water production rate for Hale-Bopp of about  $2 \times 10^{28}$  mol per second. The ISOPHOT data suggest the presence of water ice grains, which make themselves conspicuous by an increased emission at 44  $\mu\text{m}$  and 65  $\mu\text{m}$  wavelength. From the water production rate and the observed thermal emission the total mass of water ice can be estimated, the unknown characteristic grain size limiting the quality of the estimate. For a typical radius of 15  $\mu\text{m}$ ,  $2 \times 10^{10}$  kg are obtained, for 100  $\mu\text{m}$  radius, the amount is  $2 \times 10^{11}$  kg. The data also showed the ice grains to be a few degrees warmer than their corresponding blackbody temperature. This could be explained by small amounts of dust contaminating the ice particles which therefore heat up more efficiently than pure ice.

This extensive analysis has demonstrated impressively the potential of far-infrared observations of comets. Since comets as bright as Hale-Bopp are rare, it is yet uncertain whether future space missions, such as HERSCHEL (to be launched in 2007), will be equally successful. In any case, these telescopes will be much more sensitive because

of their larger mirrors compared to ISO (HERSCHEL: 3.5 m, ISO: 0.6 m). So, those observations, which have turned out to be especially interesting could be carried out at even larger distances to the Sun.

*(Dietrich Lemke, Christoph Leinert, Manfred Sticklel)*

## Staff

### In Heidelberg

**Directors:** Rix, Henning (since 1.11.)

**Scientists:** Abraham (until 22.4.), Andersen (since 15.11.), Bailer-Jones, Beetz, Birkle, Burkert, Dehnen, Feldt, Fried, Graser, Grebel, Haas, Heraudeau, T. Herbst, Hotzel (since 1.7.), Jester (since 15.9.), Hippelein, Hofferbert, Klaas, Kümmel (until 2.12.), Leinert, Lemke, Lenzen, Ligori, Marien, Meisenheimer, Mundt, Nasince, Neckel, Odenkirchen, Ollivier (until 28.8.), Phleps (since 1.10.) Röser, Slyz (until 30.6.), Staude, Stickel, Toth (since 15.10.), Vavrek (since 1.9.), Wolf, Wilke

**Ph. D. Students:** Bertschik (since 1.3.), Büchler (since 1.7.), Brunner (since 1.9.), Dib, Geyer, Harbeck, Hartung, Heitsch (until 30.6.), Hempel (since 1.8.), Hetznecker (until 14.3.), Hotzel (until 14.4.), Jesseit, Jester (until 14.9.), Khochfar, Kleinheinrich (until 31.3.), Kovács (since 1.11.), Kranz, Krause, Krdzalic (until 28.2.), Lamm, Lang, Maier, McIntosh (15.1. until 30.6.), Mühlbauer, Ofek (29.1. until 4.3.), Phleps (until 30.9.), Przygodda, Puga, Rudnick (until 14.11.), Sarzi (1.7. until 30.11.), Schuller (until 14.2.), Stolte, Walcher (since 1.11.), Weiss, Wetzstein (since 1.2.), Ziegler (since 1.10.)

**Diploma Students:** Bertschik (until 28.2.), Tschamber (since 24.4.), Walcher (until 31.7.), Wetzstein (until 31.1.), Ziegler (until 30.6.), Zimer (since 1.6.), S. Müller (1.3. until 31.8.), Mohr (since 1.9.)

**Student Assistants:** Drepper (since 1.3.), Egner (since 15.11.), Tschamber (since 15.11.), Zimer (since 15.8.)

**Scientific Services:** Bizenberger, Galperine (since 18.6.), Grözinger, Hofferbert, Laun, Mathar, Neumann, Quetz.

**Computers, Data Processing:** Briegel, Helfert, Hiller, Hippler, Rauh, Storz, Tremmel, Zimmermann.

**Electronics:** Alter, Becker, Ehret, Grimm, Klein, Mall (since 1.9.), Ridinger, Salm, Töws (1.2.-31.7.), Unser, Wagner, Werner (until 30.9.), Westermann, Wrhel.

**Fine Mechanics:** Böhm, Haffner (since 1.9.), Heitz, Meister, Meixner, Morr, Pihale, Sauer

**Drawing Office:** Baumeister, Ebert, Münch, Rohloff

**Photo Shop:** Anders-Özcan

**Graphic Artwork:** Meißner-Dorn, Weckauf

**Library:** Behme (exempted since 1.10.), Dueck (since 1.7.)

**Administration:** Apfel, Flock (exempted), Gieser, Goldberger, Kellermann, Hartmann, Heißler, Janssen-Bennynck, Kellermann, Papousado, Schleich, Voss, Zähringer.

**Secretariate:** Goldberger, Janssen-Bennynck, Rushworth (until 31.7.), Silventoinen (since 1.7.)

**Technical Services:** Behnke, Gatz (until 30.4.), Herz, M. Jung (since 15.2.), Lang, Nauss, B. Witzel, F. Witzel, Zergiebel.

**Trainees:** Fine Mechanics – Fsinceianatz (until 4.3.), Greiner (until 4.3.), Haffner (until 31.8.), Lares, Maurer (since 1.9.), Rosenberger (1.9.), Sauer (1.9.), Petri, Wesp (until 31.8.); Drawing Office – K. Jung (until 6.2.), Bender (since 1.9.)

**Free Collaborator:** Dr. Thomas Bürhrke.

**Scholarship Holders:** Butler (since 15.1.), Caldwell (since 26.4.), Chesneau (since 1.10.), Cretton (until 30.9.), Del Burgo, D'Onghia (since 1.12.), Heitsch (1.7. until 30.9.), Hetznecker (1.9. until 31.10.), Kessel (DFG), Klessen (Otto Hahn Award, until 30.9.), Kroupa (until 31.1.), Lee (since 1.11.), Nelson, Pentericci, Popescu (Otto Hahn Award, until 31.8.), Travaglio (until 30.9.)

**Guests:** Abraham, Hungary (July), Avila, Mexico (November – December), Bodenheimer, USA (December), Böker, USA (May), Ciecielag, Polen (August – September), Devriendt/France (March – April), Dodt, Germany (June), Dong, USA (June – July), Gallagher, USA (June – August), Gupta, Indien (November), B. Herbst, USA (June), Hiroshita, Japan (October), Holtzman, USA (May), Hozumi, Japan (May), Ionita, USA (August – September), Kiss, Hungary (January, September), Klapp, USA (December), Lin, USA (April – May), Looze, USA (June – August), MacLow, USA (July), Makarova, Russia (November), Mellema, Netherlands (May – June), Mochizuki, Japan (May), Morel, Frankreich (April – December), Morgan, USA (June – July), O'Dell, USA (January – March), Ofek, Israel (January – March, June – August), Sanchez, Mexiko (November – December), Schechter, USA (June – August), Shields, USA (July – August), Smith, UK (September), Steinmetz, Germany (May – June), T'oth/ Hungary (June – August), Vitvitska, Russia (June – August), Zuther, Germany (September).

Due to regular international meetings at the MPIA further guests stood at the Institute for shorter periods, who are not listed here.

**Co-operative Students:** Adelman (9.4. – 12.4.), P. Brunner (since 1.9.), Egner (20.8.– 30.9.), Eiermann (19.2. – 23.2.), Enbrecht (1.3. – 31.8.), F. Geyer (3.9. – 28.9.), Harth (since 17.9.), Link (until 28.2.), Marquart (5.3. – 8.4.), Miller (20.6. – 19.8.), Rohlf (12.3. – 22.4.), Schmitt (1.3. – 31.8.), Tamas (20.8. – 2.11.), Tristram (6.8. – 19.8., 17.9. – 30.9.)

---

## Calar Alto/Almeria

**Local Directors:** Gredel, Vives

**Astronomy, Coordination:** Thiele, Prada, Frahm

**Astronomy, Night Assistants:** Aceituno, Aguirre, Alises, Guijarro, Hoyo, Montoya (until 30.11.), Pedraz

**Telescope Techniques:** Capel, De Guindos, Garcia, Helmling, Henschke, L. Hernandez, Raul López, Morante, W. Müller, Nunez, Parejo, Schachtebeck, Usero, Valverde, Wilhelmi.

**Technical Services:** A. Aguila, M. Aguila, Ariza, Barón, Carreno, Corral, Dominguez, Gómez, Góngora, Klee, Rosario Lopez, Marquez, Martinez, F. Restoy, Romero, Saez, Sanchez, Schulz (until 30.6.), Tapia.

**Administration, Secretariate:** M. Hernández, M. J. Hernández, M. I. López, C. Restoy (until 31.5.).

---

## Working Groups and Scientific Collaborations

### Instrumental Projects

#### Adaptive Optics

Stefan Hippler, M. Feldt, M. Kasper, R.-R. Rohloff, K. Wagner, and all technical departments of MPIA and Calar Alto Observatory, in collaboration with MPI for extraterrestrial Physics, Garching, ESO, Garching, Osservatorio Arcetri, Italy, Steward Observatory, Arizona, USA

#### CONICA

Rainer Lenzen, H. Becker, P. Bizenberger, A. Böhm, M. Hartung, W. Laun, Meixner, N. Münch, R.-R. Rohloff, C. Storz, K. Wagner, in collaboration with MPI for extraterrestrial Physics, Garching

#### LAICA

Joseph Fried, H. Baumeister, W. Benesch, F. Briegel, U. Graser, B. Grimm, Klein, K. Marien, R.-R. Rohloff, C. Unser, K. Zimmermann

#### MIDI

Christoph Leinert, Uwe Graser, A. Böhm, B. Grimm, T. Herbst, W. Laun, R. Lenzen, S. Ligor, R. Mathar, K. Meisenheimer, W. Morr, U. Neumann, E. Pitz, F. Przygodda, R.-R. Rohloff, P. Schuller, C. Storz, K. Wagner, K. Zimmermann, in collaboration with ASTRON, Dwingeloo, Amsterdam University, Sterrewacht Leiden, Observatoire de Paris-Meudon, Observatoire de la Cote d'Azur, Nice, Kiepenheuer-Institut Freiburg, Thüringer Landessternwarte Tautenburg

#### OMEGA 2000

Hermann-Josef Röser, C. Bailer-Jones, M. Alter, H. Baumeister, P. Bizenberger, A. Böhm, B. Grimm, W. Laun, U. Mall, R.-R. Rohloff, C. Storz, K. Zimmermann

#### PACS for Herschel

Dietrich Lemke, V. Galperine, U. Grözinger, R. Hofferbert, U. Klaas, R. Vavrek, H. Baumeister, A. Böhm, coordination: MPI for extraterrestrial Physics, Garching in collaboration with: DLR, Berlin, Kaiserslautern University

#### LUCIFER and LINC for the LBT

R. Lenzen, Tom Herbst, H.-W. Rix, H. Baumeister, P. Bizenberger, B. Grimm, W. Laun, Ch. Leinert, R.-R. Rohloff, coordination: Landessternwarte Heidelberg

#### LINC-NIRVANA for the LBT

T. Herbst, R. Ragazzoni, H.-W. Rix, P. Bizenberger, D. Andersen, R.-R. Rohloff, H. Baumeister, in collaboration with Köln University and Osservatorio Astrofisico di Arcetri

#### ISOPHOT Data Center

Dietrich Lemke, ISOPHOT-PI and the ISO Group at the MPIA: C. del Burgo Diaz, M. Haas, P. Heraudeau, S. Hotzel, C. Kiss, U. Klaas, O. Krause, M. Stickel, R. Vavrek, K. Wilke

#### MIRI for NGST

Dietrich Lemke, Th. Henning, U. Grözinger, R. Hofferbert, R.-R. Rohloff, K. Wagner

---

## Research Programmes

### Evolution of Globules

Roland Gredel, in collaboration with: Armagh Observatory, UK, MPI for Radio Astronomy, Bonn, Joint Astronomy Center, Hawaii, Helsinki University, Finland, ESO, Chile.

### Interstellar Ice Dust

U. Klaas, D. Lemke in collaboration with: Astrophysikalisches Institut und Universitätssternwarte Jena, Konkoly Observatory, Budapest, Hungary.

### Double Stars

Ch. Leinert, T. Herbst, A. Burkert in collaboration with: Thüringer Landessternwarte, Tautenburg, University of California, San Diego, USA, Kiel University

### Chemical Evolution of the Galaxy

C. Travaglio, A. Burkert in collaboration with: Osservatorio Astrofisico di Arcetri, Italy

**Most Distant Quasar**

Laura Pentericci, Hans-Walter Rix in collaboration with: Institute of Advanced Study and Princeton University Observatoty, Princeton, USA, Space Telescope Science Institute, Baltimore, USA, University of California, Davis, USA, LLNL, Livermore, USA, Pennsylvania State University, USA, Johns Hopkins University, Baltimore, USA, Apache Point University, New Mexico, USA, University of Chicago, USA, Astrophysikalisches Institut Potsdam, ESO, Chile.

**COMBO 17**

Christian. Wolf, Klaus Meisenheimer, A. Borch, S. Phleps, H.-W. Rix, H.-J. Röser, in collaboration with: Astronomisches Institut der Universität Bonn, Physikalisches Institut der Universität Potsdam, Institute of Physics, Oxford, Institute of Astronomy, Edinburgh, Imperial College, London.

**The Deepest Image in the Infrared**

Gregory Rudnick, Hans-Walter Rix in collaboration with: Sterrewacht Leiden and Kaplyn Institute, Groningen, NL, ESO, Garching, Caltech, Pasadena, USA., Space Telescope Science Institute, Baltimore, USA.

**Dust in Clusters of Galaxies**

Manfred Stickel, U. Klaas, D. Lemke in collaboration with: Helsinki University, Finland.

**The Jet of 3C 273**

Sebastian Jester, H.J. Röser, K. Meisenheimer in collaboration with: NRAO, New Mexico, USA, Jodrell Bank Observatory, Cheshire, UK.

**Spiral Systems within Elliptical Galaxies**

Thorsten Naab, A. Burkert.

**The Sky Background in the Far Infrared**

C. Kiss, P. Abraham, U. Klaas, D. Lemke in collaboration with: Konkoly Observatory, Budapest, Hungary, Helsinki University, Finland.

**Dark Matter**

Andreas Burkert in collaboration with: MPI for Astrophysics, Garching, Carnegie Institution, Washington, USA.

**ISO Observations of the Comet Hale-Bopp**

Christoph Leinert, D. Lemke, M. Stickel and the ISO Data Center in collaboration with: MPI für Kernphysik, Heidelberg, MPI für Aeronomie, Katlenburg-Lindau, JPL, Pasadena, USA, ESO, Chile, University of Arizona, Texas, USA, Observatoire de Paris, France, Pennstate University, USA; Laboratoire d'Astrophysique Spatiale, Marseille, France, Space Telescope Science Institute, Baltimore, USA, MIT, Cambridge, USA, Universität Prag, CZ, University of Kent, UK

*Projects not Described in this Annual Report:***PRIME – A satellite for Surveys in the Near Infrared**

D. Lemke, R. Lenzen, H.-W. Rix in an international collaboration

**NGST – Next Generation Space Telescope**

D. Lemke, Th. Henning, Grözinger, Hofferbert, R.-R. Rohloff in an international collaboration

**Jets from Young Stars**

Reinhard Mundt in collaboration with: Osservatorio Astrofisico di Arcetri, Firenze, Dublin Institute of Advanced Studies, Thüringer Landessternwarte, Tautenburg, Landessternwarte Heidelberg

**Detection of Interstellar CN**

R. Gredel in collaboration with: Universität Paris, Toledo University, USA

**Discs Around Pulsars**

M. Haas in collaboration with: CEA, Saclay, France, Oxford University, UK, Exeter University, UK

**The Effects of Gas Loss on Bounded Star Clusters**

M. Geyer, A. Burkert

**Determination of Stellar Parameters with GAIA**

C.A.L. Bailer-Jones, in collaboration with the GAIA Science Team

**Spectroscopy of Star Clusters in NGC 1399**

Eva Grebel in collaboration with: Universidad de Concepcion, Chile, Texas University, USA, Universidad Catolica, Chile, Universidad Nacional de La Plata, Argentina, Lick Observatory, USA, Observatorio Astronomico Cordoba, Argentina.

**Spectroscopic Study of the Globular Cluster Palomar 5**

M. Odenkirchen, E. Grebel, W. Dehnen, H.-W. Rix in collaboration with ESO, Chile, Yerkes-Observatorium, USA.

**Double and Multiple Star Clusters in the Large Magellanic Cloud**

Eva Grebel in Collaboration with the University and Institute for Photogrammetry, Bonn.

**CADIS – Calar Alto Deep Imaging Survey**

K. Meisenheimer, J. Fried, H. Hippelein, B. v. Kuhlmann, Ch. Leinert, S. Phleps, H.-W. Rix, H.-J. Röser, Ch. Wolf

**Cosmological Evolution of Merging Galaxies**

S. Khochfar, A. Burkert.

## Collaboration with Industrial Firms

### Calar-Alto-Observatorium

DSD Dillinger Stahlbau GmbH, Saarlouis  
PEP Modular Computers GmbH,  
Kaufbeuren

### LAICA

Filtrop AG, Balzers Liechtenstein  
Reichmann Feinoptik, Brokdorf

### OMEGA 2000

Börsig, Neckarsulm  
Compumess Electronic,  
Unterschleissheim  
Comtronic GmbH, Heiligkreuzsteinach  
Cryophysics, Darmstadt, Deutschland  
EBJ, Ladenburg  
EBV-Electronic, Leonberg  
EFH, Neidenstein  
ERNI, Adelberg  
Haecker, Weinsberg, Deutschland  
Horst Göbel, Ludwigshafen  
HTF Elektro, Mannheim  
Huber + Suhner, Taufkirchen  
Janos, Townshend, USA  
Knief GmbH, Karlsruhe  
Kugler, Salem, Deutschland  
Lemo Elektronik, München  
MSC Vertriebs-GmbH, Stutensee  
Nies Electronic, Frankfurt  
Pfeifer, Asslar, Deutschland  
Reinhold Halbeck, Offenhausen  
Riekert & Sprenger, Wertheim  
Rittal-Werk, Herborn  
Roland Häfele Leiterplattentechnik,  
Schriesheim  
Scantec, Planegg  
Spoerle Electronic, Dreieich  
Swissoptic, Herrbrugg, Schweiz  
Tower Electronic Components,  
Schriesheim  
Varian, Darmstadt, Deutschland

### MIDI

AMI Doduco GmbH  
AMS, Martinsried  
B.E.S.T. Ventile und Fittinge GmbH  
Baumer electric, Friedberg  
BOC Edwards GmbH  
Börsig, Neckarsulm  
Colder Products GmbH  
Cryophysics GmbH  
Drollinger GmbH  
Edmond Industrie Optik, Karlsruhe  
Faber Industrietechnik, Mannheim  
Ferrofluidics, Nürtingen  
Gerwah Präzisions GmbH, Grosswallstadt  
Gutekunst, Metzingen

GVL Croengineering GmbH  
Hommel Werkzeuge, Viernheim  
Infrared Labs, Tucson, USA  
Infrared Multilayer Laboratory,  
University of Reading  
ISOLOC, Stuttgart  
KOBOLD Messring GmbH  
Leybold Vakuum GmbH  
Linos Photonics, Göttingen  
Melles-Griot, Bensheim  
Merck Eurolab, Bruchsal  
Metallschleiferei Christoph Höhen  
Mörz Metallbearbeitungs GmbH  
Newport, Darmstadt  
OCLI, Santa Rosa, USA  
Pfeiffer Vacuum GmbH  
Poligrat GmbH  
Polytec, Waldbrunn  
Präzisionsoptik Gera, Gera  
RETEC Instruments, Idstein  
SHI Cryogenics Europe GmbH  
Sky Blue, München  
Taylor-Hobson, Wiesbaden  
VSYSTEMS, München  
Wiebusch, Volkmarsen  
Witzenmann GmbH

### CONICA

Walpa, Walldorf, Deutschland  
Cryophysics GmbH, Darmstadt,  
Deutschland  
Janos, Townshend, Vermont, USA  
Leybold, Hanau, Deutschland  
Nosta GmbH, Höchstadt, Deutschland

### PRIME

Kayser-Threde, Bremen  
Focus Software Inc., Tucson, USA

### PACS

Agilent (früher Hewlett-Packard),  
Böblingen  
ANTEC, Kelkheim  
Astrium Friedrichshafen  
Buerklin, München  
Comtronic GmbH, Heiligkreuzsteinach  
CryoVac Tieftemperaturtechnik, Troisdorf  
Cryophysics GmbH, Darmstadt  
Fraunhofer-Institut für Betriebsfestigkeit,  
Darmstadt  
GSF Forschungszentrum,  
Unterschleissheim  
GVL Cryoengineering, Stolberg  
Hensoldt AG, Wetzlar  
Hopt GmbH, Schöenberg  
Hoschar, Karlsruhe  
Hy-Line Power Components,

Unterhaching  
IMEC Leuven/Belgien  
Kayser-Threde, München  
Mattke Servotechnik, Freiburg  
Messer-Griesheim, Ludwigshafen  
National Instruments, München  
Oxford Instruments, Wiesbaden  
Polytec GmbH, Waldbrunn  
Rohde & Schwarz, Neu-Isenburg  
SAR Systemsolution, Ottobrunn  
Scientific Instruments, Gilching  
Stöhr Armaturen, Augsburg  
Tektronix, Köln  
Vacuumschmelze, Hanau  
Zeiss, Oberkochen

### CCD Techniques

Dataman, Pliezhausen  
EEV Ltd., GB  
Heraeus, Hanau  
ITOS GmbH, Mainz  
Lockheed Martin Fairchild Syst., USA  
Micro-Optronic-Messtechnik,  
Langebrück  
New Focus, Santa Clara, USA  
Roth, Karlsruhe  
Schäfter+Kirchhoff, Hamburg  
Schott Mainz  
SITE Corp., Beaverton, Oregon, USA  
Steward Observatory, Tucson, Arizona,  
USA  
Stöhr Armaturen, Augsburg  
Tafelmeier, Rosenheim

### Computer Equipment

AKRO, Unterschleißheim  
asknet, Karlsruhe  
Additive, Friedrichsdorf  
Bechtle, Heilbronn  
Cancom, Frankfurt  
Creaso, Gilching  
Danes, Frankfurt  
DELL, Langen  
Edo, Hockenheim  
Gordion, Troisdorf  
h-soft, Stuttgart  
INMAC, Mainz  
ISPD, Poing  
Kippdata, Bonn  
LANTEC, Planegg  
PROUT, Darmstadt  
PTC, Mannheim  
Rufenach, Heidelberg  
Schulz, München  
Scientific Computers, Aachen  
Sun, Langen  
Transec, Tübingen

**Workshops**

ABB (chem. Hartmann + Braun), Alzenau	Geier Metalle, Mannheim	Physik Instrumente, Waldbronn
Almet-AMB, Mannheim	GLT, Pforzheim	Phytec Meßtechnik, Mainz
Amphenol-Tuchel Electronics, Heilbronn	Gould Nicolet Meßtechnik, Dietzenbach	Phytron, Gröbenzell
Angst+Pfister, Mörfelden	Grandpair, Heidelberg	Plastipol, Runkel
APE Elektronik, Kuppenheim	Gutekunst, Gutekunst	PSI Tronix, Tulare, California, USA
Auer Paul GmbH, Mannheim	Halm+Kolb, Stuttgart	Püschel Elektronik, Mannheim
Best Power Technology, Erlangen	Heidenhain, Traunreut	RED. Regional-Electronic-Distribution, Rodgau-Jügesheim
Binder Magnete, Villingen-Schwenningen	Hilma-Römheld GmbH, Hilchenbach	Radiall, Rödermark
Bohnenstiel, Heidelberg	Helukabel, Hemmingen	Rau-Meßtechnik, Kerkheim
Böllhoff, Winnenden	Hema, Mannheim	Räder Gangl, München
Börsig, Neckarsulm	Herz, Leister Geräte, Neuwied	Reeg, Wiesloch
Bubbenzer Bremsen, Kirchen-Wehrbach	Hewlett-Packard Direkt, Böblingen	Reinhold Halbeck, Offenhausen
Bürklin, München	HM Industrieservice, Waghäusel	Reith, Mannheim
C&K Components, Neuried b. München	Hommel-Hercules Werkzeughandel, Viernheim	Retronic, Ronneburg
C.A.P. CNC+Coating Technik, Zell. a. H.	Horst Gobel, Ludwigshafen	Riekert & Sprenger, Wertheim
CAB, Karlsruhe	Horst Pfau, Mannheim	Rittal-Werk, Herborn
Cadillac-Plastic, Viernheim	HOT Electronic, Taufkirchen	Roland Häfele Leiterplattentechnik, Schriesheim
Carl Roth, Karlsruhe	HTF Elektro, Mannheim	Roth, Karlsruhe
Cherry Mikroschalter, Auerbach	Huber + Suhner, Taufkirchen	RS Components, Mörfelden-Walldorf
Coating-Plast, Schriesheim	Hummer+Rieß, Nürnberg	RSP-GmbH, Mannheim
Com Pro, Stuttgart	IBF Mikroelektronik, Oldenburg	Rudolf, Heidelberg
Compumess Elektronik, Unterschleissheim	Infrared Labs, Tucson, USA	Rütgers, Mannheim
Comtronic GmbH, Heiligkreuzsteinach	Inkos, Reute/Breisgau	Rufenach Vertriebs-GmbH, Heidelberg
Conrad Electronic, Hirschau	iSystem, Dachau	Rutronik, Ispringen
Cryophysics, Darmstadt	Jacobi Eloxal, Altlusheim	Sartorius, Ratingen
Dannewitz, Linsengericht	Jarmyn, Limburg	Sasco, Putzbrunn
DMG-Service, Pfronten	Joisten+Kettenbaum, Bergisch Gladbach	Scantec, Planegg
Delta, Wuppertal	Kaufmann, Crailsheim	Schaffner Elektronik, Karlsruhe
Dürkes & Obermayer, Heidelberg	Kerb-Konus-Vertriebs-GmbH, Amberg	Schuricht, Fellbach-Schmidlen
Dyna Systems NCH, Mörfelden-Walldorf	Kniel, Karlsruhe	Schweizer Elektroisierungsstoffe, Mannheim
EBARA Pumpen, Dietzenbach	Knürr, München	SCT Servo Control Technology, Taunusstein
EBJ, Ladenburg	Lambda Electronics, Achern	SE Spezial-Electronic, Bückeberg
EBV-Elektronik, Leonberg	Lemo Elektronik, München	Seifert mtm Systems, Ennepetal
EC Motion, Mönchenglöblich	LPKF CAD/CAM Systeme, Garbsen	Siemens IC-Center, Mannheim
Edsyn Europa, Kreuzwertheim	Macrotron, München	Spaeter, Viernheim
EFH, Neidenstein	Mankiewicz, Hamburg	Spindler & Hoyer, Göttingen
Eldon, Büttelborn	Matsuo Electronics Europe, Eschborn	Spoerle Electronic, Dreieich
Elna Transformatoren, Sandhausen	Matsushita Automation, Holzkirchen	Stäubli, Bayreuth
elspec, Geretsried	Maxim Ges. f. elektronische integrierte Bausteine, Planegg	SUCO-Scheuffele, Bietigheim-Bissingen
ELV Elektronik, Leer	Menges electronic, Dortmund	Synatron, Hallbergmoos
ERNI, Adelberg	Metrofunkkabel-Union, Berlin	Tandler, Brauen
eurodis Enatechnik, Quickborn	Mitsubishi-Electric, Weiterstadt	Thorlabs, Gruenberg
EWf, Eppingen	MSC Vertriebs-GmbH, Stutensee	TMS Test- und Meßsysteme, Herxheim/Hayna
Farben Specht, Bammental	MTI, Baden-Baden	Tower Electronic Components, Schriesheim
Faber, Mannheim	Munz, Lohmar	TreNew Electronic, Pforzheim
Farnell Electronic Components, Deisenhofen	Nanotec, Finsing	TS-Optoelectronic, München
Farnell Electronic Services, Möglingen	Newport, Darmstadt	TWK-Elektronik, Karlsruhe
FCT Electronic, München	Nickel Schalt- und Meßgeräte, Villingen-Schwenningen	Vacuumschmelze, Hanau
Fels Spedition, Heidelberg	Nies Electronic, Frankfurt	VBE Baustoff+Eisen, Heidelberg
Fisba, St. Gallen	Noor, Viernheim	Vero Electronics, Bremen
Fischer Elektronik, Lüdenscheid	Nova Elektronik, Pulheim	W. & W. Schenk, Maulbronn
FPS-Werkzeugmaschinen GmbH, Otterfing	Oberhausen, Ketsch	Wikotec, Bramsche
Franke, Aalen	Otto Faber, Mannheim	Wilhelm Gassert, Schriesheim
Fritz Faulhaber, Schönaich	OWIS GmbH, Staufen	WS CAD Elektronik, Berk Kirchen
Future Electronics Deutschland, Unterföhring	Parametric Technology, Muenchen	Witter GmbH, Heidelberg
Ganter, Walldorf	Parcom, CH-Flurlingen	WIKI, Klingenberg
	pbe Electronic, Elmshorn	
	Pfeiffer, Mannheim	

## Teaching Activities

### Summer Term 2001

- J. W. Fried, B. Fuchs: Galaxies (Lecture)  
 K. Meisenheimer: Radio Galaxies (Lecture)  
 H.-J. Röser: Cosmological Test Observations (Lecture)  
 U. Klaas: Ultra- und hyperluminous Infrared Galaxies (Lecture)  
 M. Stickle: Astrophysical Data Analysis (Lecture)  
 Ch. Leinert, D. Lemke, R. Mundt, H.-M. Schmid, W.M. Tscharnuter, P. Ulmschneider: Introduction to Astronomy and Astrophysics III (Seminar)  
 Ch. Leinert, E. Gehlken, J. Krautter, H. Görgemanns, P. Ulmschneider: History of Astronomy (Seminar)  
 A. Burkert, B. Fuchs, A. Just, H.-W. Rix, R. Spurzem, R. Wielen: Stellar Dynamics (Seminar)  
 The Astronomy Lecturers: Astronomical Colloquium

### Winter Term 2001/2002

- W. Dehnen: Gravitational Lenses: Concepts and Applications in Astronomy (Lecture)  
 W.J. Duschl, D. Lemke, R. Mundt, H.J. Röser, W.M. Tscharnuter: Introduction to Astronomy and Astrophysics III (Seminar)  
 A. Burkert, B. Fuchs, A. Just, H.-W. Rix, R. Spurzem, R. Wielen: Structure, Kinematics and Dynamics of Stellar Systems (Seminar)  
 J. Kirk, K. Meisenheimer: Particle Acceleration and Radiation Processes in Radio Galaxies (Seminar)  
 The Astronomy Lecturers: Astronomical Colloquium

## Meetings, Talks and Public Lectures

- Workshop on "Dwarf Galaxies and Their Environment", Bad Honnef, January: E.K. Grebel (invited talk)  
 Seminar, University of Hertfordshire, England, January: L. Pentericci (invited talk)  
 The Origin of the World, Fachhochschule Regensburg, January: H.-W. Rix (talk)  
 ISO Calibration Legacy Conference, Vilspa, Spanien, February: P. Ábraham, P. (talk)  
 ISO Calibration Legacy Conference, Vilspa, Spanien, February: C. del Burgo (talk, 2 posters)  
 Universidad Complutense de Madrid, Madrid, Spanien, February: C. del Burgo (invited talks)  
 American Association for the Advancement of Science, San Francisco, USA, February: E. K. Grebel (invited review)  
 ISO Calibration Legacy Conference, Vilspa, Spanien, February: P. Héraudeau (talk, poster), U. Klaas (invited talk), D. Lemke (invited talk)  
 Massive Black Holes from  $z = 0.001$  to  $z = 4.5$ , University of Cambridge, February: H.-W. Rix (invited talk)  
 Massive Black Holes from  $z = 0.001$  to  $z = 4.5''$ , University of Oxford, February: H.-W. Rix (invited talk)  
 ISO Calibration Legacy Conference, Vilspa, Spanien, February: K. Wilke (talk)  
 The atmospheres of ultracool dwarfs, Carnegie Mellon University, Pittsburgh, PA, USA, March: C.A.T. Bailer-Jones  
 Variability and rotation in ultracool dwarfs, Zentrum für Astronomie und Astrophysik, Technische Universität, Berlin, March: C.A.T. Bailer-Jones

- The Dark Universe, Baltimore, MA, USA, March: A. Burkert (invited talk)
- IAU Symposium 207 über “Extragalactic Star Clusters”, Pucón, Chile, March: E. K. Grebel (invited review)
- SDSS Collaboration Meeting, Chicago, USA, March: E. K. Grebel (invited talk)
- Astronomisches Kolloquium, Universität Bonn und MPIfR, March: S. Jester (invited talk)
- Astronomische Großgeräte, Potsdam, March: D. Lemke
- SDSS General Collaboration Meeting, Chicago, USA, March/April: L. Pentericci
- IAU Symposium 207, Extragalactic Star Clusters, Pucon, Chile, March: A. Stolte (poster)
- INAOE, Mexico, April: C. del Burgo (invited talk)
- Kolloquium, University of Wisconsin, Madison, USA, April: E.K. Grebel
- Planetarium Stuttgart, April: E.K. Grebel (public talk)
- OPTICON Board Meeting, Catania, Italien, April: R. Gredel
- Mirror Maintenance Conference, Mt. Palomar Observatory, April: R. Gredel
- Infrarot-Kolloquium, Freiburg, April: R. Hofferbert (invited talk)
- First DIVA Thinkshop, MPIA, Heidelberg, April: K.-H. Marien
- ESO Workshop on “The Origin of Stars and Planets, Garching, April: A. Stolte (Poster)
- EBL Workshop, Helsinki, Finland, April: D. Lemke
- Black Holes at the Centers of Galaxies from  $z > 4$ , AIP, Potsdam, April: H-W. Rix (invited talk)
- Spectral classification in large, deep surveys using neural networks, Astronomisches Institut der Universität Basel, May: C.A.T. Bailer-Jones (invited talk)
- Modelling data: Analogies in neural networks, simulated annealing and genetic algorithms, Konferenz “Model-based reasoning”, Pavia, Italy, May: C.A.T. Bailer-Jones
- OMEGA 2000: a new wide field near infrared camera for Calar Alto und “Time-resolved photometric monitoring of brown dwarfs”, Calar Alto Kolloquium, Heidelberg: May: C.A.T. Bailer-Jones
- Calar Alto Colloquium, Heidelberg, May: E.K. Grebel (talk)
- GAIA Conference The termination of stellar parameters with GAIA, ESTEC/ESA, Netherlands: June: C.A.T. Bailer-Jones (invited talk)
- Dark Matter, Annual Meeting of the Max Planck Society, Berlin, June: A. Burkert (invited talk)
- XVIIth IAP Colloquium on “Gaseous Matter in Galaxies and Intergalactic Space”, Paris, Frankreich, June: E. K. Grebel (invited review)
- IAU Colloquium “184 AGN Surveys”, Armenien, June: M. Haas (invited talk)
- “Where’s The Matter? Tracing Dark and Bright Matter With The New Generation of Large-Scale Surveys, June: S. Khochfar
- Particle Astrophysics Workshop, Potsdam, June: D. Lemke (invited talk)
- Infrared and Submillimeter Space Astronomy Colloquium, Fance, June: M. Stickel (invited talk)
- “Determination of stellar parameters with GAIA” at the Konferenz “Census of the Galaxy: Challenges for photometry and spectrometry with GAIA”, Wilna, Littauen, July: C.A.T. Bailer-Jones
- Workshop on “The Lowest-Mass Galaxies and Constraints on Dark Matter”, Schloss Ringberg, July /August: E. K. Grebel (talks)
- Conference “Tracing Cosmic Evolution with Galaxy Clusters”, Sesto, Alto Adige, Italy, July: L. Pentericci
- “Galaxy Structure Research at the MPIA, talk, Heidelberg, July: H.-W.Rix
- “Galactic Nuclei: Is smaller more interesting?”, Symposium “The Lowest Mass Galaxies”, Schloss Ringerb, July: H.-W. Rix
- “Tracing Cosmic Evolution with Galaxy Clusters”, Sesto, Alto Adige, Italy: July: H.-J. Röser
- “Cosmological Galaxy Formation and Dark Matter Halos, Workshop, Santa Cruz, CA, USA, August: A. Burkert (invited talk)
- MPA/Eso/MPE/USM Joint Astronomy Conference: “Lighthouses of the Universe”, Garching, August: S. Jester (talk)
- Conference “Lighthouses of the Universe: The Most Luminous Celestial Objects and their use for Cosmology”, Garching, August: L. Pentericci
- German School and Rotary Club, Marbella, Spain, September: K. Birkle (public talk)
- “First UKAFF Conference”, Leicester, UK, September: A. Burkert (invited talk)
- Kolloquium, Observatoire de Strasbourg, Strasbourg, Frankreich, September: E.K. Grebel
- OPTICON Medium-sized Telescopes, Toulouse, Frankreich, September: R. Gredel
- OPTICON Board Meeting, München, September: R. Gredel
- 9th ESMATS, Belgium, September: R. Hofferbert (invited talk)
- Workshop on Relativistic Jets, Schloss Ringberg, September: S. Jester

- Colloquium, Astronomy & Astrophysics Department, University of Chicago, September: S. Jester
- Astronomical Colloquium, University of Minnesota, September: S. Jester (invited talk)
- Science Lunch talk, MIT Center for Space Research, Cambridge, USA, September: S. Jester
- 9th ESMATS; Belgien, September: O. Krause
- JENAM, Munich, September: C. Maier (Poster)
- Workshop “Elliptical Galaxies”, Schloss Ringberg, November: A. Burkert (invited talk)
- Physics Colloquium and Seminar talk, Bochum University, November: E. K. Grebel
- Workshop “Formation & Evolution of Giant Elliptical Galaxies”, Ringberg, November: U. Klaas (invited talk)
- “Disks of Galaxies: Kinematics, Dynamics and Perturbations”, Puebla, Mexico, November: T. Kranz (talk)
- Hochschultag, TFH Berlin, November: D. Lemke (speech of the day)
- XIII Canary Islands Winter School of Astrophysics: “Cosmochemistry”, Puerto de la Cruz, Teneriffa, November: C. Maier (poster)
- DFG-Workshop zur Sternentstehung, Bad Honnef, November: R. Mundt
- International Conference “Disks of Galaxies: Kinematics, Dynamics and Perturbations”, Puebla, Mexiko, November: H-W Rix (talk)
- “Gas vs. Stars, Jeans vs. Schwarzschild: The Pain and Gain of Detailed Dynamical Modeling”, Workshop, Schloss Ringberg. November: H-W Rix (talk)
- Colloquium, Steward Observatory, University of Arizona, Tucson, December: E.K. Grebel
- ESO, Garching, December: U. Klaas (invited talk)

## Service in Committees

- C.A.T. Bailer-Jones: member of the GAIA Science Team of ESA; Chairman of the GAIA “Classification” working group; member of DIVA working group for Photometry and Spectroscopy; member of the Scientific Organizing Committee for the conference “Census of the Galaxy: Challenges for photometry and spectrometry with GAIA.
- E. K. Grebel: member of the Canadian Program Committee for the Gemini Telescopes, member of the student selection committee at the MPIA, member of the PhD Advisory Council (PAC) at the MPIA, speaker of the MPIA in the Collaboration Council of the Sloan Digital Sky Survey, Women Speaker, member of the Board of the Scientific Ernst Patzer Foundation.
- R. Grebel: member of the Calar Alto Program Committee and of the OPTICON working group “Future of medium-sized telescopes”
- U. Klaas: member of the ISO Post Operations Coordination Committee, Co-Investigator in the HERSCHEL-PACS Consortium
- K.-H. Marien: member of the DIVA Co-Investigator Team
- R. Mundt: member of the Calar Alto Program Committee
- D. Lemke: member of the ISO Science Team of ESA; Co-Investigator in the HERSCHEL-PACS consortium; Co-Investigator for NGST-MIRI; member of the Experts Board for Astronomical Research, coordinator for MPIA in the POE-Netzwerk
- R.-R. Rohloff, member of the Sloan Digital Sky Survey (SDSS) Review Committee
- H.-J. Röser, secretary of the Calar Alto Program Committee

## Publications

- Abrahám, P., C. Kiss, L. V. Tóth, A. Moór, F. Sato, S. Nikoli and J. G. A. Wouterloot: Low mass clouds in the Cepheus-Cassiopeia void. I. Khavtassi 15. *Astronomy and Astrophysics* 363, 755-766 (2001)
- Azzaro, M., C. M. Gutiérrez and F. Prada: Morphological Analysis of Satellite Galaxies in External Systems. In: *Galaxy Disks and Disk Galaxies, Rome/Italy 2000*, (Eds.) J.G. Funes, E.M. Corsini. ASP Conference Series 230, Astronomical Society of the Pacific, San Francisco 2001, 431-432
- Bailer-Jones, C. A. L.: Automated stellar classification for large surveys: a review of methods and results. In: *Automated Data Analysis in Astronomy, Puna/India 2000*, (Eds.) R. Gupta, H.P. Singh, C.A.L. Bailer-Jones. Narosa Publishing House, New Delhi 2001, 83-98
- Bailer-Jones, C. A. L.: Surface Features, Rotation and Atmospheric Variability of Ultra Cool Dwarfs. In: *Ultracool Dwarfs: New Spectral Types L and T, Manchester 2000*, (Eds.) H.R.A. Jones, I.A. Steele. Springer, Heidelberg 2001, 271-288
- Bailer-Jones, C. A. L., R. Gupta and H. P. Singh: An introduction to artificial neural networks. In: *Automated Data Analysis in Astronomy, Puna/India 2000*, (Eds.) R. Gupta, H.P. Singh, C.A.L. Bailer-Jones. Narosa Publishing House, New Delhi 2001, 51-68
- Bailer-Jones, C. A. L. and R. Mundt: Erratum: Variability in ultra cool dwarfs: Evidence for the evolution of surface features. *Astronomy and Astrophysics* 374, 1071 (2001)
- Bailer-Jones, C. A. L. and R. Mundt: Variability in ultra cool dwarfs: Evidence for the evolution of surface features. *Astronomy and Astrophysics* 367, 218-235 (2001)
- Bailer-Jones, C. A. L., R. Mundt and D. Barrado y Navascués: A Deep Medium Band Survey for Brown Dwarfs in IC 2391. In: *Cool Stars, Stellar Systems and the Sun – 11th Cambridge Workshop, Puerto de la Cruz/Tenerife 1999*, (Eds.) Garcia Lopez, R.J., R. Rebolo, M.R. Zapatero Osorio. ASP Conference Series 223, Astronomical Society of the Pacific, San Francisco 2001, CD-1508
- Bailer-Jones, D. M. and C. A. L. Bailer-Jones: Modelling data: Analogies in neural networks, simulated annealing and genetic algorithms. In: *Model-based Reasoning, Pavia/Italy 2001*, (Ed.) L. Magnani. Kluwer/Plenum, Dordrecht 2001, 85-102
- Barrado y Navascués, D., J. R. Stauffer, J. Bouvier and E. Martín: From the Top to the Bottom of the Main Sequence: A Complete Mass Function of the Young Open Cluster. *The Astrophysical Journal* 546, 1006-1018 (2001)
- Barrado y Navascués, D., J. R. Stauffer, C. Briceno, B. Patten, N. C. Hambly and J. D. Adams: Very low-mass stars and brown dwarfs of the young open cluster IC 2391. *The Astrophysical Journal Supplement Series* 134, 103-114 (2001)
- Barrado y Navascués, D., M. R. Zapatero Osorio, V. J. S. Béjar, R. Rebolo, E. L. Martín, R. Mundt and C. A. L. Bailer-Jones: Optical spectroscopy of isolated planetary mass objects in the  $\sigma$  Orionis cluster. *Astronomy and Astrophysics* 377, L9-L13 (2001)
- Barth, A. J., L. C. Ho, A. V. Filippenko, H.-W. Rix and W. L. W. Sargent: The Broad-Line and Narrow-Line Regions of the LINER NGC 4579. *The Astrophysical Journal* 546, 205-209 (2001)
- Barth, A. J., M. Sarzi, H.-W. Rix, L. C. Ho, A. V. Filippenko and W. L. W. Sargent: Evidence for a Supermassive Black Hole in the S0 Galaxy NGC 3245. *The Astrophysical Journal* 555, 685-708 (2001)
- Béjar, V. J. S., E. L. Martín, M. R. Zapatero Osorio, R. Rebolo, D. Barrado y Navascués, C. A. L. Bailer-Jones, R. Mundt, I. Baraffe, C. Chabrier and F. Allard: The Substellar Mass Function in  $\sigma$  Orionis. *The Astrophysical Journal* 556, 830-836 (2001)
- Béjar, V. J. S., M. R. Zapatero Osorio, R. Rebolo, D. Barrado Y Navascués, C. A. L. Bailer-Jones and R. Mundt: A Deep IZ(J) Search for the Brown Dwarf Population in  $\sigma$  Orionis. In: *Cool Stars, Stellar Systems and the Sun – 11th Cambridge Workshop, Puerto de la Cruz/Tenerife 1999*, (Eds.) Garcia Lopez, R.J., R. Rebolo, M.R. Zapatero Osorio. ASP Conference Series 223, Astronomical Society of the Pacific, San Francisco 2001, CD-1519

- Berkefeld, T., A. Glindemann and S. Hippler: Multi-Conjugate Adaptive Optics with Two Deformable Mirrors: Requirements and Performance. *Experimental Astronomy* 11, 1-21 (2001)
- Bodenheimer, P. and A. Burkert: Formation of Wide Binaries by Fragmentation. In: *Birth and Evolution of Binary Stars (Posters)*, Potsdam 2000, (Eds.) B., H. Reipurth, Zinnecker. International Astronomical Union, Astrophysikalisches Institut Potsdam, Potsdam 2001. IAU Symposium 200, D. Reidel Publ. Comp., Dordrecht 2001, 13
- Boehnhardt, H., G. Tozzi, K. Birkle, O. Hainaut, T. Sekiguchi, M. Vair, J. Watanabe and G. Rupprecht: Visible and near-IR observations of transneptunian objects. Results from ESO and Calar Alto Telescopes. *Astronomy and Astrophysics* 378, 653-667 (2001)
- Böker, T., R. P. van der Marel, L. Mazzuca, H.-W. Rix, G. Rudnick, L. C. Ho and J. C. Shields: A Young Stellar Cluster in the Nucleus of NGC 4449. *The Astronomical Journal* 121, 1473-1481 (2001)
- Bonaccini, D., W. Hackenberg, M. Cullum, E. Brunetto, M. Quattri, E. Allaert, M. Dimmler, M. Tarenghi, A. van Kersteren, C. di Chirico, M. Sarazin, B. Buzzoni, P. Gray, R. Tamai, M. Tapia, R. Davies, S. Rabien, T. Ott and S. Hippler: ESO VLT Laser Guide Star Facility. *The Messenger* 105, 9 (2001)
- Brandner, W., E. K. Grebel, R. H. Barbá, N. R. Walborn and A. Moneti: Hubble Space Telescope NICMOS Detection of a Partially Embedded, Intermediate-Mass, Pre-Main-Sequence Population in the 30 Doradus Nebula. *The Astronomical Journal* 122, 858-865 (2001)
- Burkert, A.: The Formation of the Milky Way in the Cosmological Context. In: *Cosmic Evolution*, Paris 2000, (Eds.) E. Vangioni-Flam, R. Ferlet, M. Lemoine. World Scientific, New Jersey/USA 2001, 245
- Burkert, A.: Self-Interacting Cold Dark Matter Halos. In: *Dark Matter in Astro- and Particle Physics*, Heidelberg 2000, (Ed.) H.V. Klapdor-Kleingrothaus, Springer, Heidelberg 2001, 89
- Burkert, A. and P. Bodenheimer: Turbulence and Cloud Angular Momentum. In: *The Formation of Binary Stars*, Potsdam/Germany 2000, (Eds.) H. Zinnecker, R.D. Mathieu. IAU Symposium 200, International Astronomical Union, Astronomical Society of the Pacific, San Francisco 2001, 122-131
- Burkert, A. and T. Naab: Evidence for Large Stellar Disks in Elliptical Galaxies. In: *Starburst Galaxies: Near and Far*, Ringberg Castle/Germany 2000, (Eds.) L. Tacconi, D. Lutz. Springer, Heidelberg 2001, 147
- Burkert, A. and J. Silk: Star Formation-Regulated Growth of Black Holes in Protogalactic Spheroids. *The Astrophysical Journal* 554, L151-L154 (2001)
- Busso, M., R. Gallino, D. L. Lambert, C. Travaglio and V. V. Smith: Nucleosynthesis and Mixing on the Asymptotic Giant Branch. III. Predicted and Observed s-Process Abundances. *The Astrophysical Journal* 557, 802-821 (2001)
- Butler, D. J., R. Davies and M. Feldt: ALFA Crowded Field Observations: Experiences, Data Reduction, and Future Strategies. In: *Adaptive Optical Systems Technology*, Munich/Germany 2000, (Ed.) P. Wizinowich. SPIE Conference Series 4007, SPIE, Bellingham, WA. 2001, 857-863
- Cenarro, A. J., N. Cardiel, J. Gorgas, R. F. Peletier, A. Vazdekis and F. Prada: Empirical calibration of the near-infrared CaII triplet. I. The stellar library and index definition. *Monthly Notices of the Royal Astronomical Society* 326, 959-980 (2001)
- Cenarro, A. J., J. Gorgas, N. Cardiel, S. Pedraz, R. F. Peletier and A. Vazdekis: Empirical calibration of the near-infrared CaII triplet. II. The stellar atmospheric parameters. *Monthly Notices of the Royal Astronomical Society* 326, 981-994 (2001)
- Cenarro, A. J., J. Gorgas, N. Cardiel, A. Vazdekis, R. F. Peletier, S. Pedraz and F. Prada: The Near-IR CA II Triplet: Empirical Calibration and Stellar Populations Synthesis Models. In: *Highlights of Spanish Astrophysics II*, Santiago de Compostela/Spain 2000, (Eds.) J. Zamorano, J. Gorgas, J. Gallego. 4th Meeting of Spanish Astronomical Society, Kluwer Academic Publishers, Dordrecht 2001, 137-140
- Cretton, N., T. Naab, H.-W. Rix and A. Burkert: The Kinematics of 3:1 Merger Remnants and the Formation of Low-Luminosity Elliptical Galaxies. *The Astrophysical Journal* 554, 291-297 (2001)
- Cretton, N., T. Naab, H.-W. Rix and A. Burkert: The Kinematics of 3:1-Merger Remnants and the Formation of Low-Luminosity Elliptical Galaxies. In: *Galaxy Disks and Disk Galaxies*, Rome 2000, (Eds.) G. José, J.G. Funes, E.M. Corsini. ASP Conference Series 230, Astronomical Society of the Pacific, San Francisco 2001, 261-262
- Davies, R. I., M. Tecza, L. W. Looney, F. Eisenhauer, L. E. Tacconi-Garman, N. Thatte, T. Ott, S. Rabien, S. Hippler and M. Kasper: Adaptive Optics Integral Field Spectroscopy of the Young Stellar Objects in LkH $\alpha$  225. *The Astrophysical Journal* 552, 692-698 (2001)

- Dehnen, W.: Towards optimal softening in three-dimensional N-body codes – I. Minimizing the force error. *Monthly Notices of the Royal Astronomical Society* 324, 273-291 (2001)
- Dole, H., R. Gispert, G. Lagache, J.-L. Puget, F. R. Bouchet, C. Cesarsky, P. Ciliegi, D. L. Clements, M. Dennefeld, F.-X. Désert, D. Elbaz, A. Franceschini, B. Guiderdoni, M. Harwit, D. Lemke, A. F. M. Moorwood, S. Oliver, W. T. Reach, M. Rowan-Robinson and M. Stickel: FIRBACK III: Catalogue, source counts and cosmological implications of the 170  $\mu\text{m}$  ISO deep survey. *Astronomy and Astrophysics* 372, 364-376 (2001)
- Dolphin, A. E., L. Makarova, I. D. Karachentsev, V. E. Karachentseva, D. Geisler, E. K. Grebel, P. Guhathakurta, P. W. Hodge, A. Sarajedini and P. Seitzer: The stellar content and distance of UGC 4483. *Monthly Notices of the Royal Astronomical Society* 324, 249-256 (2001)
- Dye, S., A. N. Taylor, E. M. Thommes, K. Meisenheimer, C. Wolf and J. A. Peacock: Gravitational lens magnification by Abell 1689: distortion of the background galaxy luminosity function. *Monthly Notices of the Royal Astronomical Society* 321, 685-698 (2001)
- Fan, X., V. K. Narayanan, R. H. Lupton, M. A. Strauss, G. R. Knapp, R. H. Becker, R. L. White, L. Pentericci, S. K. Leggett, Z. a. n. Haiman, J. E. Gunn, Z. Ivezic, D. P. Schneider, S. F. Anderson, J. Brinkmann, N. A. Bahcall, A. J. Connolly, I. a. n. Csabai, M. Doi, M. Fukugita, T. Geballe, E. K. Grebel, D. Harbeck, G. Hennessy, D. Q. Lamb et al.: A Survey of  $z \sim 5.8$  Quasars in the Sloan Digital Sky Survey. I. Discovery of Three New Quasars and the Spatial Density of Luminous Quasars at  $z \sim 6$ . *The Astronomical Journal* 122, 2833-2849 (2001)
- Fried, J. W., B. von Kuhlmann, K. Meisenheimer, H.-W. Rix, C. Wolf, H. H. Hippelein, M. Kümmel, S. Phleps, H. J. Röser, I. Thiering and C. Maier: The luminosity function of field galaxies and its evolution since  $z = 1$ . *Astronomy and Astrophysics* 367, 788 - 800 (2001)
- Fried, J. W. and B. M. F. von Kuhlmann: The Evolution of the Luminosity Function of Field Galaxies from  $z = 1$  to  $z = 0$ . In: *The Evolution of Galaxies I. Observational Clues*, Granada/Spain 2000, (Eds.) J.M. Vilchez, G. Stasinska, E. Pérez. *Astrophysics and Space Science Supplement* 277, Kluwer Academic Publishers, Dordrecht 2001, 581
- Gallego, J., A. Delgado, J. Zamorano and M. Stickel: Far-Infrared properties of local star-forming galaxies from the UCM sample. In: *The Promise of the Herschel Space Observatory*, Toledo/Spain 2000, (Eds.) G.L. Pilbratt, J. Cernicharo, A.M. Heras et al. *ESA Special Publications SP-460*, ESA, Noordwijk 2001, 401
- Geyer, M. P. and A. Burkert: The Effect of Gas Loss on the Formation of Bound Stellar Clusters. *Monthly Notices of the Royal Astronomical Society* 323, 988-994 (2001)
- Geyer, M. P. and A. Burkert: Gas Expulsion from Star Forming Regions and the Formation of Globular Clusters. In: *Galaxy Disks and Disk Galaxies*, Rome 2000, (Eds.) J.G. Funes, E.M. Corsini. *ASP Conference Series* 230, Astronomical Society of the Pacific, San Francisco 2001, 311-312
- Grebel, E. K.: Dwarf Galaxies in the Local Group in the Local Volume. In: *Dwarf Galaxies and Their Environment*, Bad Honnef/Germany 2001, (Eds.) K.S. de Boer, R.-J. Dettmar, U. Klein. *Shaker Verlag*, Aachen 2001, 45-52
- Grebel, E. K.: A Map of the Northern Sky: The Sloan Digital Sky Survey in Its First Year. In: *Dynamic Stability and Instabilities in the Universe*, Bremen, Germany 2000, (Ed.) R. Schielicke. *Reviews in Modern Astronomy* 14, *Astronomische Gesellschaft*, Hamburg 2001, 223-243
- Grebel, E. K.: Star Formation Histories of Nearby Dwarf Galaxies. *Astrophysics and Space Science* 277, 231-239 (2001)
- Grebel, E. K.: Stellar Populations in Local Group Dwarf Galaxies and Beyond. In: *Science with the Large Binocular Telescope*, Ringberg Castle/Germany 2000, (Ed.) T. Herbst. *Max-Planck Society and LBT Beteiligungsgesellschaft*, Heidelberg 2001, p. 79-85
- Gredel, R.: The Calar Alto Observatory: present and future instrumentation. *New Astronomy Review* 45, 33-36 (2001)
- Gredel, R., J. H. Black and M. Yan: Interstellar C2 and CN toward the Cyg OB2 association. A case study of X-ray induced chemistry. *Astronomy and Astrophysics* 375, 553-565 (2001)
- Grün, E., M. S. Hanner, S. B. Peschke, T. Müller, H. Boehnhardt, T. Y. Brooke, H. Campins, J. Crovisier, C. Delahodde, I. Heinrichsen, H. U. Keller, R. F. Knacke, H. Krüger, P. Lamy, C. Leinert, D. Lemke, C. M. Lisse, M. Müller, D. J. Osip, M. Solc, M. Stickel, M. Sykes, V. Vanysek and J. Zarnecki: Broadband infrared photometry of comet Hale-Bopp with ISOPHOT. *Astronomy and Astrophysics* 377, 1098-1118 (2001)

- Guenther, E. W., V. Joergens, R. Neuhäuser, G. Torres, N. Stout Batalha, J. Vijapurkar, M. Fernández and R. Mundt: A Spectroscopic and Photometric Survey for Pre-Main Sequence Binaries. In: *The Formation of Binary Stars*, Potsdam/Germany 2000, (Eds.) H. Zinnecker, R.D. Mathieu. IAU Symposium 200, International Astronomical Union, Astronomical Society of the Pacific, San Francisco 2001, 165-168
- Guenther, E. W., R. Neuhäuser, V. Joergens, M. Fernández, N. S. Batalha, R. Mundt, C. Leinert, J. Vijapurkar and G. Torres: A Search for Pre-main Sequence Spectroscopic Binaries. In: *Cool Stars, Stellar Systems and the Sun – 11th Cambridge Workshop*, Puerto de la Cruz/Tenerife 2000, (Eds.) R.J. Garcia Lopez, R. Rebolo, M.R. Zapatero Osorio. ASP Conference Series 223, Astronomical Society of the Pacific, San Francisco 2001, CD-515
- Guenther, E. W., G. Torres, N. Stout Batalha, V. Joergens, R. Neuhäuser, J. Vijapurkar, M. Fernández and R. Mundt: RXJ1603.8-3938 – A Surprising Pre-Main Sequence Spectroscopic Binary. *Astronomy and Astrophysics* 366, 965-971 (2001)
- Gupta, R., H.P. Singh, C.A.L. Bailer-Jones (Eds.): *Automated Data Analysis in Astronomy*, IUCAA, Puna/ India, 2000. Narosa Publishing House, New Delhi 2001, 364 pp
- Haas, M.: Dust in PG Quasars As Seen By ISO. *New Astronomy Reviews* 45, 617-624 (2001)
- Haas, M., U. Klaas, K. Meisenheimer, D. Lemke, S. A. H. Müller and R. Chini: The infrared spectra of quasars as seen by ISO. In: *The Promise of the Herschel Space Observatory*, Toledo/Spain 2000, (Eds.) G.L. Pilbratt, J. Cernicharo, A.M. Heras et al. ESA Special Publication Series SP-460, ESA, Noordwijk 2001, 139-142
- Haas, M., U. Klaas, S. A. H. Müller, R. Chini and I. Coulson: The PAH 7.7  $\mu\text{m}$ /850 m ratio as new diagnostics for high extinction in ULIRGs – increasing evidence for a hidden quasar in Arp 220. *Astronomy and Astrophysics* 367, L9-L13 (2001)
- Harbeck, D., E. K. Grebel, J. Holtzman, P. Guhathakurta, W. Brandner, D. Geisler, A. Sarajedini, A. Dolphin, D. Hurley-Keller and M. Mateo: Population Gradients in Local Group Dwarf Spheroidal Galaxies. *The Astronomical Journal* 122, 3092-3105 (2001).
- Heitsch, F., M.-M. MacLow and R. S. Klessen: Gravitational Collapse in Turbulent Molecular Clouds. II. Magnetohydrodynamical Turbulence. *The Astrophysical Journal* 547, 280-291 (2001)
- Henning, T., M. Feldt, B. Stecklum and R. Klein: High-resolution imaging of ultracompact HII regions. III. G11.11-0.40 and G341.21-0.21. *Astronomy and Astrophysics* 370, 100-111 (2001)
- Herbst, T. M., P. Bizenberger, M. Ollivier, H.-W. Rix and R.-R. Rohloff: Fizeau Interferometry on the Large Binocular Telescope. In: *Science with the Large Binocular Telescope*, Ringberg Castle/Germany 2000, (Ed.) T. Herbst. Max-Planck Society and LBT Beteiligungsgesellschaft, Heidelberg 2001, 193-201
- Herbst, W., C. A. L. Bailer-Jones and R. Mundt: The Mass Dependence of Stellar Rotation in the Orion Nebula Cluster. *The Astrophysical Journal* 554, L197-L200 (2001)
- Hinz, J. L., H.-W. Rix and G. M. Bernstein: A comparison of coma cluster S0 galaxies with the Tully-Fisher Relation for late-type spirals. *The Astronomical Journal* 121, 683 - 691 (2001)
- Hirashita, H., A. Burkert and T. T. Takeuchi: Chemical Evolution of the Galaxy Based on the Oscillatory Star Formation History. *The Astrophysical Journal* 552, 591-600 (2001)
- Hofferbert, R., D. Lemke, O. Krause, U. Grözinger, A. Böhm, W. Bollinger and J. Katzer: A cold focal plane chopper for HERSCHEL-PACS – critical components and reliability. In: *9th ESMATS (European Space Mechanism and Tribology Symposium)*, Liège/Belgium 2001, (Ed.) R.A. Harris. ESA Special Publication Series SP-480, ESA, Noordwijk 2001, 221-229.
- Hotzel, S., J. Harju, D. Lemke, K. Mattila and C. M. Walmsley: Dense gas and very cold dust in the dark core B217. *Astronomy and Astrophysics* 372, 302-316 (2001)
- Huang, J.-S., D. Thompson, M. W. Kümmel, K. Meisenheimer, C. Wolf, S. V. W. Beckwith, R. Fockenbrock, J. W. Fried, H. Hippelein, B. von Kuhlmann, S. Phleps, H.-J. Röser and E. Thommes: The Calar Alto Deep Imaging Survey: K-band Galaxy number counts. *Astronomy and Astrophysics* 368, 787-796 (2001)
- Ibata, R., G. Lewis, M. Irwin, E. Totten and T. Quinn: Great circle tidal streams: evidence for a nearly spherical massive dark halo around the Milky Way. *The Astrophysical Journal* 551, 294-311 (2001)

- Jensen, B. L., J. U. Fynbo, J. Gorosabel, J. Hjorth, S. Holland, P. Möller, B. Thomsen, G. Björnsson, H. Pedersen, I. Burud, A. Henden, N. R. Tanvir, C. J. Davis, P. Vreeswijk, E. Rol, K. Hurley, T. Cline, J. Trombka, T. McClanahan, R. Starr, J. Goldsten, A. J. Castro-Tirado, J. Greiner, C. A. L. Bailer-Jones, M. Kümmel et al.: The afterglow of the short/intermediate-duration gamma-ray burst GRB 000301C: A jet at  $z = 2.04$ . *Astronomy and Astrophysics* 370, 909-922 (2001)
- Jester, S., H.-J. Röser, K. Meisenheimer, R. Perley and R. Conway: HST optical spectral index map of the jet of 3C 273. *Astronomy and Astrophysics* 373, 447-458 (2001)
- Juvela, M., K. Mattila, K. Lehtinen, D. Lemke, R. Laureijs and T. Prusti: Far infrared and molecular line observations of Lynds L183- studies of cold gas and dust. *Astronomy and Astrophysics* 383, 502-518 (2001)
- Juvela, M., K. Mattila and D. Lemke: Far Infrared Extragalactic Background Radiation: Source Counts with ISOPHOT. In: *The extragalactic infrared background and its cosmological implications*, Manchester 2000, (Eds.) M. Harwit, M.G. Hauser. IAU Symposium 204, International Astronomical Union, Astronomical Society of the Pacific, San Francisco 2001, 261
- Kaltcheva, N., R. Gredel and C. Fabricius: The association surrounding NGC 2439. *Astronomy and Astrophysics* 372, 95-104 (2001)
- Kaltcheva, N., R. Gredel and C. Fabricius: NGC 2439  $u$ - $v$  photometry. *VizieR Online Data Catalog* 337, 20095 (2001)
- Karachentsev, I. D., M. E. Sharina, A. E. Dolphin, D. Geisler, E. K. Grebel, P. Guhathakurta, P. W. Hodge, V. E. Karachentseva, A. Sarajedini and P. Seitzer: A new galaxy near the Local Group in Draco. *Astronomy and Astrophysics* 379, 407-411 (2001)
- Karachentsev, I. D., M. E. Sharina, A. E. Dolphin, D. Geisler, E. K. Grebel, P. Guhathakurta, P. W. Hodge, V. E. Karachentseva, A. Sarajedini and P. Seitzer: WFPC2 observations of two dwarf spheroidal galaxies in the M 81 group. *Astronomy and Astrophysics* 375, 359-365 (2001)
- Kasper, M., M. Feldt and T. M. Herbst: Spatially resolved imaging spectroscopy of T Tauri. *The Astrophysical Journal* 567, 262-272 (2001)
- Keller, S. C., E. K. Grebel, G. J. Miller and K. M. Yoss: UBV $I$  and  $H_{\alpha}$  Photometry of the  $h$  and  $\chi$  Persei Cluster. *The Astronomical Journal* 122, 248-256 (2001)
- Khanzadyan, T., M. Smith, R. Gredel, T. Stanke and C. J. Davis: Active Star Formation in the Large Bok Globule CB 34\*. *Astronomy and Astrophysics* 383, 502-518 (2001)
- Khochfar, S. and A. Burkert: Redshift Evolution of the Merger Fraction of Galaxies in Cold Dark Matter Cosmologies. *The Astrophysical Journal* 561, 517-520 (2001)
- Kiss, C., P. Ábrahám, U. Klaas, M. Juvela and D. Lemke: Sky confusion noise in the Far-Infrared: Cirrus, Galaxies and the Cosmic Far-Infrared Background. *Astronomy and Astrophysics* 379, 1161-1169 (2001)
- Klaas, U., M. Haas, S. A. H. Müller, R. Chini, B. Schulz, J. Coulson, H. Hippelein, K. Wilke, M. Albrecht and D. Lemke: Infrared to millimetre photometry of ultraluminous IR galaxies: new evidence favouring a 3-stage dust model. *Astronomy and Astrophysics* 379, 823-844 (2001)
- Klessen, R. S. and A. Burkert: The Formation of Stellar Clusters: Gaussian Cloud Conditions. II. *Astrophysical Journal* 549, 386-401 (2001)
- Klessen, R. S. and A. Burkert: Fragmentation of Molecular Clouds: The Initial Phase of a Stellar Cluster. In: *New Horizons of Computational Science*, Tokyo/Japan 2001, (Eds.) T. Ebisuzaki, J. Makino. Kluwer Academic Publishers, Dordrecht 2001, 239
- Kley, W., G. D'Angelo and T. Henning: Three-Dimensional Simulations of a Planet Embedded in a Protoplanetary Disk. *The Astrophysical Journal* 547, 457-464 (2001)
- Koch Miramond, L., P. Podsiadlowski, M. Haas, T. Naylor and M. Sauvage: Determination of Mass Limits around Pulsars at 10 and 90 micron with ISO-0.3 cm. In: *Black Holes in Binaries and Galactic Nuclei*, Garching 1999, (Eds.) L. Kaper, E.P.J. van den Heuvel, P.A. Woudt. ESO Astrophysics Symposia, Springer, Berlin 2001, 139
- Kochanek, C. S., E. E. Falco, C. D. Impey, J. Lehár, B. A. McLeod, H.-W. Rix, C. R. Keeton, J. A. Muñoz and C. Y. Peng: The Evolution of Gravitational Lens Galaxies. In: *Gravitational Lensing: Recent Progress and Future Goals*, Boston, MA. 1999, (Eds.) T.G. Brainerd, C.S. Kochanek. ASP Conference Series 237, Astronomical Society of the Pacific, San Francisco 2001, 159-168
- Koresko, C. D. and C. Leinert: The Infrared Companions of T Tauri Stars: Clues to the Formation and Early Evolution of Binaries. In: *The formation of Binary Stars*, Potsdam 2000, (Eds.) H. Zinnecker, R.D. Mathieu. ASP Conference Series 200, Astronomical Society of the Pacific, San Francisco 2001, 265 - 274

- Kranz, T., A. Slyz and H. W. Rix: Measuring Stellar and Dark Mass Fractions in Spiral Galaxies. In: *Dark Matter in Astro- and Particle Physics*, Heidelberg 2000, (Ed.) H.V. Klapdor-Kleingrothaus. Springer, Heidelberg 2001, 33-37
- Kranz, T., A. Slyz and H.-W. Rix: Probing for Dark Matter within Spiral Galaxy Disks. *The Astrophysical Journal* 562, 164-178 (2001)
- Kranz, T., A. Slyz and H.-W. Rix: The Submaximal Disk of NGC 4254. In: *Galaxy Disks and Disk Galaxies*, Rome 2000, (Eds.) J.G. Funes, E.M. Corsini. ASP Conference Series 230, Astronomical Society of the Pacific, San Francisco 2001, 261-262
- Krause, O.: Stellare CCD-Photometrie: Vom Halbleiter zum Alter des Universums. Max-Planck-Institut für Astronomie, Heidelberg 2001, 21 pp.
- Krause, O., U. Grözinger, D. Lemke, A. Böhm and R. Hofferbert: Magnetoresistive position sensors for cryogenic space applications. In: *9th ESMATS (European Space Mechanism and Tribology Symposium)*, Liège/Belgium 2001, (Ed.) R.A. Harris. ESA Special Publication Series SP-480, ESA, Noordwijk 2001, 335-338
- Kroupa, P. and A. Burkert: On the Origin of the Distribution of Binary Star Periods. *The Astrophysical Journal* 555, 945-949 (2001)
- Kümmel, M., K. Meisenheimer, J.-S. Huang, D. Thompson, C. Wolf, J. Fried, H. Hippelein, B. von Kuhlmann, S. Phleps and H. J. Röser: The CADIS Picture Evolution in Range. *Astrophysics and Space Science Supplement* 277, 599 (2001)
- Kümmel, M., K. Meisenheimer, H. J. Röser, C. Wolf, J. Fried, H. Hippelein, C. Maier, B. von Kuhlmann and S. Phleps: The Data Flow in the Calar Alto Deep Imaging Survey. In: *Mining the Sky*, Garching/Germany 2000, (Eds.) A.J. Banday, S. Zaroubi, M. Bartelmann. ESO Astrophysics Symposia, Springer, Berlin 2001, 564-570
- Kurk, J. D., L. Pentericci, H. J. A. Röttgering and G. K. Miley: A proto-cluster around a radio galaxy at redshift 2.16. *Astrophysics and Space Science Supplement* 277, 543-546 (2001)
- Lai, S.-P., Y.-H. Chu, C.-H. R. Chen, R. Ciardullo and E. K. Grebel: A Critical Examination of Hypernova Remnant Candidates in M 101. I. MF 83. *The Astrophysical Journal* 547, 754-764 (2001)
- Lehtinen, K., L. K. Haikala, K. Mattila and D. Lemke: A far-infrared view of low mass star formation in the Cederblad 110 nebula of Chamaeleon I. *Astronomy and Astrophysics* 367, 311-332 (2001)
- Leinert, C., T. L. Beck, S. Ligori, M. Simon, J. Woitas and R. R. Howell: The near-infrared and ice-band variability of Haro 6-10. *Astronomy and Astrophysics* 369, 215-221 (2001)
- Leinert, C., M. Haas, P. Abraham and A. Richichi: Halos around Herbig Ae/Be stars - more common than for the less massive T Tauri stars. *Astronomy and Astrophysics* 375, 927-936 (2001)
- Leinert, C., H. Jahreiß, J. Woitas, S. Zucker, T. Mazeh, A. Eckart and R. Köhler: Dynamical mass determination for the very low mass stars LHS 1070 B and C. *Astronomy and Astrophysics* 367, 183-188 (2001)
- Lemke, D., P. Abraham, M. Haas, P. Héraudeau, S. Hotzel, C. Kiss, U. Klaas, O. Krause, C. Leinert, K. Meisenheimer, M. Stickel and L. V. Tóth: ISOPHOT surveys and the extragalactic background. In: *The extragalactic infrared background and its cosmological implications*, Manchester 2000, (Eds.) M. Harwit, M.G. Hauser. IAU Symposium 204, The Astronomical Union, The Astronomical Society of the Pacific, San Francisco 2001, 247-259
- Mandel, H., I. Appenzeller, D. Bomans, F. Eisenhauer, B. Grimm, T. M. Herbst, R. Hofman, M. Lehmitz, R. Lemke, M. Lehnert, R. Lenzen, T. Luks, R. Mohr, W. Seifert, A. Seltmann, N. Thatte, P. Weiser and W. Xu: LUCIFER – A NIR Spectrograph and Imager for the LBT. In: *Science with the Large Binocular Telescope*, Ringberg Castle/Germany 2000, (Ed.) T. Herbst, Max-Planck Society and LBT Beteiligungsgesellschaft, Heidelberg 2001, 177-186
- Márquez, I., J. Masegosa, T. Morel, A. Efstathiou, A. Verma, P. Väisänen, D. Alexander, P. Héraudeau, C. Surace, I. Pérez-Fournón, F. Cabrera-Guerra, J. I. González-Serrano, E. A. González-Solares, S. Serjeant, S. Oliver, M. Rowan-Robinson and E. Consortium: Mid-FIR properties of ELAIS sources. In: *The Promise of the Herschel Space Observatory*, Toledo/Spain 2000, (Eds.) G.L. Pilbratt, J. Cernicharo, A.M. Heras et al. ESA Special Publication Series SP-460, ESA, Noordwijk 2001, 147
- Meisenheimer, K., M. Haas, S. A. H. Müller, R. Chini, U. Klaas and D. Lemke: Dust emission from 3C radio galaxies and quasars: New ISO observations favour the unified scheme. *Astronomy and Astrophysics* 372, 719-729 (2001)

- Meisenheimer, K., C. Maier, H. Hippelein, H.-J. Röser, J. Fried, M. W. Kümmel, B. von Kuhlmann, S. Phleps, H.-W. Rix and C. Wolf: The CADIS Search for Lyman-Alpha Galaxies. In: *Deep Fields, Garching/Germany, 2000*, (Eds.) S. Christani, A. Renzini, R.E. Williams. Springer, Berlin 2001. ESO Astrophysics Symposia, 102
- Muñoz, J. A., E. E. Falco, C. S. Kochanek, J. Lehar, B. A. McLeod, B. R. McNamara, A. A. Vihklinin, C. D. Impey, H.-W. Rix, C. R. Keeton, C. Y. Peng and C. R. Mullis: Multifrequency Analysis of the New Wide-Spread Gravitational Lens Candidate RXJ 0921+4529. *The Astrophysical Journal* 546, 769 - 774 (2001)
- Muñoz, J. A., E. E. Falco, C. S. Kochanek, B. A. McLeod, J. Lehar, C. D. Impey, C. R. Keeton, C. Y. Peng and H.-W. Rix: Host Galaxies: A New Approach to Distinguish Lensed and Binary Quasars. In: *Highlights of Spanish Astrophysics II, Santiago de Compostela/Spain 2000*, (Eds.) J. Zamorano, J. Gorgas, J. Gallego. 4th Meeting of Spanish Astronomical Society, Kluwer Academic Publishers, Dordrecht 2001, 57-60
- Naab, T. and A. Burkert: The Formation of Disks in Elliptical Galaxies. *The Astrophysical Journal* 555, L91-L94 (2001)
- Naab, T. and A. Burkert: Gas Dynamics and Disk Formation in 3:1 Mergers. In: *Galaxy Disks and Disk Galaxies, Rome/Italy 2000*, (Eds.) G. José, S.J. Funes, E.M. Corsini. ASP Conference Series 230, Astronomical Society of the Pacific, San Francisco 2001, 451-452
- Naab, T. and A. Burkert: Formation of Ellipticals by Unequal Mass Mergers. In: *Galaxy Disks and Disk Galaxies, Rome/Italy 2000*, (Eds.) G. José, S.J. Funes, E.M. Corsini. ASP Conference Series 230, Astronomical Society of the Pacific, San Francisco 2001, 453-454
- Naab, T. and A. Burkert: Gas Dynamics and Inflow in Gas-Rich Galaxy Mergers. In: *The Central Kiloparsec of Starbursts and AGN: The La Palma Connection, Los Cancejos, La Palma/Spain 2001*, (Eds.) J.H. Knapen, J.E. Beckman, I. Shlosman et al. ASP Conference Series 249, Astronomical Society of the Pacific, San Francisco 2001, 735-738
- Nikoli, S., C. Kiss, J. G. A. Wouterloot, L. Johanson and L. V. Tóth: L1274: a multiwavelength study of a dark cloud in the Cep-Cas void. *Astronomy and Astrophysics* 367, 694-704 (2001)
- Odenkirchen, M., E. K. Grebel, D. Harbeck, W. Dehnen, H.-W. Rix, H. J. Newberg, B. Yanny, J. Holtzman, J. Brinkmann, B. Chen, I. Csabai, J. J. E. Hayes, G. Hennessy, R. B. Hindsley, Z. Ivezić, E. K. Kinney, S. J. Kleinman, D. Long, R. H. Lupton, E. H. Neilsen, A. Nitta, S. A. Snedden and D. G. York: New Insights on the Draco Dwarf Spheroidal Galaxy from the Sloan Digital Sky Survey: A Larger Radius and No Tidal Tails. *The Astronomical Journal* 122, 2538-2553 (2001)
- Odenkirchen, M., E. K. Grebel, C. M. Rockosi, W. Dehnen, R. Ibata, H.-W. Rix, A. Stolte, C. Wolf, J. E. Anderson Jr., N. A. Bahcall, J. Brinkmann, I. Csabai, G. Hennessy, R. B. Hindsley, Z. Ivezić, R. H. Lupton, J. A. Munn, J. R. Pier, C. Stoughton and D. G. York: Detection of Massive Tidal Tails around the Globular Cluster Palomar 5 with Sloan Digital Sky Survey Commissioning Data. *The Astrophysical Journal* 548 L165 - L169 (2001)
- Odenkirchen, M., V. V. Makarov, C. Soubiran and S. Urban: The tidal extension of the Coma star cluster revealed by HIPPARCOS, Tycho-2 and spectroscopic data. In: *Dynamics of Star Clusters and the Milky Way, Heidelberg/Germany 2000*, (Eds.) S. Deiters, B. Fuchs, A. Just et al. ASP Conference Series 228, Astronomical Society of the Pacific, San Francisco 2001, 535.
- Ofek, E., D. Maoz, T. Kolatt and H.-W. Rix: A survey for large separation-lensed FIRST quasars. *Monthly Notices of the Royal Astronomical Society* 324, 463 - 472 (2001)
- Patsis, P. A., P. Héraudeau and P. Grosboel: Spiral arms in near-infrared bands. Broad- and narrow-band NIR photometry. *Astronomy and Astrophysics* 370, 875-880 (2001)
- Pentericci, L., P. McCarthy, H. Röttgering, G. Miley, W. van Breugel and R. Fosbury: NICMOS Observations of High-Redshift Radio Galaxies: Witnessing the Formation of Bright Elliptical Galaxies? *The Astrophysical Journal Supplement Series* 135, 63-85 (2001)
- Phleps, S., K. Meisenheimer, B. Fuchs and C. Wolf: CADIS deep star counts: Galactic structure and the stellar luminosity function. *Astronomy and Astrophysics* 356, 108-117 (2001)
- Pizzella, A., E. M. Corsini, J. C. Vega Beltrán, J. E. Beckman, J. G. Funes, W. W. Zeilinger, M. Sarzi and F. Bertola: Kinematics of Gas and Stars in 20 Disk Galaxies. In: *Galaxy Disks and Disk Galaxies, Rome/Italy 2000*, (Eds.) J.G. Funes, E.M. Corsini. ASP Conference Series 230, Astronomical Society of the Pacific, San Francisco 2001, 279-280

- Popescu, C. C., R. Tuffs, H. Völk, D. Pierini and B. F. Madore: Cold Dust in Late-Type Virgo Cluster Galaxies. *The Astrophysical Journal* 567, 221-236 (2001)
- Rifatto, A., P. Rafanelli, S. Ciroi, M. Radovich, J. Vennik, G. Richter and K. Birkle: The Active Merging System ESO 202-G23 (Carafe Nebula). *The Astrophysical Journal* 122, 2301-2317 (2001)
- Rix, H.-W., E. Falco, C. Impey, C. Kochanek, J. Lehár, B. A. McLeod, J. Muñoz and C. Y. Peng: Host Galaxies of Lensed Luminous Quasars at  $z \sim 2$ . In: *Gravitational Lensing: Recent Progress and Future Goals*, Boston, MA. 1999, (Eds.) T.G., Brainerd, C.S. Kochanek. ASP Conference Series 237, Astronomical Society of the Pacific, San Francisco 2001, 169-175
- Rousselot, P., C. Arpigny, H. Rauer, R. Gredel, J. Manfroid and A. Fitzsimmons: A fluorescence model of the C3 radical in comets. *Astronomy and Astrophysics* 368, 689-699 (2001)
- Rudnick, G., M. Franx, H.-W. Rix, A. Moorwood, K. Kuijken, L. van Starckenburk, P. van der Werf, H. Röttgering, P. van Dokkum and I. Labbé: A K-Band-Selected Photometric Redshift Catalog in the Hubble Deep Field South: Sampling the Rest-Frame V Band to  $z = 3$ . *The Astronomical Journal* 122, 2205-2221 (2001)
- Rudnick, G., H.-W. Rix and M. Franx: FIRES at the VLT: Measuring the Rest-Frame V-Band Luminosity of Galaxies from  $z \sim 3$  to Now. In: *Galaxy Disks and Disk Galaxies*, Rome/Italy 2000, (Eds.) J.G. Funes, E.M. Corsini. ASP Conference Series 230, Astronomical Society of the Pacific, San Francisco 2001, 261-262
- Rusin, D., C. S. Kochanek, M. Norbury, E. E. Falco, C. D. Impey, J. Lehár, B. A. McLeod, H.-W. Rix, C. R. Keeton, J. A. Muñoz and C. Y. Peng: B1359-154: A Six Image Lens Produced by a  $z = 1$  Compact Group of Galaxies. *The Astrophysical Journal* 557, 594-604 (2001)
- Sarzi, M., F. Bertola, M. Cappellari, E. M. Corsini, J. G. Funes, A. Pizzella and J. C. Vega Beltrán: The Orthogonal Bulge-Disk Decoupling in NGC 4698. *Astrophysics and Space Science* 276, 467-473 (2001)
- Sarzi, M., H.-W. Rix, J. C. Shields, G. Rudnick, L. C. Ho, D. McIntosh, A. V. Filippenko and W. L. W. Sargent: Supermassive Black Holes in Bulges. *The Astrophysical Journal* 550, 65 - 74 (2001)
- Sarzi, M., H.-W. Rix, J. C. Shields, G. Rudnick, D. H. McIntosh, L. C. Ho, A. V. Filippenko and W. L. W. Sargent: Supermassive Black Holes from the Survey of Nearby Nuclei with STIS. In: *Galaxy Disks and Disk Galaxies*, Rome/Italy 2000, (Eds.) J.G. Funes, E.M. Corsini. ASP Conference Series 230, Astronomical Society of the Pacific, San Francisco 2001, 261-262
- Schuller, P. and C. Leinert: Performance of Optical Path Length Modulators in MIDI. In: *Summer School on Space and Ground Based Optical and InfraRed Interferometry*, Leiden 2000, (Eds.) I.J. Percheron, I. Montilla, L. D'Arcio. NEVEC Leiden Observatory, Leiden 2001, 371.
- Singh, H. P., C. A. L. Bailer-Jones and R. Gupta: Principal component analysis and its application to stellar spectra. In: *Automated Data Analysis in Astronomy*, Puna/India 2000, (Eds.) R. Gupta, H.P. Singh, C.A.L. Bailer-Jones. Narosa Publishing House, New Delhi 2001, 69-82
- Slyz, A., J. E. G. Devriendt, A. Burkert, K. Prendergast and J. Silk: Star formation in Viscous Galaxy Disks. In: *Galaxy Disks and Disk Galaxies*, Rome/Italy 2000, (Eds.) J.G. Funes, E.M. Corsini. ASP Conference Series 230, Astronomical Society of the Pacific, San Francisco 2001, 333-334
- Stickel, M., U. Klaas, D. Lemke and K. Mattila: Far-Infrared Emission from Dust in Abell Clusters. In: *Deep Fields*, Garching/Germany 2000, (Eds.) S. Cristiani, A. Renzini, R.E. Williams. ESO Astrophysics Symposia, Springer, Berlin 2001, 216
- Stickel, M., D. Lemke, U. Klaas, C. A. Beichman, M. Rowan-Robinson, A. Efstathiou, S. Bogun, M. F. Kessler and G. Richter: The ISOPHOT 170 Micron Serendipity Sky Survey: A Plea to FIRST. In: *The Promise of FIRST*, Toledo/Spain 2000, (Eds.) G.L. Pilbratt, J. Cernicharo, A.M. Heras et al. ESA Special Publication Series SP-460, ESA, Noordwijk 2001, 109
- Taylor, A. N., S. Dye, E. Thommes, C. Wolf and K. Meisenheimer: Gravitational Lens Magnification and the Distortion of the Galaxy Luminosity Function. In: *Gravitational Lensing: Recent Progress and Future Goals*, Boston 1999, (Eds.) T.G. Brainerd, C. Kochanek. ASP Conference Series 237, Astronomical Society of the Pacific, San Francisco 2001, 295
- Torres, S., E. García-Berro, A. Burkert and J. Isern: The Impact of a Merger Episode in the Galactic Disc White Dwarf Population. *Monthly Notices of the Royal Astronomical Society* 328, 492-500 (2001)

- Tovmassian, G. H., G. Stasínska, V. H. Chavushyan, S. V. Zharikov, C. Gutierrez and F. Prada: SBS 1150+599A: An extremely oxygen-poor planetary nebula in the Galactic halo? *Astronomy and Astrophysics* 370, 456-467 (2001)
- Travaglio, C., A. Burkert and D. Galli: Inhomogeneous chemical evolution of the Galactic halo. *Astrophysics and Space Science Supplement* 277, 211-211 (2001)
- Travaglio, C., D. Galli and A. Burkert: Inhomogeneous Chemical Evolution of the Galactic Halo: Abundance of *r*-Process Elements. *The Astrophysical Journal* 547, 217-230 (2001)
- Travaglio, C., R. Gallino, M. Busso and A. Dalmazzo: Galactic enrichment of heavy s-elements: from Ba to Bi. *Memorie della Società Astronomica Italiana* 72, 381-390 (2001)
- Travaglio, C., R. Gallino, M. Busso and R. Gratton: Lead: Asymptotic Giant Branch Production and Galactic Chemical Evolution. *The Astrophysical Journal* 549, 346-352 (2001)
- Travaglio, C., S. Randich, D. Galli, J. Latanzio, L. M. Elliott, M. Forestini and F. Ferrini: Galactic chemical evolution of Lithium: Interplay between stellar sources. *The Astrophysical Journal* 559, 909-924 (2001)
- Van den Bosch, F. C., A. Burkert and R. A. Swaters: The angular momentum content of dwarf galaxies: new challenges for the theory of galaxy formation. *Monthly Notices of the Royal Astronomical Society* 326, 1205-1215 (2001)
- Woitas, J., R. Koehler and C. Leinert: T Tauri binary systems orbital motion. *VizieR Online Data Catalog*, originally published in *Astronomy and Astrophysics* 336, 90249 (2001)
- Woitas, J., R. Köhler and C. Leinert: Orbital motion in T Tauri binary systems. *Astronomy and Astrophysics* 369, 249-262 (2001)
- Woitas, J., C. Leinert and R. Koehler: Near-IR observations of young binaries. *VizieR Online Data Catalog*, originally published in *Astronomy and Astrophysics* 337, 60982 (2001)
- Woitas, J., C. Leinert and R. Köhler: Mass ratios of the components in T Tauri binary systems and implications for multiple star formation. *Astronomy and Astrophysics* 376, 982-996 (2001)
- Wolf, C., K. Meisenheimer, S. Dye, M. Kleinheinrich, H.-W. Rix and L. Wisotzki: Deep BVR-band photometry of the Chandra Deep Field South from the COMBO-17 survey. *Astronomy and Astrophysics* 377, 442-449 (2001)
- Wolf, C., K. Meisenheimer and H.-J. Röser: Classification and Redshift Estimation in Multi-Color Surveys. In: *Mining The Sky*, Garching, Germany 2000, (Eds.) A.J. Banday, S. Zaroubi, M. Bartelmann. *ESO Astrophysics Symposia*, Springer, Berlin 2001, 337-343
- Wolf, C., K. Meisenheimer and H.-J. Röser: Efficiency of Medium-Band Surveys. In: *The New Era of Wide Field Astronomy*, Preston/UK 2000, (Eds.) R., A. Clowes, Adamson, G. Bromage. *ASP Conference Series* 232, Astronomical Society of the Pacific, San Francisco 2001, 320
- Wolf, C., K. Meisenheimer and H.-J. Röser: Object Classification in Astronomical Multi-color Surveys. *Astronomy and Astrophysics* 365, 660-680 (2001)
- Wolf, C., K. Meisenheimer, H. J. Röser, S. W. V. Beckwith, F. H. Chaffee, J. Fried, H. H. Hippelein, J.-S. Huang, M. Kümmel, B. von Kuhlmann, C. Maier, S. Phleps, H.-W. Rix, E. Thommes and D. Thompson: Multi-color classification in the Calar Alto deep imaging survey. *Astronomy and Astrophysics* 365, 681-698 (2001)
- Zapatero Osorio, M. R., V. J. S. Béjar, E. L. Martín, R. Rebolo, D. Barrado y Navascués, C. A. L. Bailer-Jones and R. Mundt: Discovery of a Very Young Planetary-Mass Population in  $\sigma$  Orionis: the Substellar Mass Function. In: *From Darkness to Light: Origin and Evolution of Young Stellar Clusters*, Cargèse, Corsica/France 2000, (Eds.) T. Montmerle, P. André. *ASP Conference Series* 243, Astronomical Society of the Pacific, San Francisco 2001, 477-486
- Zapatero Osorio, M. R., V. J. S. Béjar, E. L. Martín, R. Rebolo, D. Barrado Y Navascués, C. A. L. Bailer-Jones and R. Mundt: Evidence for Free-floating Planetary-mass Objects in the  $\sigma$  Orionis Star Cluster. In: *Cool Stars, Stellar Systems and the Sun – 11th Cambridge Workshop*, Tenerife/Spain 2000, (Eds.) R.J. Garcia Lopez, R. Rebolo, M.R. Zapatero Osorio. *ASP Conference Series* 223, Astronomical Society of the Pacific, San Francisco 2001, 70

**Diplomarbeiten**

Walcher, J.: Detecting Tidal Tails With Field Cameras. Diploma thesis Ruprecht-Karls-Universität, Heidelberg 2001

Ziegler, M.: Velocity and Density Structure of Molecular Cloud Cores. Diploma Thesis Ruprecht-Karls-Universität, Heidelberg 2001

---

**Doktorarbeiten**

Heitsch, F.: Turbulence and Fragmentation in Molecular Clouds. PhD Thesis Ruprecht-Karls-Universität, Heidelberg 2001

Hetznecker, H.: Die Entstehungsgeschichte der dichten Kerne von CDM-Halos. PhD Thesis Ruprecht-Karls-Universität, Heidelberg 2001

Hotzel, S.: The 170  $\mu\text{m}$  Zufallsdurchmusterung mit ISO. Strukturen im kalten Staub der Milchstraße. PhD Thesis Ruprecht-Karls-Universität, Heidelberg 2001

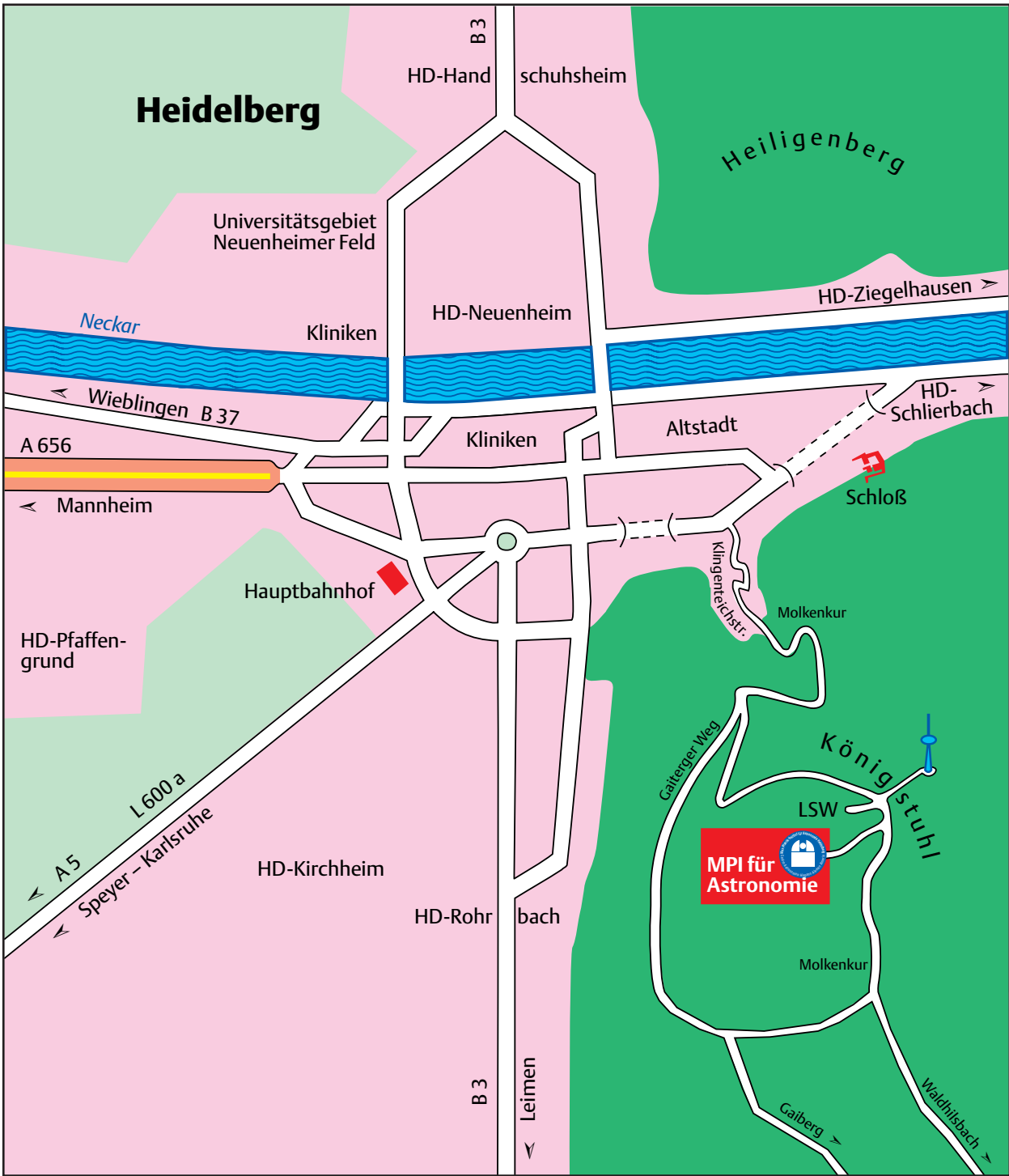
Jester, S.: High-resolution multi-wavelength study of the jet in 3C 273. PhD Thesis Ruprecht-Karls-Universität, Heidelberg 2001

Phleps, S.: The Evolution of the Large Scale Structure of the Universe since  $z = 1$ . PhD Thesis Ruprecht-Karls-Universität, Heidelberg 2001

---

**Habilitationsschrift**

Haas, M.: Quasars in the Infrared. Habilitationsschrift Ruprecht-Karls-Universität, Heidelberg 2001



Heidelberg – City map

# The Max Planck Society

The Max Planck Society for the Promotion of Sciences was founded in 1948. In succession to the Kaiser Wilhelm Society, which was founded in 1911, the Max Planck Society operates at present 78 Institutes and other facilities dedicated to basic and applied research. With an annual budget of around 1.25 billion € in the year 2001, the Max Planck Society has about 11 600 employees, of which one quarter are scientists. In addition, annually about 7000 junior and visiting scientists are working at the Institutes of the Max Planck Society.

The goal of the Max Planck Society is to promote centers of excellence at the forefront of the international scientific research. To this end, the Institutes of the Society are equipped with adequate tools and put into the hands of outstanding scientists, who have a high degree of autonomy in their scientific work.

Max-Planck-Gesellschaft zur Förderung der Wissenschaften  
Public Relations Office  
Hofgartenstr. 8  
D-80539 München

Tel.: 0049-89-2108-1275 or -1277

Fax: 0049-89-2108-1207

Internet: <http://www.mpg.de>



---

MAX-PLANCK-GESELLSCHAFT